ENVIRONMENTAL PROGRESS

Vol.12, No. 4 • November 1993

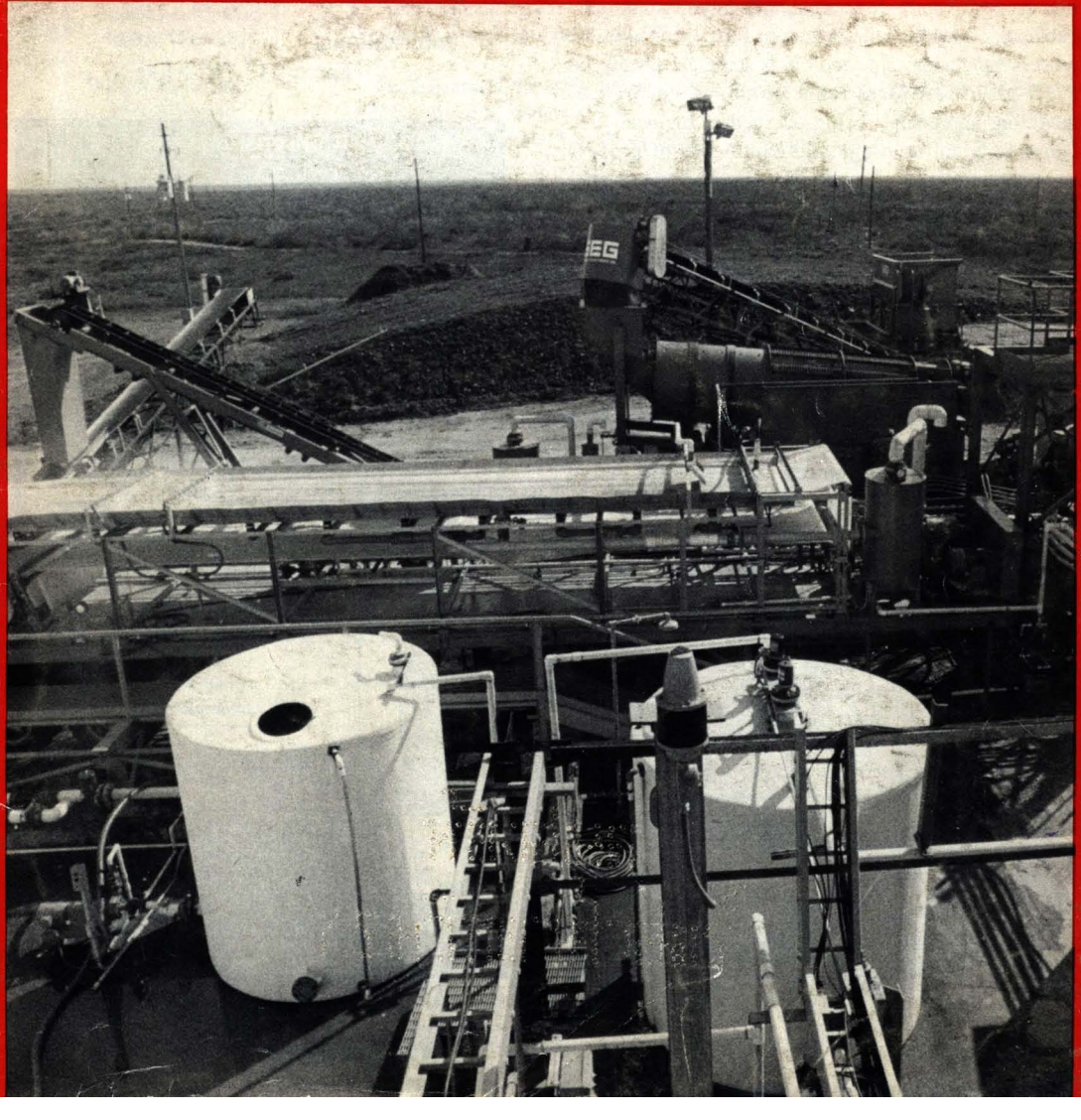

Environmental Considerations in Process Design and Simulation

Prepared by J. Eisenhauer and S. McQueen, Energetics Inc.

The Environmental Protection Agency, The Department of Energy, and The Center for Waste Reduction Technologies, brings a new publication which identifies how environmental factors should be incorporated into process simulation and design tools for the chemical process industries.

Authored by leading U.S. experts drawn from the industrial user community, software designers, university researchers, and federal R&D managers—this publication identifies the important R&D needed in the process simulation area and offers some perspective on R&D priorities. Ideas range from new theoretical modeling approaches being pursued in the academic community to the pragmatic data needs of process engineers who must find ways to meet environmental regulations for current operating facilities.

Issues and R&D needs addressed:

- The pertinent environmental considerations and how they should be brought into the optimization/design process
- New process models or modifications required to accommodate environmental factors in process simulation
- Current concepts of process simulators and design tools modified to incorporate environmental factors
- Data required to support process simulation and design with environmental factors

Nearly all of the recommended R&D activities are expected to produce significant results within ten years. And nearly half of the R&D activities proposed will provide results in three years or less.

CENTER FOR
Waste Reduction
TECHNOLOGIES
AMERICAN INSTITUTE OF CHEMICAL ENGINEERS

1993, 78 pages, Pub #C-3
ISBN 0-8169-0614-9
List: $25.00 International: $35.00

Call AIChExpress or mail coupon to order this invaluable book today!

U.S. 1-800-242-4363
International 1-212-705-7657
Fax 212-705-8400

Mail to: AIChExpress, 345 East 47th St, New York, NY 10017-2395

TYPE OR PRINT CLEARLY

Please send me _____ copies of "Environmental Considerations in Process Design & Simulation" @ $25.00 each (International: $35.00) for a total of _____.

[ ] Check enclosed (Payable to: AIChE)
[ ] Charge to my [ ] Visa [ ] Mastercard

Acct. # _____

Exp. Date _____

Signature _____

[ ] Check here if you would like a copy of the AIChE Publications Catalog.

Name _____

Title _____

Tel. ( ) _____

Company _____

Address _____

City _____

State _____

Zip _____

ENVIRONMENTAL PROGRESS

Environmental Progress is a publication of the American Institute of Chemical Engineers. It will deal with multifaceted aspects of the pollution problem. It will provide through coverage of abatement, control, and containment of effluents and emissions within compliance standards. Papers will cover all aspects including water, air, liquid and solid wastes. Progress and technological advances vital to the environmental engineer will be reported.

Published four times a year (February, May, August, and November) by the American Institute of Chemical Engineers, 345 E 47th St., New York, N.Y. 10017 [ISSN 0278-4491]. Manuscripts should be submitted to the Manuscript Center, AIChE 345 E 47th St., New York, N.Y. 10017. Statements and opinions in *Environmental Progress* are those of the contributors,and the American Institute of Chemical Engineers assumes no responsibility for them. Subscription price per year $125. AIChE Environmental Division Members $29 included in dues. Outside the U.S. please add $12 per subscription for postage and handling. Single copies $37. Outside the U.S. please add $3 for postage and handling. Payment must be made in U.S. dollars. Second-class postage paid at New York, N.Y. and additional mailing offices. Copyright 1993 by the American Institute of Chemical Engineers.

Contents

Cover: Mobile soil washing system. Photo courtesy of Scientific Ecology Group Inc., Pittsburgh, PA

Departments

Partnering - Gimmick or Opportunity?

Paul L. Busch

The environmental arena has been rife with litigation for years. Everyone - even the lawyers - are fed up with how adversarial the situation has become. When the courts decide, there are usually clear winners and losers. What can we do to create a system with no losers - *all winners?* Alternative dispute resolution systems are often proposed to eliminate the court system; but these systems come into use only after disputes exist. Many people think alternative dispute resolutions are an improvement over the courts, but they involve so much compromise that often they are seen as producing only losers - *no winners!*

Partnering has been proposed as a method to stem the tide of adversarial relationships. Even though it is not a partnership in the legal sense "partnering" endeavors to emulate what we require in a partner, namely competence and trust. We work together with our partner to achieve specific project goals: economic, regulatory, schedule, and quality.

Many say that clients (owners), contractors, equipment suppliers, and consultants have always tried to be partners but that differing objectives make success unlikely. After all, trust and competence may not be consistent with individual economic, quality, and schedule interests. However, the U.S. Army Corps of Engineers - committed to partnering - claims immense savings, improved schedules and virtually no litigation (and no litigation costs) with partnering. Other government entities and private corporations are claiming similar results.

The key to making it work seems to be "formal" partnering sessions at the outset of a project - between owner and engineer at the start of planning or design; or among owner, contractor and engineer at the beginning of construction - the earlier the better. With the help of a professional facilitator each party agree on what's important to all: for example, no increase in project costs; high quality; no schedule extensions; adequate profit for engineer and contractor; timely payments, etc. They discuss barriers to achieving goals, and actions that would help eliminate these barriers; they might create shared incentives for reducing total cost or improving the schedule; they agree to meet periodically to look for ways to improve the project "system", and to discuss lessons learned - not to be repeated. Finally, *they agree in advance to reach agreement or compromise for reasonable cause on issues which normally could lead to disputes.* At the end of the session the group writes a formal "partnering charter" which all the principal players sign and hang on their office walls for the duration of the project. This serves as a powerful reminder that everyone is part of the project team committed to helping each other for the benefit of the project.

Does the above sound too good to be true? Well, we're doing it with both owners and contractors. Half the time we have suggested it and half the time they have. So there *must* be something in this for all of us. We've found that building trust through formal partnering is remarkably effective. Costs are reduced and schedules contained. Creating a project "team" which includes all the principal players dedicated to the same goals is a real morale booster. While formal "partnering" must not replace contracts, its success thus far gives cause to believe it can improve a system which most of us have been dissatisfied with for decades.

Paul L. Busch, Ph.D., is President and CEO of Malcolm Pirnie Inc., Environmental Engineers, Scientists and Planners, White Plains, New York. He is Past President of the American Academy of Environmental Engineers, and Vice Chair of the Water Environment Research Foundation.

Free Clean Air Act Assistance Available

The Clean Air Act Amendments of 1990 can be a nightmare for environmental managers. Assistance, however, is available in that Environmental Compliance Reporter Inc., is distributing a free catalog of private and federal agency documents designed to help environmental managers make their way through the regulatory maze.

The document include technical assistance on reducing pollution, including EPA guidance on reducing emissions of NO_x, VOCs and hazardous air pollutants. Guidebooks published by private firms, provide common sense advice on meeting the law's complex requirements while holding down administrative and capital expenditures.

For more information call ECR Inc., at 1 (800) 729-1964.

CWRT Chair Speaks at Pollution Prevention Luncheon

Earl Beaver, technology director, waste elimination for Monsanto Company and Advisory Board chair for the Center for Waste Reduction Technology (CWRT), was the featured speaker at the luncheon which wrapped up the Topical Conference on Pollution Prevention held in conjunction with the AIChE Summer National Meeting in Seattle last August.

"I'm going to challenge you to move what you personally do toward pollution prevention. I'm going to challenge the companies represented here to take a different view of pollution prevention - not to think of other companies as competition, but of the opportunity to cooperate." he said. Beaver discussed how Monsanto has worked to reduce its waste, and said that "we believe that organizations like CWRT give us the leverage " to help accomplish company goals. He also described CWRT's publishing program. *Environmental Considerations in Process Design & Simulation* was based on a workshop cosponsored by the Environmental Protection Agency and the Department of Energy. *Current and Potential Future Industrial Practices for Reducing and Controlling Volatile Organic Compounds* is a survey of needs and technology. He feels that *Pollution Prevention: Homework and Design Problems for Engineering Curricula,* authored by David Allen of UCLA and others, "provides the curricula development necessary to incorporate pollution prevention in the learning experience of today's engineers so that they come out with a different mindset."

Washington Environmental Newsletter

Superfund

In his February State of the Union Address, President Clinton chose to let the nation know that his administration believes that the Superfund law "needs to be fixed." It was not by chance that he said this as private sector interest groups in Washington D.C., had lobbied the President's staff to get the message inserted in his speech. That's all history now, but congressional action to amend Superfund is not. To date 20 bills have been introduced in Congress to "fix Superfund." Numerous hearings have been held already with more to follow. The debate will easily spill over into next year

.

What is Superfund and What Needs Fixing?

The Comprehensive Environmental Response, Compensation and Liability Act (CERCLA), or Superfund as it is commonly known, was enacted in 1980 in response to the discovery of hazardous waste dumps at Love Canal, N.Y., and elsewhere. CERCLA requires that the Environmental Protection Agency (EPA) determine the nation's most serious abandoned hazardous waste sites and gives the agency the power to force those responsible to clean up the sites.

To ensure prompt action, EPA can conduct cleanups itself and later sue the responsible parties to recover the costs. To cover EPA's cleanup costs, CERCLA established a "superfund" consisting of targeted taxes and general revenues. CERCLA's "strict liability" system makes all those connected with a contaminated site potentially responsible for the entire cleanup cost without regard to fault. Courts can divide the costs among liable parties based on fairness considerations, and the parties can sue one another for cleanup expenses.

To date, EPA had identified approximately 36,000 potential Superfund sites. The sites considered to be the most hazardous have been placed on the National Priorities List (NPL) for Superfund cleanup; there currently are over 1,200 sites on the NPL, and about 100 sites are added each year. Cleanups, which have been averaging 11 years and $25 million per site, have been completed at 183 NPL sites and cleanup activities have commenced at more than 1,000 other NPL sites. It is estimated that the Superfund and private parties have spent over $30 billion in the past 13 years to clean up Superfund sites. The cleanup effort could cost $500 billion and take decades to complete.

CERCLA has been amended and reauthorized twice since 1980. The current authorization expires at the end of FY 1994 (September 30, 1994).

Superfund Issues to be Debated

Risk Assessment

CERCLA requires that a risk assessment be performed at each NPL site to assure that EPA selects a cleanup plan that is protective of human health and the environment. It is claimed that EPA's risk assessments are flawed because they frequently use default assumptions rather than site-specific data, the default assumptions are worst-case rather than realistic, and EPA uses a single-value (deterministic) method rather than a group of values (probabilistic) method for variables. This leads many to conclude that EPA overestimates the risks of harm from Superfund sites.

Affected parties are asking if EPA's risk assessment process is scientifically valid and whether it should be replaced with a system that looks at the realistic risks at the site. Congress will consider this issue very carefully.

Cleanup Standards

Current law states that cleanups must be adequate to ensure the protection of human health and the environment and must also be cost-effective. Cleanups should be permanent and utilize alternative treatment technologies to the maximum extent practicable. Remedial actions that permanently and significantly reduce the volume, toxicity, or mobility of hazardous wastes are preferred over remedial actions that do not involve such treatment. CERCLA itself does not establish cleanup standards; rather it incorporates legally applicable or relevant and appropriate requirements (ARARs) from other State and Federal laws.

Congress will consider whether the preferred level of cleanup should be uniform or whether it should it be determined on a case-by-case basis, looking at the current and future use of the land and the environmental risk posed by wastes.

(continued on following page)

Innovative Technologies

Although CERCLA requires use of alternative treatment technologies to the maximum extent practicable, EPA has been accused of stifling innovative remediation technologies by imposing regulatory impediments to the development and implementation of more cost-effective and reliable methods to remediate hazardous waste and by not providing the flexibility needed for demonstration projects.

Congress will consider how EPA can support the development and implementation of innovative remediation technologies.

The "Polluter Pays" System

CERCLA established a "polluter pays" strict liability system under which the costs of site cleanups generally is borne by the parties that contributed hazardous waste to the site, regardless of whether there is any causal link between the wastes disposed of and the conditions requiring remediation. Liability for cleanup costs is determined by oftentimes complex and time-consuming lawsuits against and among those who are identified as contributing hazardous wastes.

Congress will consider whether the "polluter pays" system should be replaced by a broad-based publicly funded system under which EPA would be responsible for Superfund cleanups.

Other Issues

Other issues which Congress will be addressing are: Joint and Several Liability, Retroactive Liability, Municipal Liability, De Minimus Contributor Liability, Lender Liability, Insurer Liability and Legal Fees - a complex mixture of important issues.

Future Action

The Administration has committed to submit its Superfund bill to Congress on November 30, but it likely will present only a set of principles to be used to draft legislation. EPA Administrator Carol Browner is being assisted in the development of the proposal by an interagency Superfund reauthorization task force. The task force's work has been complicated by the fact that Treasury officials have endorsed a proportional liability approach, which is strongly opposed by EPA and the Department of Justice.

The Superfund Evaluation Committee of the National Advisory Council for Environmental Policy and Technology recently submitted position papers on Superfund reauthorization to Administrator Browner. The committee's Superfund Evaluation Committee includes a broad spectrum of potentially responsible parties, environmental groups, and other interested entities. The position papers indicate a lack of agreement within the committee on how to resolve major Superfund issues. The Remedy Selection Reform Subcommittee agreed that "a more streamlined method for remedy selection that is protective of human health and the environment is merited" and that remedy selection should be land-use based. It suggested that national standards "may be a viable alternative," with site-specific standards being used where national standards to not apply.

There are several major industry-supported groups working on Superfund. The Coalition on Superfund is a group of approximately 20 manufacturing firms and insurance companies. They advocate setting priorities for Superfund cleanups, basing the level and extent of cleanups on the actual risks of the sites and the current and planned uses of the sites, and promoting innovative technologies through certifications and credits. The "No Name Group," consisting of small businesses and the food and oil industries, has put forth a fix on retroactive liability. The Business Roundtable has enunciated a set of principles that endorse a broad-based funding mechanism and remediation based on realistic risks and actual land uses.

Others also are involved. The Chemical Manufacturers Association has unveiled its Superfund reform proposal, a proportional liability system. The National Environmental Trust Fund, which is funded by the insurance industry proposes a broad-based trust fund to pay for cleanups. The Hazardous Waste Cleanup Project, whose eight members are trade associations in the industrial sector advocates reforming Superfund to focus on actual rather than hypothetical risks. The NAACP has endorsed a limit on retroactive liability because of the current system's failure to achieve cleanups of Superfund sites in minority and low-income communities. It advocates creating a trust fund supported by increased taxes on business to pay for cleanups.

This newsletter was prepared by AIChE's Washington staff, Dale Brooks and Sean Bersell, 1300 I Street, N.W., Suite 1090, East Tower, Washington, D.C. 20005. Telephone (202) 962-8690 • FAX: (202) 962-8699

Alum Sludge in the Aquatic Environment, by Dennis B. George, Sharon G. Berk, V. Dean Adams, Eric L. Morgan, Robert O. Roberts, Cynthia A. Holloway, R. Craig Lott, Lissa K. Holt, Rebecca S. Ting, and Amy W. Welch. AWWA Research Foundation and the American Water Works Assoc., Denver, Colorado, (1991). 224 pages [ISBN No.: 0-89867-531-6] U.S. List Price: $ 36.50

This report describes the toxicity of alum sludges towards a variety of organisms, ranging from bacteria to benthic macroinvertebrates. Alum sludge is a residual from the production of potable or process water whenever alum or other aluminum salts are used as the primary coagulants. In many cases, disposal of alum sludge to steams and rivers is not allowed and alternative techniques (such as land application, disposal in landfills, or regeneration and reuse) must be evaluated. However, nearly 50% of alum sludges are still disposed to surface waters.

The authors obtained alum sludges from ten water treatment plants throughout the United States and Canada, representing a variety of raw water alkalinity, disinfection techniques, and other chemical parameters. All plants were of conventional design, with sedimentation tanks and rapid filters. Although the chemical conditions during coagulation (especially the pH and alum dose) are not explicitly described, these conditions can be inferred from the contents of the report.

In general, extracts from the alum sludges were non-toxic to the tested organisms unless the pH was artificially lowered or raised, and then they were only toxic to the test algal species, *Selenastrum capricornutum*. Extracts taken at various pH values from the alum sludges were non-toxic to *Photobacterium phosphoreum* (bacterium), *Tetrahymena pvriformis* (protozoan), *Ceriodaphnia dubia* (arthropod), and *Pimephales* (fathead minnows). Acute toxicity towards the algal species corresponded to increases in the concentration of "monomeric aluminum", which was determined by means of chemical fractionation tests and which was implicitly considered to be the only toxic substance.

Some extracts has a chronic toxicity effect on fathead minnows. Thus fish lost weight relative to controls when exposed to two of the sludge extracts. In addition, both field studies and laboratory ecosystem studies revealed decreases in the populations of benthic macroinvertebrates when alum sludge was sufficient to cover the original sediment. The authors proposed that this was due to a lack of organic carbon

nutrients, and discovered similar effects from the addition of bentonite to laboratory ecosystems.

This study offers specific information regarding the toxicity of alum sludges, and also provides a format for conducting studies of potentially toxic effects due to the disposal of other residuals in streams and rivers. The study indicates that the disposal of water treatment residuals to receiving streams will have minimal impact on stream biota if there is sufficient flow and hydraulic scour to prevent immediate deposition of the residual solids and if the receiving water has circumneutral pH and sufficient pH buffer capacity to prevent substantial diurnal or seasonal changes in pH.

Brian A. Dempsey, Ph.D.
Associate Professor
Department of Civil Engineering
The Pennsylvania State
University
University Park, PA 16802

Electrical and Instrumentation Safety for Chemical Processes, by Richard J. Buschart, Van Nostrand Reinhold Publishing Co., New York, NY, (1991) 241 pages [ISBN No:0-442-23833-9] U.S. List Price: S49.95

The author should be congratulated for preparing a timely and much needed book in electrical and instrumentation safety in the chemical process industry. Although the chemical and petroleum process industries rely heavily on electrical devices and instrumentation, in many chemical process units, there are no experienced electrical engineers to make design and safety decisions pertaining to electrical devices and instrumentation. This book covers a wide spectrum of electrical and electronic phenomena and the effects on chemical process safety.

The book contains eleven chapters, beginning with an introduction to general safety criteria, safety philosophy and principles, and electrical and control safety incidents. Chapter 2 addresses the process conditions that influence safety, the process operation, and the plant layout. The National Electric Code terminology, flammability characteristics, leak and release sources, ventilation, vapor barriers, and electrical classifications are discussed in Chapter 3.

Chapter 4 presents an excellent discussion of electrical equipment in class I locations. The discussion includes explosion proof apparatus, intrinsic safety and oil immersion. Chapter 5 addresses the importance of dust electrical safety in chemical process facilities, while Chapter 6 presents a good discussion of electrical safety in chemical processes.

Chapters 7 through 9 deal with the issue of process control safety and the role of instrumentation and different process control schemes in chemical process safety. Chapter 10 presents a good discussion of safety in maintenance operations and Chapter 11 discusses safety in work practices.

This book is highly recommended for those involved in the design, operation, maintenance, and management of chemical, petroleum, and similar processes.

Hamid R. Kavianian, Ph.D.
Professor
Dept., of Chemical Engineering
California State University
Long Beach, CA 90840

Manual of Design for Slow Sand Filtration by David Hendricks, AWWA Research Foundation and the American Water Works Association, Denver, CO, (1991) 247 pages [ISBN No: 0-89867-551-0] U.S. List Price: $55.00

With the new drinking water regulations many water supply systems that previously did not require filtration will now have to provide this treatment. The two most commonly used methods of filtration are slow rate and rapid rate filtration through sand, although diatomaceous earth filtration is a valid consideration. As a general rule, slow rate filtration through sand has advantages for a small system. A major advantage is the requirement of operational time, although new monitoring regulations require frequent sampling which may offset the operating time benefits. This book is designed to provide information on selecting the best filtration alternative, and, in the event that slow sand filtration is chosen, to provide guidance in the design and construction of a slow sand filtration system.

The book is very elementary. Its stated purpose is to provide design guidance for the engineer who may wish to consider recommending and designing a slow sand filtration system. Being very basic, the book could be used as a text for an undergraduate engineering course. It seems to assume that the reader has no previous knowledge of sand filtration, and starts from there. It is so basic that a non-engineer could understand it and use it to evaluate the advantages of a slow sand filtration system and its design. The authors constantly caution, however, that a professional engineer should conduct the actual design.

The chapters adequately cover background and principles of slow sand filtration, choosing the best system, design of a slow sand filter, pilot plant studies, construction, and operation. An additional chapter is devoted to modifications including pretreatment. The final chapter, Guidelines, is really a condensed summary of all the steps to be followed in choosing, designing, constructing, and operating a slow sand filter.

Each chapter adequately stands on its own. A reader can read only one chapter and fully understand the portion discussed without referring to information in a previous chapter. Unfortunately, for the individual reading the entire book, this results in frequent repetition from chapter to chapter.

The book suffers from the problems common to books in which several authors each write a chapter. Styles vary, and one author repeats what another has written.

The book also contains errors common to most first editions. Some figures lack sufficient identification such as keys to lines and directions of flow. Example 3.5 has several typographical errors in it, and example 3.9 is completely off. There are several instances

of the most common English grammatical error: A number...are. Whereas the use of photographs is encouraged, pictures of an earthen covered filter (Fig. 3.19), a propane tank (Fig. 3.20), and the outside of a chlorination building (Fig. 3.24) add little to the usefulness of the book.

For basic information, the authors rely heavily on two references: Hazen, 1913, and Huisman and Wood 1974. Reviewing their works and incorporating them into this book is useful. However, all the recent studies refer to research conducted by the various authors. Whereas one expects authors to expound on their own work, one gets the impression that the slow sand filtration system at Empire, CO, is the most important modern facility. As a matter of fact, all the system discussed in detail are west of Denver, including Canada. It would be interesting to know if there are any new facilities east of the Rockies.

In this regard, the authors have not even mentioned what was at one time the largest slow sand filtration system in the world. Their historical data, provided by Hazen, 1913, lists only slow sand filtration plants in the United States prior to 1900. In the early 1900s, Philadelphia, PA, had what they claimed was the largest slow sand filtration system in the world. It seems that this could have at least been mentioned for completeness.

This book is useful to an engineer who has little previous knowledge of slow sand filters. It also is useful to individuals in a community who want to consider the use of a slow sand filter as a means of bringing their water supply up to regulations.

Donald B. Aulenbach, Ph.D., P.E., DEE
Environmental Engineering Consultant
Clifton Park, N.Y. 12065

Municipal Waste Incineration Risk Assessment, Contemporary Issues in Risk Analysis, Volume 5 by Curtis C. Travis, Plenum Press, New York, N.Y. (1991) 314 pages [ISBN No: 0-306-44016-4] U.S. List Price: $85.00

Risk assessment of emissions resulting from incineration operations is of significant interest since it evokes immediate public interest. Many communities in the U.S. are weary of having a municipal incinerator in their backyard. In Europe, safe incineration of waste materials has been practiced for many years. Much of the concern in the U.S. is indeed press sensationalism. Scientific literature on this topic abounds. This book is a good compilation of some of the aspects of multimedia exposure from incinerator emissions.

There are 16 chapters in this book with contributions by 33 authors. Some of the chapters have direct relevance to incinerator risk assessments and some others are of general applicability to air pollution in general.

The first five chapters are concerned with dry and wet deposition of particulates and particle-bound contaminants from air. Chapter 1 by Yambert *et al.*, is a discussion of recently developed EPA recommended models. (CSCST and ISCLT) for the influence of complex terrains on pollutant deposition. Chapter 2 by Kapahi is concerned with the process of fine particle deposition, which is an area that presently lacks satisfactory models. Chapter 3 by Campbell *et al.*, is a good review of the various approaches to estimating wet deposition of toxic air pollutants. Not to be outdone, the authors have even devised a new acronym, namely TAPs for toxic atmospheric pollutants. Chapter 4 by Travis and Yambert deals with comparisons of three separate models for dry deposition of particles. Chapter 5 by Bidleman is perhaps the best contribution in this book. It is an excellent review of the methods of determining gas-particle distributions of semi-volatile organic compounds. High-volume and denuder samplers are discussed.

Chapters 6 through 11 deal with food chain accumulation. Dioxin, the most toxic of compounds is a combustion product from municipal solid waste incinerators. Chapter 6 by Hattemer-Frey and Travis discusses a probabilistic risk assessment approach to dioxin exposure. Chapter 7 by Paterson and Mackey is an excellent discussion of the fugacity approach to modelling plant uptake by exposure to hydrophobic chemicals from air and soil. Plant uptake and release kinetics of hydrophobic organic vapors by plant leaves is discussed by Bacci and Clamari in Chapter 8. A model for uptake, translocation, accumulation, and biodegradation of toxic organic chemicals in terrestrial plants is discussed by McFarlane in Chapter 9.

In Chapter 10, Washburn and Kahn elaborate on the uncertainties in estimating chemical degradation and accumulation in the environment and consequent difficulties in assessing risks from incinerator emissions. Chapter 11 by Belcher *et al.*, deals with the uncertainties in the modelling of food chain magnification from exposure to incinerator emissions. Chapter 12 is an assessment of uncertainty for exposure estimates of incinerator emissions through air/milk and air/meat pathways. Chapter 13 by Tyler *et al.*, is a critique of the use of worst case assumption to address uncertainty in estimates of exposure. A stochastic approach to risk analysis is recommended. A case study of health risk assessment due to ambient concentration of toxic compounds is provided by Edgerton *et al.*, in Chapter 14. Chapter 15 by Chambers *et al.*, concerns the EPA proposal for setting risk-based emissions standards for hazardous air pollutants. Chapter 16 by Rao and Brown describes the scientific basis for establishing a health-based dioxin standard in the state of Connecticut.

In conclusion, this book is an excellent collection of articles on multimedia exposure pathways for pollutants resulting from incinerator emissions. This book is recommended for environmental engineers, regulatory personnel, and environmental chemists. The book, however, is costly.

K.T. Valsaraj, Ph.D
Assistant Research Professor
Department of Chemical Engineering
Louisiana State University
Baton Rouge, LA 70803

Software For Preparing Meteorological Data For Industrial Source Complex Models

Ashok Kumar and Madhavan Ranganathan

The Department of Civil Engineering, The University of Toledo, Toledo, OH 43606

Introduction

Meteorological data are vital ingredients for the proper execution of any air quality model. Typically, meteorological data include wind speed, ambient temperature, atmospheric stability, and mixing heights and are obtained from observations at weather stations. The purpose of this paper is to discuss software needed to prepare meteorological data for the execution of the widely used Industrial Source Complex (ISC2) model [*1*]. Utility programs available from the U.S. Environmental Protection Agency (EPA) are capable of preparing most of the data required for the execution of the ISC model. However, during an application of the ISC2 model for demonstrating the compliance of the National Ambient Air Quality Standards (NAAQS) of lead from a plant, it was found that utility programs to prepare monthly and quarterly averages of temperature and mixing height are not public domain. For this purpose, two computer codes were developed and are discussed in this paper.

Industrial Source Complex Model

The U.S. Environmental Protection Agency maintains a "Guideline on Air Quality Models" [*2*] which provides the agency's guidance on regulatory applicability of air quality models in general. Any regulatory application of the model should be carried out in accordance with a modeling protocol that is reviewed and approved by the appropriate agency prior to conducting the modeling. For example, the ISC2 model is recommended for single and/or multiple sources. There are two versions of the ISC2 model namely the ISCLT2 (Industrial Source Complex Long Term) which calculates long-term pollutant concentrations, and ISCST2 (Industrial Source Complex Short Term) which calculates short-term pollutant concentrations produced at a large number of receptors due to emissions from point, area and volume sources.

The two basic types of input needed to run the ISC2 model are: 1) Runstream file setup which consists of selected modeling options, source location/parameter data, receptor locations, meteorological data for specifications and output options, and 2) the meteorological data files themselves.

The current version of the ISC2 models were developed on an IBM-compatible PC using the Microsoft FORTRAN optimizing compiler (version 5.1) [*1*]. A math coprocessor chip is optional but recommended for fast execution. These models have also been uploaded on the EPA's IBM 3090 and the DEC VAX mainframe systems. Execution time is considerably minimized when the mainframe systems are used.

Available Utility Programs

In order to prepare meterological data for the ISC2 models, the following utility programs are essential [*1*]. These programs are:

1) PKUNZIP
2)MET144
3) STAR
4) PCRAMMET
5) BINTOASC

The above listed programs can be downloaded from the EPA's Bulletin Board System [*3*]. The Bulletin Board can also be accessed through INTERNET using the following address:

Telnet TTNBBS.RTPNC.EPA.GOV

At this point it should be noted that STAR is used only for the ISCLT2 and not for the ISCST2. A brief description of each program is provided below.

1) PRUNZIP

PRUNZIP is a dearchiving program that 'unzips' or dearchives files making them fit to be used. The archived files which require this program in order to be dearchived, exist in the *.zip format.

2) MET144

MET144 is an Edit/Expansion utility program that is essential to reformat meteorological data to the required format. It performs two important functions namely;

*Identify all missing data parameters for the entire Surface data file, and

*Restructure the Surface data file to the CD144 format required by PCRAMMET and STAR.

These surface data files are stored in a unique format in the SCRAM BBS.

Parameter	Location (Col #)
NWS Station Number	1-5
Year	6-7
Month	8-9
Day	10-11
Hour	12-13
Ceiling Height	14-16
Wind Direction	17-18
Wind Speed	19-21
Dry Bulb Temperature	22-24
Total Cloud Cover	25-26
Opaque Cloud Cover	27-28

Following is the layout of the surface file in the CD144 format:

Parameter	Location (Col #)
NWS Station Number	1-5
Year	6-7
Month	8-9
Day	10-11
Hour	12-13
Ceiling Height	14-16
Wind Direction	39-40
Wind Speed	41-42
Dry Bulb Temperature	47-49
Total Cloud Cover	56
Opaque Cloud Cover	79

3) STAR

STAR processes the expanded and restructured (CD144 format) surface data file (SFC.DAT) and generates joint frequency distributions of six wind-speeds, sixteen wind directions, and six stability categories for the respective station and time period specified. The output consists of:

* Number of entries for each wind-speed/wind direction category corresponding to each stability class.

* Percent frequency for each wind speed/wind direction category corresponding to each stability class.

STAR can be operated by the following command:

STAR.EXE < TEST.IN SFC.DAT > FILE.OUT OUT.MOD

STAR can be operated by the following command:

STAR.EXE < TEST.IN SFC.DAT > FILE.OUT OUT.MOD

where TEST.IN is the control file which contains only one record.

This executes the test case and sends the result to an external file. The OUT.MOD file contains the STAR summaries. To send the result directly to the printer, the command used is;

STAR.EXE <TEST.IN SFC.DAT> PRN

For the output to appear on the screen, the '>PRN' from the above command must be eliminated.

4) PCRAMMET

The program processes hourly surface meteorological observation data to determine a Pasquill stability class for each hour and interpolates between twice-daily mixing height data (an input card for each day) to obtain a mixing height value for each hour.

PCRAMMET reads two external data files, surface and twice daily mixing height values. The execution time of the program is

reduced considerably if a math coprocessor chip is installed. The program uses the following syntax for execution.

At the prompt type:

PCRAMMET.EXE SFC.DAT MIX.DAT RAM.BIN

where, SFC.DAT is the surface data file, MIX.DAT is the mixing height data file and RAM.BIN is the output file. The output file is in binary format and for conversion to text format, the program PCRAMPRT is used.

At the prompt type:

PCRAMPRT.EXE RAM.BIN > RAM.PRT

This directs output to a file.

5) BINTOASC

BINTOASC converts unformated (binary) meteorological data files generated by PCRAMMET to the default ASCII format, which is required by the ISCST2 model.

New Programs

The two new programs are written in FORTRAN and are called AVTEMP and AVMIX. Both programs read appropriate data from the output file generated by PCRAMPRT. PCRAMPRT is the program that converts the binary output generated by PCRAMMET into text form. AVTEMP and AVMIX are discussed briefly below.

AVTEMP:

AVTEMP reads temperature data for the various stabilities and calculates both monthly and quarterly averages corresponding to each stability. The temperature averages calculated are time-weighted averages based on the number of hours of occurrence of each stability value. These averages are then used by the ISCLT2 model.

AVMIX:

AVMIX reads mixing height values from the same output file as AVTEMP does. This program calculates monthly and quarterly averages for various wind speeds and corresponding stabilities. AVMIX also calculates time-weighted averages. By default, thisprogram reads the urban mixing height values and for rural mixing height values, the appropriate change must be instituted in the source code.

The listings of both these programs can be found in Appendix A.

Procedure for Preparing Meterological Data

There are certain steps to be followed to prepare meteorological data for either the ISCLT2 or the ISCST2 [*4,5*]. These steps are as follows:

Step 1: Access the EPA Bulletin Board System and enter the SCRAM option.

Step 2: Within the SCRAM option, access the option entitled "METEOROLOGICAL DATA".

Step 3: Select the desired option, i.e, surface data or mixing height data.

Step 4: Download the selected file for the desired state (eg., Ohio).

Step 5: The surface air data files exist as archived files as they are voluminous in nature. They are dearchived using the PKUNZIP program.

Step 6: The MET144.EXE program is used to fill in the missing data in the dearchived surface air file. This is further restructured to the CD144 format (text) which is ready to be input into STAR and PCRANMET. It must be noted here that the file in the CD144 format contains all input parameters namely, ceiling height, wind speed, dry bulb temperature and opaque cloud cover.

Step 7: The dearchived Surface air data file cannot be processed by STAR.EXE without the control file. This file contains only one record and it must be constructed in the following layout.

Columns	Contents
1-5	Station number
6-7	Year (2-digits)
8	'1' (output file option)
19-28	Title
29-36	Latitude (xx.xxx)
37-44	Longitude (xx.xxx)
45-47	Central Meridan of zone
48	Model Selection ('2' for ISCLT)
49	Monthly Selection: "o" for yearly; "1" to include monthly selection
50-61	'1' to select month and "0" for month not used

Once this is achieved, the STAR program is then used to develop the stability windrose which is required exclusively by the ISCLT.

Step 8: Before the expanded (CD144 format) surface air and mixing height data files are input into PCRAMMET, the mixing height data file needs to be refurbished. This data file is opened using a text editor. The first record must be the control card and is to be created. The following layout defines the format of this record.

Parameter	Location (column
Surface Station #	1-5
Year	6-7
Latitude	13-18
Longitude	22-28
Time Zone	30

The second record in this file must be the last record of the previous year and has got to be inserted. From the third record onwards starts the data for the present year. Again, the last record in this file must be the first data record (and not the control card of the next year) of the succeeding year and this too has got to be inserted.

The following layout describes the mixing height cards which are the remaining records in the file.

Parameter	Location (Col #)
Station number	1-5
Year	6-7
Month	8-9
Day	10-11
AM Type	12
Blank	13
AM Mixing Value	14-17
AM Mixing Depth Wind Speed	18-21
AM Surface Wind Speed	22-25
Blank	26-29
PM Mixing Value	32-35
PM Mixing Depth Wind Speed	36-39
PM Surface Wind Speed	40-43

Once these processes have been performed, the mixing height data file along with the surface data file is input to PCRAMMET.

Step 9: The output of PCRANMET is then converted to text form by executing PCRAMPRT. The PCRAMMET output is also converted to the default ASCII format by running BINTOASC which is the format required by ISCST2.

Step 10: Run the new programs AVTEMP and AVMIX which read the required data from the output generated by PCRANPRT and calculate monthly and quarterly averages of temperatures and mixing heights.

Step 11: Use the values obtained of average temperature and average mixing height from the output of AVTEMP and AVMIX as input for the ISCLT2 model.

An overview of this procedure is provided in the form of a flowchart in Figure 1.

Conclusions

Appropriate meteorological data are very important for the successful application of air dispersion models. This paper presents a procedure to obtain best available data to run the Industrial Source Complex models. Two new programs are provided for the use of readers. It is hoped this information will be helpful for industrial work.

References

1. U.S. EPA, "User's Guide for the Industrial Source Complex (ISC2) Dispersion Models", U.S. Environmental Protection Agency, Office of Air Quality Planning and Standards, Research Triangle Park, N.C., March 1992.
2. U.S. EPA, "Guideline on Air Quality Models (Revised) Supplement A (1987) and Supplement B (1993)" EPA 450/2-78-027R, U.S. EPA, 1986.
3. Kumar, A. and Mohan, S., "Use of Bulletin Board System for Air Quality Modeling," Vol. 10, No. 1, pp. F8-F11, *Environmental Progress*, 1991.
4. "Lee, R., "Preparing Meteorological Data for ISCLT2 and Other Long-term Models", SCRAM News (U.S. EPA), Vol. 4, No. 2, Summer 1993.
5. Lee, R.,"Preparing Meteorological Data for ISCST2", SCRAM News (U.S. EPA), Vol. 3, No. 2, Summer 1992.

Figure 1:
Flowchart for Preparing Meteorological Data for ISC2 Model

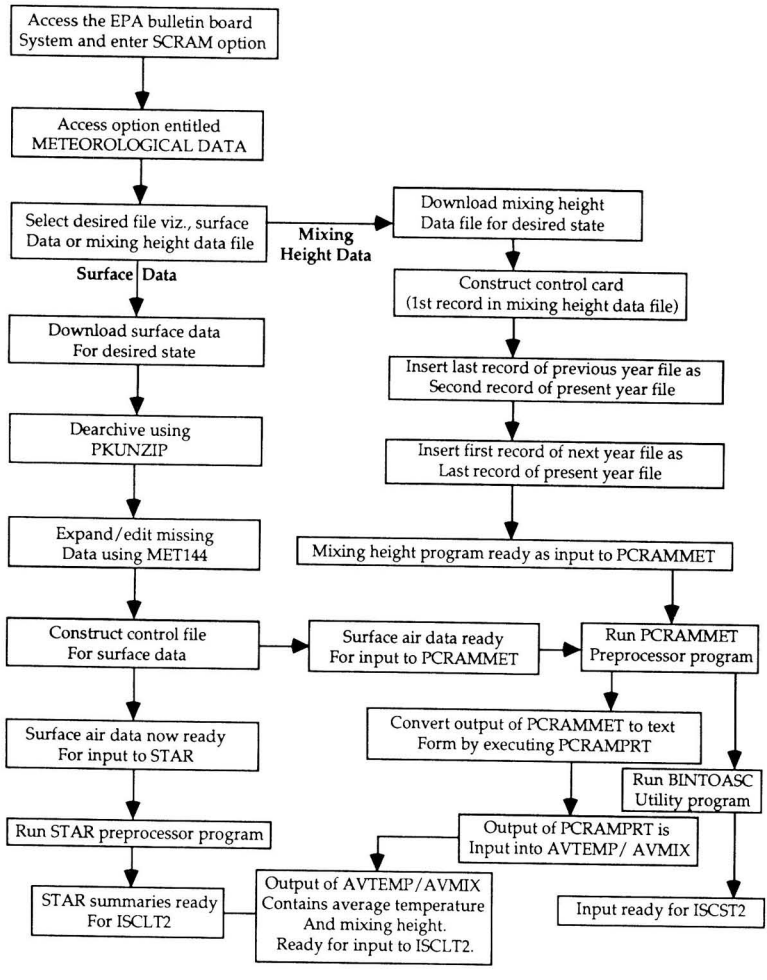

```
C     ***********************************************************************
C                                AVTEMP
C
C       This program calculates monthly and quarterly averages of
C     temperature—It reads data from the output file of PCRAMPRT.
C     Please refer to the paper for a detailed procedure.
C
C     Authors: Ashok Kumar & Madhavan Ranganathan
C     Incept Date: 10/01/93. (Ver. 1.01)
C     ***********************************************************************
C       Dimensions of parameters to be read from the output file obtained
C     by executing PCRAMPRT.
C     ***********************************************************************
      DIMENSION KST(24),SPEED(24),TEMP(24),AFV(24),FVR(24),HLH(2,24)
      DIMENSION ATEMP(6,12),ICNT(6,12),TKST(6)
      CHARACTER *12 NAME,NAME1
      WRITE(6,*)'NAME OF INPUT DATA FILE : '
      READ(6,5)NAME
      WRITE(6,*)'NAME OF OUTPUT DATA FILE : '
      READ(6,5)NAME1
5     FORMAT(A12)
      OPEN(UNIT=15,FILE=NAME,STATUS='OLD')
      OPEN(UNIT=16,FILE=NAME1)
      IMOC=1
      IMOC1=1
      CALL TEMPINI(TKST)
      READ(15,101)ISS,ISY,IUS,IUY
      WRITE(16,100)ISS,ISY,IUS,IUY
C     ***********************************************************************
C     KST: Stability, TEMP: Temperature, AFV: Average Flow Vector
C     FVR: Random Flow Vector
C     ***********************************************************************
10    READ(15,201)IYEAR,IMONTH,DAY1,KST,SPEED,TEMP,AFV,FVR,
     *((HLH(J,L),L=1,24),J=1,2)
100   FORMAT(1X,I5,2X,I2,2X,I5,2X,I2)
101   FORMAT(I5,2X,I2,2X,I5,2X,I2)
201   FORMAT(4X,I2,5X,I2,6X,F4.0///
     *7X,I3,11I5/,7X,I3,11I5/
     *5X,12F5.1/5X,12F5.1/6X,12F5.0/6X,12F5.0/
     *6X,12F5.0/6X,12F5.0/
     *6X,12F5.0/6X,12F5.0/
     *6X,12F6.0/6X,12F6.0/6X,12F6.0/6X,
     *12F6.0/)
      IF (IMOC .NE. IMONTH) GOTO 1005
1010  DO 1000 II=1,6
      DO 1001 I=1,24
      IF(KST(I) .EQ. II)TKST(II)=TKST(II)+TEMP(I)
      IF(KST(I) .EQ. II)ICNT(II,IMOC)=ICNT(II,IMOC)+1
1001  CONTINUE
1000  CONTINUE
      IMOC=IMONTH
      IF (DAY1 .EQ. 365) GOTO 1005
      GOTO 10
1005  DO 3005 JJ=1,6
      ATEMP(JJ,IMOC)=0.
      IF(ICNT(JJ,IMOC) .EQ. 0) GOTO 3005
      ATEMP(JJ,IMOC)=TKST(JJ)/FLOAT(ICNT(JJ,IMOC))
      IF(FLOAT(ICNT(JJ,IMOC)) .EQ. 0)ATEMP(JJ,IMOC)=0
3005  CONTINUE
      DO 1020 J=1,6
```

```
      WRITE(16,4001)J,IMOC,ATEMP(J,IMOC),ICNT(J,IMOC)
4001  FORMAT(1X,'STBLTY',I2,'      AVG MTHLY',I2,'=',F7.3,'   HRS=',I4)
1020  CONTINUE
      WRITE(16,4002)
4002  FORMAT(//)
      IF ((IMOC .EQ. 12).AND.(DAY1 .EQ. 365)) GOTO 998
      CALL TEMPINI(TKST)
      IMOC=IMONTH
      GOTO 1010
998   DO 7001 I=1,6
      IC=0
      DO 7002 J=1,4
      SUM=0.
      JC=0
      DO 7003 JJ=1,3
      IC=IC+1
      SUM=SUM+ATEMP(I,IC)*ICNT(I,IC)
7003  JC=JC+ICNT(I,IC)
      SUM=SUM/FLOAT(JC)
      WRITE(16,4003)I,J,SUM
4003  FORMAT(1X,'STAB',I1,'  AQT',I2,'=',F12.3)
7002  CONTINUE
7001  CONTINUE
      CLOSE(15)
      CLOSE(16)
999   STOP
      END
C     SUBROUTINE TO BE CALLED IN THE PROGRAM
      SUBROUTINE TEMPINI(TKST)
      DIMENSION TKST(6)
      DO 3000 I=1,6
      TKST(I)=0.
3000  CONTINUE
      RETURN
      END
```

```
C     ***********************************************************************
C                                    AVMIX
C
C       This program calculates monthly and quarterly averages of mixing
C     heights. It reads data from the output file of PCRAMPRT. Please refer
C     to paper for detailed procedure.
C
C     Authors: Ashok Kumar & Madhavan Ranganathan
C     Incept Date: 10/01/93. (Ver. 1.01)
C     ***********************************************************************
C       Dimensions of parameters to be read from the output file obtained by
C     executing PCRAMPRT.
C     ***********************************************************************
      DIMENSION KST(24),SPEED(24),TEMP(24),AFV(24),FVR(24),HLH(2,24)
      DIMENSION ATEMP(12,6,6),ICNT(6,6,12),TKST(6,6),RSPEED(6,2)
C     ***********************************************************************
C       The program reads Urban values of mixing height data by default.
C     If Rural values are desired, the attribute HLH(2,24) must be replaced
C     by HLH(1,24) in the program.
C     ***********************************************************************
      CHARACTER *12 NAME,NAME1
      WRITE(6,*)'NAME OF INPUT DATA FILE : '
      READ(6,5)NAME
      WRITE(6,*)'NAME OF OUTPUT DATA FILE : '
      READ(6,5)NAME1
5     FORMAT(A12)
      OPEN(UNIT=15,FILE=NAME,STATUS='OLD')
      OPEN(UNIT=16,FILE=NAME1)
C     ***********************************************************************
C     Specification of wind speed ranges for STAR summaries.
C     ***********************************************************************
      RSPEED(1,1)=1.
      RSPEED(1,2)=3.
      RSPEED(2,1)=4.
      RSPEED(2,2)=7.
      RSPEED(3,1)=8.
      RSPEED(3,2)=12.
      RSPEED(4,1)=13.
      RSPEED(4,2)=18.
      RSPEED(5,1)=19.
      RSPEED(5,2)=24.
      RSPEED(6,1)=24.000001
      RSPEED(6,2)=100000.0
      IMOC=1
      CALL TEMPINI(TKST)
      READ(15,101)ISS,ISY,IUS,IUY
      WRITE(16,100)ISS,ISY,IUS,IUY
C     ***********************************************************************
C     KST: Stability, TEMP: Temperature, AFV: Average Flow Vector
C     FVR: Random Flow Vector
C     ***********************************************************************
10    READ(15,201)IYEAR,IMONTH,DAY1,KST,SPEED,TEMP,AFV,FVR,
     *((HLH(J,L),L=1,24),J=1,2)
100   FORMAT(1X,I5,2X,I2,2X,I5,2X,I2)
101   FORMAT(I5,2X,I2,2X,I5,2X,I2)
201   FORMAT(4X,I2,5X,I2,6X,F4.0///
     *7X,I3,11I5/,7X,I3,11I5/
     *5X,12F5.1/5X,12F5.1/6X,12F5.0/6X,12F5.0/
     *6X,12F5.0/6X,12F5.0/
     *6X,12F5.0/6X,12F5.0/
```

```
     *6X,12F6.0/6X,12F6.0/6X,12F6.0/6X,
     *12F6.0/)
      IF (IMOC .NE. IMONTH) GOTO 1005
1010  DO 1000 III=1,6
      DO 1001 II=1,6
      ICOUNT=0
      DO 1002 I=1,24
      IF(KST(I) .NE. III) GOTO 1002
      ICOUNT=ICOUNT+1
      IF((SPEED(I).GE.RSPEED(II,1)).AND.(SPEED(I).LE.RSPEED(II,2)))
     *TKST(III,II)=TKST(III,II)+HLH(1,I)
      IF((SPEED(I).GE.RSPEED(II,1)).AND.(SPEED(I).LE.RSPEED(II,2)))
     *ICNT(III,II,imoc)=ICNT(III,II,imoc)+1
1002  CONTINUE
      IF (ICOUNT .EQ.0) GOTO 1000
1001  CONTINUE
1000  CONTINUE
      IMOC=IMONTH
      IF (DAY1 .EQ. 365) GOTO 1005
      GOTO 10
1005  DO 3005 JJ=1,6
      DO 3006 JJJ=1,6
      ATEMP(IMOC,JJ,JJJ)=0.
      IF(ICNT(JJ,JJJ,imoc) .EQ. 0) GOTO 3007
      ATEMP(IMOC,JJ,JJJ)=TKST(JJ,JJJ)/FLOAT(ICNT(JJ,JJJ,imoc))
      WRITE(16,4001)JJ,RSPEED(JJJ,1),RSPEED(JJJ,2),IMOC,
     *ATEMP(IMOC,JJ,JJJ),ICNT(JJ,JJJ,imoc)
      GOTO 3006
3007  ATEMP(IMOC,JJ,JJJ)=0.
3006  CONTINUE
4001  FORMAT(1X,'STAB',I2,' SPRL',F4.1,'  SPRU',F4.1,'   AVG MTHLY',
     *I2,'=',F12.3,'   HRS=',I4)
3005   CONTINUE
      WRITE(16,4002)
4002  FORMAT(//)
      IF ((IMOC .EQ. 12).AND.(DAY1 .EQ. 365)) GOTO 998
      CALL TEMPINI(TKST)
      IMOC=IMONTH
      GOTO 1010
998   DO 7001 I=1,6
      DO 7002 J=1,6
      IC=0.
      DO 7003 KK=1,4
      SUM=0.
      JC=0
      DO 7004 K=1,3
      IC=IC+1
      JC=JC+ICNT(I,J,IC)
7004  SUM=SUM+ATEMP(IC,I,J)*ICNT(I,J,IC)
      SUM=SUM/FLOAT(JC)
      WRITE(16,4007)I,RSPEED(J,1),RSPEED(J,2),KK,SUM
4007  FORMAT(1X,'STAB',I1,'  SPRL',F4.1,'  SPRU',F4.1,'AQT',I1,
     *'=',F12.3)
7003  CONTINUE
7002  CONTINUE
7001  CONTINUE
      CLOSE(15)
      CLOSE(16)
999   STOP
      END

      SUBROUTINE TEMPINI(TKST)
      DIMENSION TKST(6,6)
      DO 3000 I=1,6
      DO 3000 II=1,6
      TKST(I,II)=0.
3000  CONTINUE
      RETURN
      END
```

The Use of a Secondary Catalyst Bed to Increase Incinerator Destruction Efficiency

Jeff Erb

IBM Inc., 11400 Burnet Road, Austin, TX 78758

Many incinerators in Texas and the USA are required to achieve 95-99% destruction efficiency. Over time incinerator efficiency may drop due to leaks developing in older equipment, resulting in bypass of catalyst beds or heat exchangers. The use of an additional catalyst bed on the incinerator exhaust stack is an economical way to boost the efficiency back to acceptable levels. The secondary catalyst bed is also efficient in converting CO to CO2 and oxidizing other products of incomplete combustion (PICs).

Following is a case history of a 12 year old incinerator at IBM-Austin which was retrofitted with a secondary catalyst bed and successfully achieved 99% destruction in VOCs and reduction in PICs by an order of magnitude.

BACKGROUND

A 5000 cfm fluidized bed catalytic incinerator was installed at IBM-Austin in 1980 to abate the exhaust from a "treater tower" which manufactures epoxy/fiberglass cloth used as the dielectric in printed circuit boards. The treater tower is a large oven in which approximately 150 lb/hr of a solvent mixture of Methyl Ethyl Ketone (MEK) and a Glycol Ether (GE) are evaporated from epoxy impregnated fiberglass cloth. The Texas Air Control Board (TACB) permit requires 99% destruction efficiency at peak inlet loading and sets maximum hourly and yearly mass emission rates for the incinerator.

Emissions from the incinerator are continuously monitored by three different devices: a Flame Ionization Detector (FID), a Mass Spectrometer (MS), and non-dispersive Infrared (IR) monitor. Articles analyzing the operation of the FID and MS have previously been published [*1*, *2*, *3*].

A Beckman Industrial™ Model 400A FID continuously monitors for total MEK/GE. The FID cannot speciate between chemicals and gives an emission rate relative to a known calibration standard. The FID is insensitive to some small oxygenated carbon compounds such as carbon monoxide (CO) and formaldehyde (HCOH) and gives little or no response to these chemicals.

A Perkin Elmer ICAMS™ mass spectrometer (MS) is used to analyze the exhaust about once each hour for MEK, GE, and several possible PICs: formaldehyde, isopropyl alcohol, methanol and acetone. PICs are measured by the MS but are at a concentration that is too low to measure accurately with the MS without significantly slowing down the cycle time of the unit to a point where it would no longer be useful as an on-line analyzing device. Therefore measurements of the PICs with the MS are more a qualitative measurement of the relative concentration of all PICs as opposed to a quantitative measurement of each individual PIC. The MS like the FID cannot measure carbon monoxide. Carbon monoxide in the incinerator exhaust stack is continuously measured by a Horiba VIA-500™ non-dispersive IR analyzer.

The fluidized bed incinerator is pictured in Figure 1. Exhaust from the treater tower passed through a pre-heat heat exchanger where the exhaust from the incinerator was used to

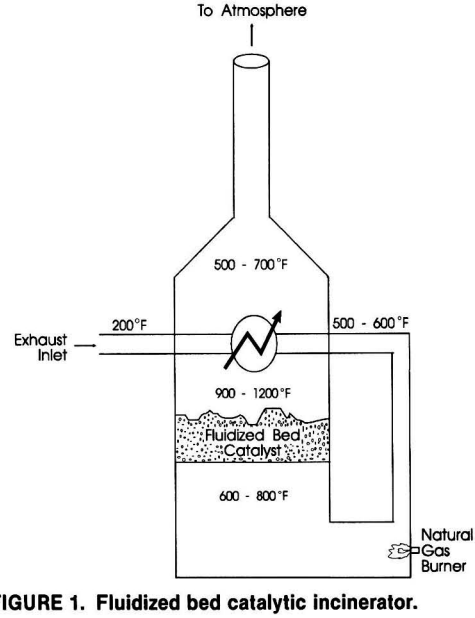

FIGURE 1. Fluidized bed catalytic incinerator.

heat the incoming process air from 100°C to 300°C. Next a natural gas burner is used to raise the temperature below the bed to 300–450°C. Then the gas passes through the catalyst bed where combustion of the solvents raises the gas temperature to 500–650°C. The exhaust then passed on the outside of the shell and tube heat exchanger and then through the exhaust stack to atmosphere at 250–400°C.

CONVERSION FROM FLUIDIZED BED TO THERMAL OPERATION

The fluidized bed incinerator with a chromium trioxide based catalyst performed satisfactorily for several years but eventually developed a leak around the catalyst bed resulting in deteriorating performance. The incinerator was constructed of carbon steel with two inner linings of refractory. The first lining next to the steel was 2″ of a relatively soft fire brick and the second lining was 6″ of a hard cast refractory. Over time, cracks developed in the hard cast refractory and the inner fire-brick eroded, allowing a short circuiting of the process gas through the wall and around the catalyst bed, resulting in a drop in overall efficiency. Instead of repairing the refractory which would have involved a complete rip out and new installation of the catalyst and refractory, it was decided to convert the incinerator to thermal operation in January 1988.

The incinerator was designed to operate at a maximum of 730°C (1350°F). At this temperature, 99% destruction of the incoming solvents was achieved and both hourly and yearly mass emission limits were readily obtained; however, the combustion of MEK/GE to CO2 was incomplete and a relatively large emission of CO resulted. The CO concentration was due to the relatively low combustion temperature and not to a lack of oxygen. There was a large excess of oxygen due to the nature of the exhaust stream since for safety reasons the LEL of the exhaust was kept below 50%. The oxygen in the exhaust stream dropped from 20% in the inlet to about 19% in the exhaust of the incinerator. Short term tests on the incinerator showed the concentration of CO could be significantly reduced if the incinerator was operated at 800°C (1475°F); however, the materials of construction of the incinerator could not withstand this high temperature over a long time period without destroying the incinerator. Other than carbon monoxide, products of incomplete combustion were at an acceptable level (Table 1).

Because of the high carbon monoxide emissions, it was decided to convert the incinerator back to catalytic operation. The chrome based fluidized bed catalyst had much lower CO emissions than the 730°C thermal operation but still had a significant CO emission. Noble metal catalysts are very efficient at oxidizing CO at low temperatures [4]. Converting the incinerator to a fixed bed noble metal catalytic incinerator would reduce carbon monoxide emissions to a very low level.

CATALYTIC OPERATION

In April 1991 an Allied Signal PURZAUST™ honeycomb fixed catalyst bed was installed in the same location as the original fluidized bed. Initial carbon monoxide emission results were very good. CO emissions were reduced by over 90%; however, MEK emissions increased by almost a factor of three (see Table 1).

Using an FID, it was determined that VOC concentrations were low immediately above the catalyst bed but concentrations were high in the exhaust stack. This indicated that the catalyst was performing satisfactorily but that the pre-heat heat exchanger was probably leaking incoming air directly to the exhaust stack.

The heat exchanger was taken apart and all the tubes were checked for leaks by pressure test. No leaking tubes were found. Several bolts which sealed the heat exchanger to the incinerator were found to have broken and a 1/8″ short circuiting gap existed. All bolts were replaced and the unit was reassembled and regasketed to eliminate the gap. After this repair the incinerator efficiency increased significantly—FID readings and CO emissions were both decreased by 40%. However, MEK emissions were still not satisfactory. The hourly MEK emission limit set by the Texas Air Control Board (TACB) could be met but the yearly emission rate would not allow for full capacity operation for an entire year. Also MS data indicated VOC PICs were at higher concentrations than in the thermal mode.

Replacing the heat exchanger would be very expensive—a replacement shell and tube heat exchanger cost $100K not including installation costs. Also there was no guarantee that the new heat exchanger would not leak just as badly at the sheet ends. To re-engineer this connection point in the existing incinerator would be very expensive.

It was also possible that a significant portion of the leak could be from bypassing of the catalyst bed. The catalyst bed was installed directly to the steel frame of the incinerator (refractory was removed and the catalyst frame was welded in place) so bypassing through the refractory was not possible. However each individual catalyst frame was gasketed into a catalyst cell and leaking was possible at these locations. Because of the laminar flow through the catalyst cells it would be

Table 1 Relative Incinerator Mass Emissions

Species	Thermal Operation 1350 F (730 C)	Catalytic Operation at Start Up	Catalytic Operation After Heat Exchanger "Repair"	Catalyst Operation W/Secondary Catalyst Bed
MEK	0.53	2.34	2.11	0.16
GE	0.33	0.10	0.08	0.00
MEK/GE	0.86	2.44	2.19	0.16
Formaldehyde	0.05		0.10	0.13
IPA	0.04		0.93	0.08
Methanol	0.04		2.18	0.00
Acetone	0.03		0.00	0.00
Total PICs	0.16		3.21	0.21
CO	8.74	0.56	0.32	0.00
Total Emissions	9.76		5.72	0.37
FID	0.64	2.69	1.54	0.29

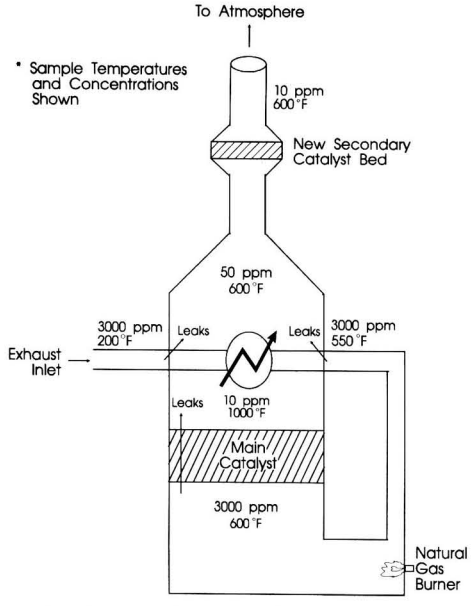

FIGURE 2. Fixed bed catalytic incinerator.

difficult to find a leak. The incinerator was sampled at 10 different points about two feet above the catalyst and no leak was found; however, to be certain no leaking was taking place would require sampling at hundreds of sample points because of the laminar flow. Each movement of the FID sample point required a shutdown of the incinerator and repositioning of a stainless steel sample tube in the incinerator. The above bed temperature in the incinerator was 590°C (1100°F) during operation so it was possible the stainless steel sample tubing could act as a catalyst for MEK/GE combustion, hiding a leak in the catalyst bed by combusting the solvent before it reached the FID for measurement.

SECONDARY CATALYST BED

Because of the expense and uncertainty of success of finding and correcting the suspected bypassing problem, a new approach was taken. A small secondary catalyst bed was installed in the exhaust stack (Figure 2). The heat exchanger was rated for only 42% efficiency. This meant a fairly high exhaust stack temperature—anywhere from 260 to 370°C (500 to 700°F), depending on solvent loading from the manufacturing area. Thus the catalyst would be effective in the stack without adding an additional burner or other source of heat.

The secondary catalyst bed was installed in the incinerator exhaust stack in November 1991. The catalyst was Allied Signal PZM 12981™, a low pressure drop honeycomb noble metal catalyst. This catalyst bed was approximately one-fourth the size of the main bed and the installed cost was also one-fourth the cost—$20,000 compared to $80,000.

From Table 1 it can be seen that the secondary catalyst bed significantly reduced emissions of both VOCs and CO. MEK and GE emissions were reduced 80% from the original thermal operation and were reduced by 93% from the single catalyst bed operation. VOC PICs were increased by 30% from the thermal mode but at the low concentrations in both modes there is a high degree of inaccuracy of using the on line mass spectrometer as a means of measurement. Carbon monoxide was reduced 100% and is no longer at measurable levels on the existing CO monitor (50 ppm full scale).

CONCLUSIONS

A method was described for achieving greater than 99% VOC destruction efficiency in an incinerator in which fumes are by-passing the main catalyst bed due to leaks through the catalyst bed or the primary heat exchanger. A small secondary catalyst bed was installed in the incinerator exhaust stack to destroy VOCs which bypassed the main catalyst bed and PICs which were created because of the leaks. The secondary catalyst was an inexpensive method (around $20K) to reduce the emissions due to the leaks within the incinerator. MEK/GE emissions were reduced by over 90%, VOC PICs were reduced by over 90% and CO was reduced by virtually 100%.

This secondary catalyst bed should have application anywhere an incinerator is not performing satisfactorily due to by-passing of a catalyst bed or heat exchanger or PIC formation due to thermal operation at too low a temperature and where the stack temperature is above 260°C (500°F).

The use of an additional catalyst bed on the incinerator exhaust stack is an economical way to boost the efficiency which has been lost due to leaks developing in older equipment. The secondary catalyst bed is also very efficient in converting CO to CO2 and oxidizing other PICs.

LITERATURE CITED

1. Erb, A. J., E. Ortiz and G. Woodside, "On-Line Characterization of Stack Emissions," *Chemical Engineering Progress*, **86**(5), pp. 40–45 (1989).
2. Bauer, C. L., A. J. Erb, and G. Woodside, "A Comparison of Methods for Monitoring Industrial Emissions," paper presented at Air and Waste Management 83rd Annual Meeting, June 24–29, Pittsburgh, PA (1990).
3. Erb, A. J., and G. Woodside, "Air Emissions Monitoring Using an On-Line Mass Spectrometer: A Performance Evaluation," *Semiconductor Safety Association Journal*, **5**(4), pp. 27–33 (1991).
4. Herbert, K. J., "Catalysts for Volatile Organic Compound Control in the 1990's," paper presented at the 1990 Incineration Conference, San Diego, CA (May 1990).

Use of Sedimentation Ponds for Removal of Metals from Ash Transport Waters

Kathleen M. Lagnese
Chester Environmental, P.O. Box 15851, Pittsburgh, PA 15244

David A. Dzombak
Department of Civil Engineering, Carnegie Mellon University, Pittsburgh, PA 15213

This study investigated the feasibility of using existing ash sedimentation ponds at coal-fired power plants as treatment reactors to reduce concentrations of metals in bottom ash and fly ash transport waters by precipitation and/or adsorption onto iron oxyhydroxide. Intrapond treatment offers economic advantages over construction of a plant for treatment of ash pond effluent. Bench-scale experiments were conducted with bottom ash and fly ash suspensions to investigate pH control and removals of aluminum, manganese, and arsenic under different chemical conditions, including addition of ferric chloride to promote adsoption on iron oxyhydroxide. The effects of pH and iron addition on ash-water partitioning of the metals of interest were studied via batch experiments. In addition, the ability to control pH and promote removal of manganese in an intrapond treatment process was investigated using semi-continuous, bench-scale, pond-simulation reactors. Results of the reactor experiments indicated that the pH could be maintained in range of 8 to 8.5 by dosing the influent with the proper amount of base as determined by batch titration, and that by doing so the influent manganese concentration of 2 ppm could be consistently lowered to less than 0.2 ppm. The effects of accumulation of settled ash were examined in the reactor studies and with the use of a coupled hydraulic/sedimentation model for ash ponds. Overall, results of this study suggest that concentrations of most metals of interest in ash pond water can be kept low with control of pH, in situ precipitation of iron oxyhydroxide, and effective sedimentation of particles. Further examination of the intrapond treatment approach is warranted.

INTRODUCTION

Over the past 15 years, the electric power industry has been researching means of removing trace elements from large volume wastewater flows, especially ash transport waters associated with coal-fired power plants. Of particular concern has been effluent from the sedimentation ponds that are widely used at such plants to settle ash particles from fly ash and bottom ash transport streams. The effluent sluicing water contains a variety of dissolved chemical species, primarily inorganic, derived from leaching of the bottom ash and fly ash and sometimes from addition of plant liquid wastes to the sluice stream. The chemical species of most concern in sluice waters are metal cations such as Al^{3+}, Cd^{2+}, and Ni^{2+}, and metal oxyanions such as AsO_4^{3-}, SeO_4^{2-}, and MoO_4^{2-} [*1*, *2*]. Ash pond effluent is usually discharged into a stream or lake, though in some plants a portion or all of the sluice water is recycled.

A number of research studies have examined the fate and transport of inorganic species in ash ponds [*3–7*]. These studies included investigation of hydraulics and chemistry of ash ponds, and means by which pond operation can be modified to achieve optimum removal of the inorganic species most often occurring as contaminants defined by regulatory agencies. Adsorption onto ash particles and added iron oxyhydroxide ($Fe(OH)_3(s)$) has been investigated as a means of removing inorganic cations and anions from ash suspensions. Subsequent engineering studies have focused on adsorption treatment of pond effluents using iron oxide and conventional treatment process hardware [*2*, *8*, *9*]. However, the use of the ash sedimentation ponds as treatment reactors has also been identified as a potentially feasible and more cost effective treatment alternative [*2*, *6*, *8*]. Detailed studies of the intrapond treatment approach heretofore have not been performed because of various uncertainties associated with the method.

The purpose of this study was to investigate the feasibility of intrapond treatment for metal removal in ash pond applications. Ash samples and operational data from actual bottom ash and fly ash sedimentation ponds at the Duquesne Light Company Cheswick Power Station (Springdale, Pennsylvania) were utilized in the study which included experiments and process modeling. Batch and continuous-flow bench-scale ex-

periments were performed to investigate pH control and removals of several metal cations and anions by precipitation and adsorption. A physical-chemical model for ash pond performance was utilized to help investigate design and operational approaches for optimum performance of an intrapond treatment system. Results of the study are presented in greater detail by Lagnese [*10*].

BACKGROUND

The feasibility of removing metals from ash transport waters by adsorption/coprecipitation with ash and/or iron oxyhydroxide has been the subject of several studies. This research has spanned from laboratory studies of fundamental mechanisms [*3–7*] to the development and field operation of a pilot-scale processing unit [*2, 8, 9, 11, 12*]. In addition, mathematical models have been developed to describe the hydraulics, solid settling, and adsorption/precipitation chemistry associated with ash ponds [*3, 6, 7*]. The results from these various projects formed the framework for this study.

Precipitation and Adsorption

Removal of metals in ash ponds or in iron coprecipitation treatment of ash pond effluents is achieved primarily by precipitation and adsorption. Both precipitation and adsorption involve a transfer of dissolved components from the aqueous phase to a solid phase. Metal oxides are the solid adsorbents of interest in ash ponds and in the iron coprecipitation process. The latter involves precipitation of iron oxyhydroxide which has a high affinity to adsorb dissolved ionic constituents.

The predominant method of metal removal typically employed in wastewater treatment processes is precipitation by addition of lime or sodium hydroxide, with separation of the resulting solids by sedimentation [*13, 14*]. This process exploits the tendency of most metals to form hydroxide and/or carbonate precipitates at higher pH values in aqueous systems. For precipitation of metal hydroxides, as pH is increased a minimum in solubility is observed at some point above neutral pH. Precipitation treatment can be effective but has several limitations. First, some metals are sufficiently soluble that dissolved concentrations are undesirably large even after precipitation and establishment of equilibrium conditions. Another limitation of the process is that it is difficult to maximize removal of several metals simultaneously because the optimum pH, i.e., the pH of minimum solubility, varies from metal to metal.

Removal of metals from the aqueous phase can also occur by adsorption onto a solid which has a reactive surface. In ash ponds and in the iron coprecipitation process, hydrous metal oxides act as adsorbents. These solids possess a hydroxylated surface which provides highly-reactive sites capable of interaction with dissolved species [*15*]. Because of their hydroxylated surfaces, metal oxides in water exhibit amphoteric behavior, i.e., they can both accept and donate protons. Thus, metal oxides serve as pH buffers in aqueous systems.

In addition to protonation and deprotonation reactions, the surface sites on an oxide particle can also adsorb other ions via surface complexation. Interactions between the surface sites and dissolved cations or anions depend on the solution characteristics, most importantly pH.

For metals that exist as cations in solution, 0% to 100% adsorption occurs over a narrow pH range of 1 to 2 pH units. This phenomenon is commonly described with an "adsorption edge," as illustrated in Figure 1. Previous work has also shown that, at a given pH, as the adsorbate/adsorbent ratio is increased, the fraction sorbed decreases [*16*]. This indicates that as available surface sites associated with a solid become occupied, the affinity of the solid for the adsorbate decreases

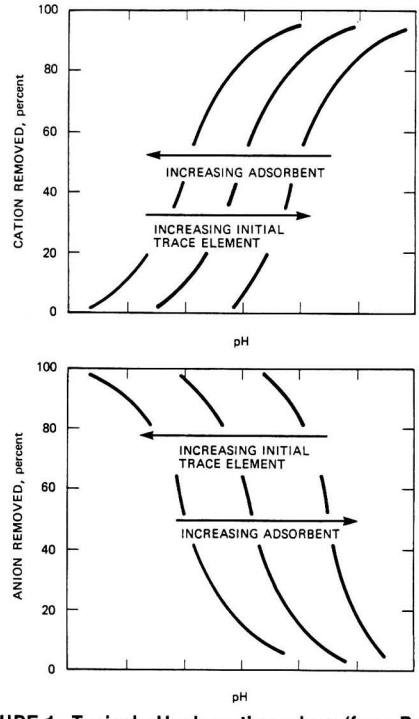

FIGURE 1. Typical pH-adsorption edges (from Ref. [*8*])

(shift from strong to weak binding sites). Figure 1 shows that, as a result, the adsorption edges for cations shift to higher pH values as the adsorbate/adsorbent ratio is increased.

Anion adsorption on hydrous oxides is greatest at low pH and decreases as the pH increases. Thus, adsorption of anions is often called the "mirror image" of cation adsorption, though the adsorption edges for anions are not as steep as those for cations. Figure 1 shows that 0% to 100% adsorption of anions occurs over a pH range of typically 3–4 pH units. At a given pH, an increase in the adsorbate/adsorbent ratio results in a lower fraction of anion being adsorbed, as evidenced by the shift in the adsorption edge to lower pH and the concurrent flattening of the curves shown in Figure 1. Therefore, similar to cation adsorption, anion adsorption also depends on both pH and the amount of solid adsorbent present in the system.

In addition to the solution pH and adsorbate/adsorbent ratio, the adsorption of trace metals onto metal oxides can also be affected by other factors, including competing adsorbates and complexation reactions in solution [*15*]. The degree of competition for surface sites depends on both the relative concentrations and the relative potentials for adsorption of the ions, as well as the solution pH.

Use of Iron Oxyhydroxide for Adsorptive Removal of Metals

Much of the research on trace element removal from ash transport waters has focused on the use of adsorption/coprecipitation with iron oxyhydroxide. Iron oxyhydroxide is an amorphous precipitate that forms when a ferric iron salt such as ferric chloride is added to water:

$$FeCl_3 + 3\ H_2O = Fe(OH)_3(s) + 3\ Cl^- + 3\ H^+$$

Research sponsored by the Electric Power Research Institute (EPRI) on iron coprecipitation has progressed through three

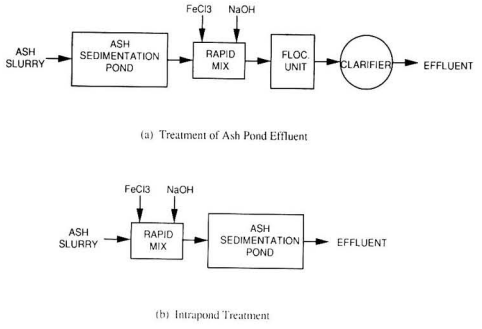

FIGURE 2. Different process schemes for iron coprecipitation treatment of ash pond water

main phases. The first phase was a laboratory study of the fundamental mechanisms associated with adsorption which identified the effectiveness of iron oxyhydroxide as an adsorbent [*3*, *4*]. This led to the second phase of the work, an engineering evalution of the feasibility for applying adsorption/coprecipitation technology to actual wastewater streams [*2*]. Based on the results of the first two phases, a pilot-scale treatment process was developed and tested under different field conditions [*8*, *9*, *11*, *12*].

In the engineering feasibility study [*2*], technical and economic aspects of treating ash pond effluents by coprecipitation with iron oxyhydroxide were evaluated. Results from this investigation, which included bench-scale treatability tests, indicated that the iron coprecipitation process can achieve removal of elements of interest (e.g., arsenic and selenium) from ash pond effluent. It was also concluded that iron coprecipitation would be more cost effective than metal precipitation induced by lime or soda ash addition. Subsequent field and engineering studies [*8*, *9*, *11*, *12*] have focused on implementation of iron coprecipitation in a "back end" process for treatment of ash pond effluent (Figure 2a).

A potentially lower-cost alternative for removal of metals from ash transport waters via iron coprecipitation is treatment in the existing ash pond. For this option, base and an iron(III) salt would be added directly to the influent ash slurry and the precipitated iron oxyhydroxide would settle in the pond along with the ash (Figure 2b). This "intrapond" treatment option offers several advantages over a back-end treatment system that would employ conventional treatment equipment. These advantages include: lower cost, minimal additional space requirements, potential for more effective sedimentation because of long hydraulic detention times in the ponds, and the elimination of the need for continuous sludge processing systems. Several uncertainties associated with the intrapond treatment concept have also been identified, however [*2*]. The primary concern is the possibility of remobilization or release of the adsorbed metals from the solids back into the aqueous phase. Desorption could be caused by a shift in pond pH, due to either changes in the influent composition or to equilibration with atmospheric carbon dioxide. Metal remobilization due to the partial dissolution of the iron oxide solids under reducing conditions is also a concern. In addition, the possible difficulty of adequately controlling intrapond treatment has been noted.

During the feasibility studies [*8*], some bench-scale experiments were performed to assess in an approximate manner the potential for release of metals from ash sediments that had been treated with iron. An attempt was made to simulate ash pond conditions during intrapond treatment by simply leaving two buckets of ash-laden water samples, both of which were first treated with iron, in contact with the ash sediment and open to the atmosphere for about one month. For comparison purposes, two additional bucket tests were run using ash-free samples. All four samples were dosed with the same amount of iron (50 mg/L) at the same time. Throughout the month, the pH of all four (unstirred) samples varied over a relatively narrow range of pH 7.4 to pH 8.2. The results indicated that the dissolved concentrations of the target element, As, were reduced sharply in all four buckets upon the addition of iron. However, after a month of water/sediment contact in the ash-laden samples, these concentrations returned to almost the same values measured prior to iron treatment, while the dissolved As concentrations in the ash-free samples continued to decrease slightly. Based on the results obtained for the ash-free samples, it was reasoned that the increase in As concentrations observed in the ash slurry supernatants was due to continued leaching of As from the settled ash particles and an inability of the iron solids to adsorb the newly-leached As. Although additional tests to simulate better the dynamic conditions of an ash pond were not run, the investigators decided that the possibility for release of metals from ash pond sediments was sufficient reason to eliminate the intrapond treatment approach as an option for the pilot testing program. Subsequent work was directed at developing and implementing a pilot-scale test unit which utilized conventional treatment technology to remove arsenic and selenium from ash pond effluents.

Ash Pond Modeling

Farley *et al.* [*6*] developed a model that considers ash pond hydraulics and solids sedimentation. With the input of certain parameters to describe the existing conditions of the pond and its influent, this model is able to provide estimates of the flow patterns in the pond and the effluent solids concentration. Results from the application of the model to an actual fly ash pond were shown to be in close agreement with the observed operating conditions [*6*]. The model is also useful for identifying the optimal pond design criteria for solids removal, as well as possible chemical treatment alternatives. The sedimentation submodel is unique because unlike previous analyses of ash sedimentation rates, it is not based solely on discrete particle settling. Farley *et al.* [*6*, *17*] developed a second-order rate expression to describe fly ash coagulation/sedimentation kinetics and verified it through numerical simulations and laboratory experiments. This rate expression is incorporated in the sedimentation submodel used to predict the solids concentrations of ash pond effluents.

Through simulation with the ash pond model, Farley *et al.* [*6*] found that solids removal in an ash pond is dependent on both hydraulic transport and sedimentation kinetics. Solids removal can be improved by: increasing the influent solids concentration (using less sluice water), increasing the length to width ratio of the pond, and/or modifying the design of the inflow and outflow structures. Finally, the chemical behavior of a ponding facility can be estimated by using the predicted solids concentrations in a chemical equilibrium model that includes acid/base chemistry, surface adsorption reactions, and surface precipitation reactions.

EXPERIMENTAL METHODS

Three sets of laboratory experiments were performed using ash samples (both bottom ash and fly ash) collected from the Duquesne Light Company Cheswick Power Station, Springdale, Pennsylvania.

- Titration and dosing experiments to determine the acid and base requirements as well as the kinetics of pH adjustment in well mixed ash-water systems.
- Batch adsorption experiments to investigate the effects of acid/base and iron addition on system pH and overall metal removals under weak mixing conditions.
- Bench-scale reactor tests to simulate the dynamic conditions of operational sedimentation ponds.

The procedures used for these experiments are described below. Additional sets of experiments were performed to examine the effects of carbon dioxide exchange reactions between the ash slurry and the atmosphere and to determine the surface charge characteristics (e.g., point of zero charge or PZC) of the ash particles. The results of these additional experiments are discussed in Lagnese [*10*].

The laboratory studies focused on the removal of dissolved aluminum, manganese, and arsenic from ash suspensions under weak mixing conditions typical of ash ponds. Based on a comparison of historical ash pond effluent data with proposed discharge limitations, aluminum and manganese were identified as two elements of interest for the Cheswick Power Station. Arsenic, although not detected in the Cheswick ash transport waters, was selected for study because it has been identified as an element of concern at other coal-fired power plants [*1*, *2*].

Ash Sources and Collection Methods

The Cheswick Power Station is a coal-fired electric power generating facility which utilizes approximately 250 tons of coal per hour and is capable of generating 570,000 kw of electricity when operating at full capacity. During a normal day's operation, the Cheswick plant produces about 350 tons of fly ash and 150 tons of bottom ash. The majority of the ash is collected, slurried with river water, and pumped to designated disposal locations. The use of sluice water is a common practice in ash handling operations because it eliminates the need for more complex dry ash handling systems with dust control provisions. The Cheswick facility operates several ash sedimentation basins which serve as clarifiers for ash-water slurries. The clarified supernatant is discharged to tributaries of the Allegheny River.

The two sets of sedimentation basins that were targeted in this study were the bottom ash ponds and the miscellaneous waste ponds. As the names imply, the bottom ash ponds are used to handle bottom ash slurries and the miscellaneous waste ponds receive a variety of wastewaters, most of which contain fly ash. Each set consists of two adjacent ponds to provide for continuous operation. One pond is operated until it accumulates a large amount of settled ash, at which time the influent is sent to the adjacent pond. Typically, each pond is operated for about one year before removal of the accumulated ash is performed.

The bottom ash pond receives an average of 1.85 million gallons per day of ash-water slurry on a semi-continuous basis. Inflow occurs for about 90 minutes every 6 hours. Each of the bottom ash ponds has dimensions of 80-ft W × 225-ft L × 20-ft D, with inflow along one end and outflow at the opposite end. When empty (i.e., little or no accumulated ash), the bottom ash pond provides a hydraulic residence time of approximately 1.5 days.

The bottom ash sample used in this study was obtained by collecting multiple buckets of the influent to the bottom ash pond during an inflow period. Five-gallon buckets were used to sample the influent at various locations along the length of the inlet distribution pipe. The contents of each bucket were allowed to settle quiescently for several minutes, the supernatant was decanted, and the settled ash was composited in a single ash collection container. The procedure was repeated continuously throughout the inflow period and approximately 100 gallons of influent was processed. The composite ash sample was transported to the laboratory and dried in an oven at 104°C for several hours. The dried sample was used in subsequent tests.

Compared to the bottom ash ponds, operation of the miscellaneous waste ponds is much more variable. The influent to the miscellaneous waste ponds originates from several different sources, with the primary source being the overflow from a fly ash slurry collection sump. This sump is used to pump the fly ash slurry from the electrostatic precipitators to its final disposal location, an abandoned mine. Influent flow to the miscellaneous waste ponds is intermittent, averaging about 2 million gallons per day, and its composition can vary significantly. Cationic polymer is added to the influent to aid particle settling and coagulation. The miscellaneous waste pond dimensions are 80-ft W × 130-ft L × 13-ft D, and when there is no significant accumulation of settled ash, each miscellaneous waste pond provides a hydraulic residence time of roughly 12 hours.

Because the influent flow to the miscellaneous waste ponds is intermittent and contains a mixture of various waste streams, the fly ash sample used in the study was obtained directly from the base of the electrostatic precipitator fly ash hoppers prior to being slurried with water. Individual ash samples were collected from each of six hoppers. The samples were composited on a percent by weight basis to provide a single sample representing the total mixture of fly ash that is removed from the flue gas stream by the precipitators. This composite sample was used throughout the laboratory study.

Titration and Dosing Experiments

Because the solubility of metals is highly pH dependent, success of the intrapond treatment method rests on the ability to adjust and control the pH of the pond water within a certain optimal range by dosing the ash-laden influent with the proper amount of acid or base. Ash contains a mixture of metal oxides which have reactive surfaces and tend to buffer the solution. The presence of ash particles will therefore affect both the amount of acid or base required and the kinetics of pH adjustment. Kinetics play a major role in the intrapond treatment process because, unlike conventional treatment systems, the ponds are not agitated and the ash-water contact time is dictated by the hydraulics of the pond. Thus, determination of the acid and base dosages required for pH adjustment of ash-water slurries and the associated kinetics was the focus of the initial set of experiments.

A series of base titrations was performed on samples of ash slurries, some prepared with an inert electrolyte ($NaNO_3$) and others in simulated ash transport waters. The experiments performed with the inert electrolyte focused on the kinetics of hydroxyl ion exchange reactions between the solution and the ash particles, without the effect of competing ions. The simulated ash transport water consisted of deionized water dosed with the same concentrations of major inorganic ions detected in the ash transport waters at the Cheswick Power Station (see Table 1).

For each test, a 5 g/L ash suspension (reflecting the approximate solids concentration in the ash pond influent streams) was prepared using either 0.1M $NaNO_3$ or simulated transport

Table 1 Compositions of Synthetic Wastewaters

a) Bottom Ash Pond Synthetic Wastewater

Compound	Concentration (mg/L)	Concentration (mol/L)
$CaSO_4 \cdot 2H_2O$	155	9×10^{-4}
NaCl	41	7×10^{-4}
$KF \cdot 2H_2O$	8.5	9×10^{-5}

b) Miscellaneous Waste Pond Synthetic Wastewater

Compound	Concentration (mg/L)	Concentration (mol/L)
$CaSO_4 \cdot 2H_2O$	258	1.5×10^{-3}
NaCl	59	1×10^{-3}
$KF \cdot 2H_2O$	75	8×10^{-4}

water. The suspensions were agitated continuously and titrated with NaOH using a programmable autotitrator interfaced with both a microcomputer and a chart recorder. Equilibrium titration curves were developed by conducting series of "incremental" base titrations. An incremental titration involved adding equal aliquots of base at a fixed time increment. Each titration was performed using a successively longer time interval until approximately the same curve was obtained for two consecutive titrations. This indicated that the shorter of the two time increments was sufficient to achieve equilibrium, and the curve was therefore considered an equilibrium titration curve. Equilibrium titration curves were developed for both fly ash and bottom ash suspensions, with and without iron addition.

After generation of the equilibrium titration curves, several dosing experiments were conducted to check response of the well mixed ash-water suspensions following the introduction of a single large dose of base. An aliquot of sodium hydroxide was added to an agitated ash suspension and the change in pH was monitored over time. Two different dosages were tested for each type of suspension. Plots of pH versus time were used to verify the approximate time required for the pH to stabilize, as well as the final "equilibrated" pH value. The results of the dosing experiments were then compared with the equilibrium titration curves. Ideally, if a titration curve represents a truly equilibrated system, the final pH and equilibration time determined from the curve should match those determined by the dosing experiments.

Batch Adsorption Experiments

The next set of experiments focused on identifying the pH range and iron dose required to minimize the concentrations of aluminum, manganese, and arsenic in the aqueous phase of ash-water systems. In addition, a secondary objective was to study the kinetics of pH adjustments and metal removal under weak mixing conditions. The titration and dosing experiments described above were performed in well-mixed systems, but ash sedimentation ponds are generally quiescent except during the short-term periods of intermittent influent flow. The low degree of mixing and solid/liquid contact that occurs in sedimentation ponds can affect the overall kinetics of the reactions that occur in ash-water systems.

Small batch experiments were conducted on ash-water samples spiked with known amounts of aluminum, manganese, and arsenic. Each sample was prepared by adding 50 mg of ash to 10 mL of simulated ash transport water in a 15-mL polystyrene test tube. The samples were spiked with 1 ppm cationic polymer (Calgon POL-E-Z 2466), 1 ppm aluminum, 2 ppm manganese, and 0.1 ppm arsenic. The type and dosage of polymer was determined based on the results of column settling tests performed by Cullen [*10*, *18*]. Cationic and anionic polymers were found to enhance sedimentation rates equally at pH 7, and the cationic polymer was selected because of its use at the Cheswick ash ponds. The aluminum and manganese dosages represent the highest concentrations measured historically in the Cheswick ash pond effluents. The arsenic dosage was selected based on concentrations reported for other ash transport waters [*1*, *2*].

The batch adsorption experiments were conducted for a 10-day period using both bottom ash and fly ash slurries. The duration of the tests was extended to 10 days, which is significantly longer than the hydraulic residence times in the full-scale ponds, in order to examine metal resolubilization over time. Three target pH values (6.5, 7.5, and 8.5) were examined for each type of ash. Sodium hydroxide was used for pH adjustment, and the approximate dose required to achieve the target pH values were estimated from the results of the titration and dosing experiments. A single aliquot of sodium hydroxide was added to each sample at the start of the 10-day test, after which no additional measures were taken to adjust the pH to the target value.

In addition to pH, the effect of iron addition was also investigated. For each pH value, three different iron doses were examined (0 ppm, 10 ppm, and 50 ppm). The iron was added once, at the start of the experiment, in the form of a ferric chloride solution.

After preparing each sample, the test tubes were capped, agitated for 30 minutes using a wrist-action shaker, and allowed to settle quiescently for another 30 minutes. The short-term agitation was done to simulate the turbulence that occurs in ash ponds during the intermittent influent flow. After 30 minutes of settling, the pH in each tube was measured and a 1-mL sample of supernatant liquid was withdrawn. The supernatant sample was preserved with redistilled HNO_3 to a pH of less than 2 and retained for metal analysis. Analyses for Al, As, and Mn were performed by atomic absorption spectrophotometry.

Twenty-four hours later, the tubes were again agitated, allowed to settle, and the pH was measured. If appropriate, another supernatant sample was withdrawn and preserved. The cycle was repeated over a ten-day period, with 30 minutes of agitation performed each day. An attempt was made to collect supernatant samples to represent the range of pH values exhibited in each tube over the ten-day test (i.e., if the pH did not vary significantly from one day to the next, no sample was collected). Typically, a total of two to four supernatant samples were collected from each tube over the ten-day period and each sample was preserved for metal analyses.

Bench-Scale Reactors

Using the information obtained from the titration and batch adsorption experiments, bench-scale reactors or "ponds" were used to investigate the effectiveness of intrapond treatment for manganese removal in flow-through systems. The bench-scale tests were conducted over a 30-day period and were designed to simulate the flow-through operation of the fly ash sedimentation ponds (miscellaneous waste ponds) at the Cheswick Power Station. The study focused on manganese because historical data indicated that it was the primary metal of interest for the Cheswick fly ash ponds.

A total of three reactors were used in the experiment, each consisting of a polyethylene basin with a capacity of three liters. The length:width:depth ratio of the basins were similar to that of the full-scale fly ash ponds. Each reactor was equipped with a perforated influent distribution pipe and an effluent discharge pipe, as shown in Figure 3. To limit the amount of floating solids entering the effluent pipe, a baffle consisting of a thin strip of polystyrene was suspended across the width of the basin, just in front of the discharge port. Throughout the 30-day experiment, the reactors were covered with transparent plastic wrap to minimize the effects of evaporation.

Each of the three reactors was operated under slightly different conditions, as summarized in Table 2. Reactors #1 and #2 were used as controls to simulate the existing conditions (without intrapond treatment) of the fly ash ponds at the Cheswick plant and to examine the effect of ash buildup on the effluent quality. Both reactors were operated under the same conditions, except that Reactor #1 initially contained no fly ash and Reactor #2 was initially half filled with fly ash (i.e., ash was evenly distributed along the bottom of the reactor to one-half the height of the reactor walls). Reactor #3 was used to test the feasibility and effectiveness of an intrapond treatment process including both pH adjustment and iron addition.

The reactors were all operated in a semi-continuous manner, similar to the operation of full-scale ponds. Once a day, each reactor was dosed with one liter of a fly ash slurry. The average hydraulic residence time for the reactors that were initially empty (Reactors #1 and #3) was approximately 3 days, and

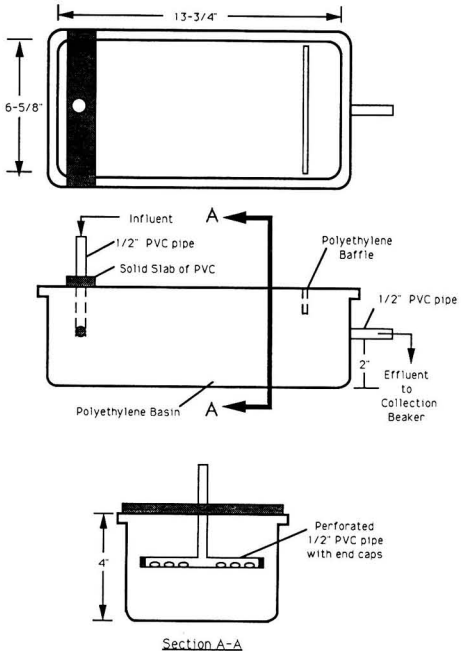

FIGURE 3. Schematic of bench-scale reactor

the average residence time in the reactor one-half full of ash was approximately 1.5 days. These residence times are average values based on the total throughput and reactor volumes assuming no short circuiting; no dye tests were performed. For Reactors #1 and #2, the influent consisted of 5 grams of fly ash in one liter of simulated ash transport water spiked with 2 ppm manganese. Prior to introducing the slurry into the reactor, each liter of influent was dosed with 1 ppm cationic polymer and adjusted to within the pH range of 6.5 to 7.0 using sodium hydroxide. The pH values measured in the influents to the Cheswick ash ponds were typically within this pH range.

The influent for Reactor #3 contained the same ash, polymer, and manganese concentrations as the other two reactors. However, the slurry was dosed with 50 ppm iron as ferric chloride and the pH was adjusted to approximately 9.5 prior to pouring the solution into the reactor. The desired pH in the reactor was 8.5 but, because the ash particles react with hydroxyl ions, the influent pH used was slightly higher to account for the decrease in pH that occurs as the hydroxyl ions are removed from solution over time. The amount of base required was estimated from the results of the titration and dosing experiments.

Table 2 Operating Conditions of Bench-Scale Reactors

Reactor	Start-Up Conditions	Influent Composition
1	empty (no ash buildup)	5 g/L fly ash 1 ppm cationic polymer 2 ppm Mn Misc. Waste Pond Syn. Wastewater
2	ash buildup = approx. 50% of reactor volume	same as Reactor 1
3	empty (no ash buildup)	same as Reactor 1 plus: 50 ppm iron 3.5 mM NaOH (influent pH = 9.5)

The pH of the influent and effluent, as well as the pH within the reactor, was monitored daily. Also, the influent and effluent from each reactor were sampled daily and the samples were combined to form 3-day composites. Prior to compositing, each influent sample was first filtered through a 0.45-micron membrane to remove suspended solids. The composited influent filtrates were analyzed for dissolved manganese. The effluent samples were not filtered prior to compositing because discharge limits for the ash ponds are usually given in terms of total (suspended plus dissolved) metal concentrations. The 3-day effluent composites from each reactor were analyzed for total suspended solids (TSS) and total manganese, and the effluent composites from Reactor #3 were also analyzed for iron.

RESULTS AND DISCUSSION

pH Adjustment of Well-Mixed Ash Slurries

The results of the titration and dosing experiments were similar for fly ash and bottom ash slurries. In both cases, the overall kinetics of pH adjustment in well-mixed systems were observed to be slow in the range of pH 7 to 9, i.e., near the PZC values for the ashes ($PZC_{BA} \approx 8$; $PZC_{FA} \approx 9.5$) as determined via rapid titrations by Lagnese [*10, 18*]. Previous studies performed by Onoda and DeBruyn [*19*] revealed that proton exchange reactions in aqueous suspensions of metal oxides follow a two-step kinetic process. The first step is generally considered a rapid exchange that occurs at the solid/solution interface, followed by a much slower second step that is believed to result from exchange reactions within the interior of the oxide particles. The pH versus time plots generated during this study indicated the same type of two-step kinetics.

Figure 4 illustrates pH time course plots (pH versus time)

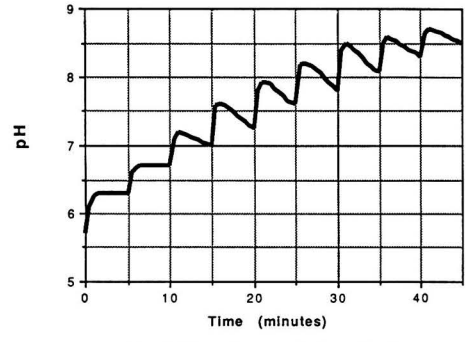

(a) 5-Minute Incremental Base Titration Performed with 0.01N NaOH (5 min/ueqv)

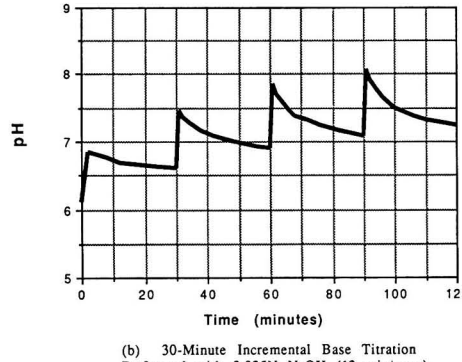

(b) 30-Minute Incremental Base Titration Performed with 0.025N NaOH (12 min/ueqv)

FIGURE 4. pH time course plots for base titrations of bottom ash suspensions in 0.01 M $NaNO_3$

generated during two separate incremental base titrations of bottom ash slurries in inert electrolyte, one performed by adding 0.1-mL aliquots of 0.01N NaOH at five-minute time intervals (i.e., 5 minutes/microequivalent of base) and the other by adding 0.1-mL of 0.025N NaOH at 30-minute intervals (i.e., 12 minutes/microequivalent of base). Both plots exhibit a series of vertical steps corresponding to the change in pH resulting from the introduction of hydroxyl ions into solution. The plot corresponding to the 5-minute titration (Figure 4(a)) shows that, within the pH range of 6 to 7, the pH of the bottom ash suspension stabilized quickly following the addition of an aliquot of base. However, in the pH range of 7 to 8.5, the initial increase in pH corresponding to the addition of an aliquot of base was followed by a rapid decrease as the hydroxyl ions reacted with the surface of the ash particles and were removed from solution. At the end of each 5-minute interval, the pH was still declining, an indication that additional time was required for pH stabilization. By comparison, the plot generated during the 30-minute incremental titration (Figure 4(b)) demonstrates that the rapid pH decline observed during the first five minutes gradually slowed over time and that at the end of 30 minutes, the pH was approaching stabilization.

The titration curves corresponding to the two pH time course plots described above are included in Figure 5, along with two additional curves. These four curves represent incremental base titrations of bottom ash slurries performed at different rates. The results indicate that, as the time between base additions was increased, the slope of the titration curve decreased (i.e., the increase in pH was less for a given amount of base added). By allowing more time between titrant additions, more hydroxyl ions are removed from solution and thus the pH at the end of the time increment is lower. The titration curve generated by allowing 10 minutes per microequivalent base added is similar to the curve generated for a rate of 12 minutes per microequivalent, indicating that the latter approximates an "equilibrium" titration curve for the bottom ash suspension.

The results from the two dosing experiments performed on bottom ash suspensions in inert electrolyte were used to determine how closely the 12 minutes-per-microequivalent titration curve approximates an equilibrium titration curve. This comparison is illustrated in Figure 6. The time interval between every two data points on the titration curve was 30 minutes. As shown, both the final pH and equilibration time determined for each dosing experiment is in close agreement with the titration curve. Thus, the 12-minute-per-microequivalent titration curve was close to an "equilibrium" curve and was used to estimate both the dosage and equilibration time required to achieve a particular pH in a well-mixed suspension of bottom ash (5 g/L) in inert electrolyte.

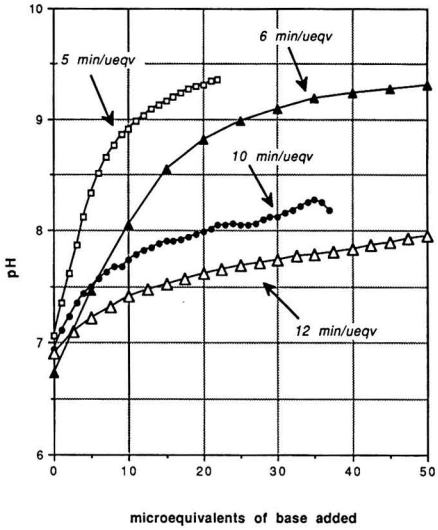

FIGURE 5. Comparison of different incremental titration rates for bottom ash suspensions in 0.01 M $NaNO_3$

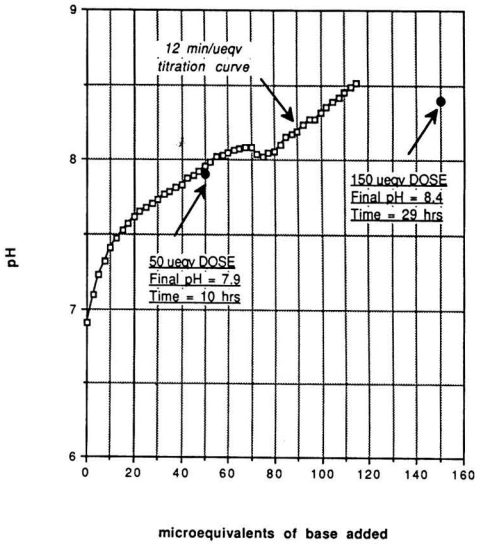

FIGURE 6. Comparison of titration and dosing experiment results for bottom ash suspensions in 0.01 M $NaNO_3$

The results obtained for ash suspensions prepared in simulated ash transport water were similar to those for the suspensions prepared in inert electrolyte. The presence of specifically adsorbing ions other than H^+ and OH^- did not have a significant effect on the acid/base chemistry of the suspensions.

pH Adjustment of Ash Slurries Under Weak Mixing Conditions

The pH measurements taken during the 10-day batch adsorption experiments conducted on fly ash slurries under weak mixing conditions are illustrated in Figure 7. Figure 7(a) depicts the change in pH over time for the three samples that had a target pH of 6.5, and Figures 7(b) and 7(c) present the data for the samples with pH goals of 7.5 and 8.5, respectively. In the cases of the latter two, the pH in the samples were initially higher than the target pH but decreased with time and gradually approaches the target value. The most significant decrease in pH occurred with the first two days, followed by a much more gradual decline over the remaining eight days. These two distinct pH adjustment rates correspond to the two-step kinetics that was recognized during the titration studies, except in this case the rates were slower because the samples were not well mixed. Thus, it appears that the enhanced solid/water contact achieved in the mixed systems facilitated hydroxyl exchange reactions and the kinetics were faster. However, in an intrapond treatment process where the intermittent influent is dosed with base, additional time will be required to achieve a stable pH under the weak mixing conditions of the pond.

The graphs presented in Figure 7 also show that, by the end of the 10-day period, the pH of each sample was close to the target pH value. The amount of base added to each sample at the start of the experiment was determined from the results of the titration and dosing experiments. The fact that the target pH values were achieved indicates that, although the equili-

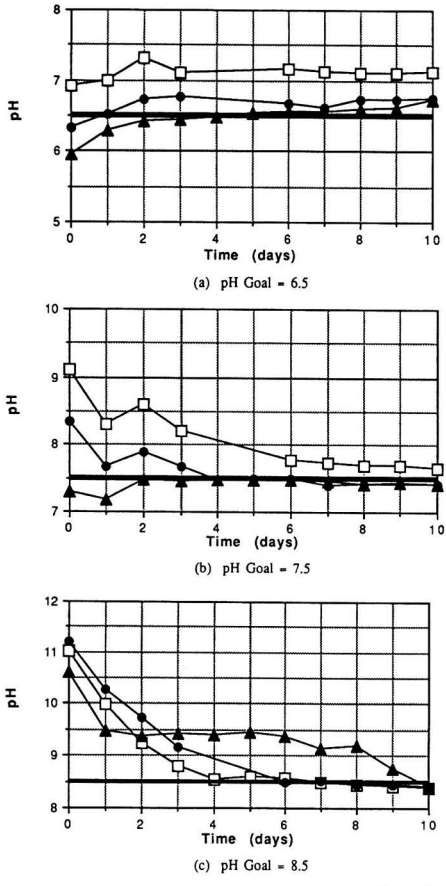

FIGURE 7. Fly ash batch adsorption experiments: pH variation with time. No Fe added (□), 10 ppm Fe (●); 50 ppm Fe (▲); pH goal (——)

bration times required in the well-mixed titration and dosing experiments were not applicable to the weak-mixing batch adsorption experiments, the base requirements were approximately the same. Thus, the extent of mixing affects the kinetics of pH adjustment but does not appear to have a marked effect on the amount of base that is needed to obtain a certain pH.

Effects of pH and Iron Dosage on Metal Concentrations

The batch adsorption experiments were also used to investigate the effects of pH and iron dosage on the concentrations of aluminum, manganese, and arsenic in the supernatant of a settled ash slurry. The concentrations detected in each sample at the final equilibrated pH were plotted against the equilibrated pH values. Plots generated for the experiments conducted with fly ash slurries, which are similar to the plots developed for bottom ash slurries, are presented in Figure 8. The initial dosage of each metal and the corresponding proposed NPDES limit for the Cheswick ash pond effluents are also indicated on the graphs. In the case of arsenic, there is no proposed limit.

As shown in Figure 8, the concentrations of both manganese and aluminum exhibited a strong dependency on pH, and the plots generated from the batch adsorption experiment data are similar to typical metal cation solubility curves. Variations in the concentrations of manganese and aluminum over time were related to variations in pH (i.e., any resolubilization that occurred was due to a lack of pH control). For manganese, the minimum concentration (less than 0.1 mg/L) were obtained at pH 8.5. At this pH, the addition to iron had no effect on the manganese concentration in solution, indicating that the dissolved concentration is fixed by the solubility of the precipitated form of manganese, most likely manganese carbonate as determined from chemical equilibrium modeling [*10*]. However, in the pH range below about 7.5 where the manganese concentrations were much higher, the presence of iron did have an effect. The concentrations were lower in the iron-treated samples than in the samples containing no iron. These results suggest that, in the lower pH range, a solid form of precipitated manganese is not present and the dissolved concentration of manganese can thus be reduced by adsorption onto the iron oxide solids.

The results for aluminum were similar to those for manganese except that the pH of minimum solubility was close to pH 7. At this pH, the initial spike concentration of 1 mg/L aluminum was reduced to approximately 0.5 mg/L, close to the minimum solubility for aluminum hydroxide predicted by chemical modeling [*10*]. The addition of iron did not enhance

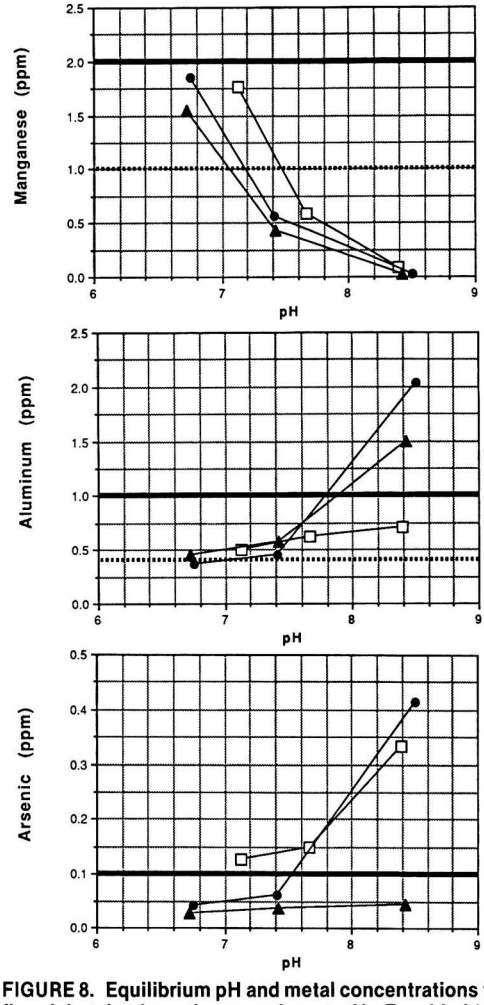

FIGURE 8. Equilibrium pH and metal concentrations for fly ash batch adsorption experiments. No Fe added (□), 10 ppm Fe (●); 50 ppm Fe (▲); spike (——); NPDES limit (- - -)

the removal of aluminum over the pH range of the tests. In fact, in the pH range above 7.5, the aluminum concentrations were unexplainably higher in the iron-treated samples.

In contrast to manganese and aluminum, the concentrations of arsenic were strongly affected by the presence of iron. As shown in Figure 8(c), the arsenic concentrations were consistently reduced from 0.1 mg/L to less than 0.05 mg/L over the pH range of 6.5 to 8.5 by the addition of 50 mg/L iron. It is also interesting to note that, for the samples containing no iron, the dissolved arsenic level at pH 8.5 was more than three times greater than the initial spike concentration of 0.1 mg/L and that the arsenic level decreased as the pH decreased. It appears that arsenic was leached from the ash particles in the higher pH range and that the decrease in concentration with pH resulted from adsorption of the arsenic onto the ash particles. As previously discussed, arsenic exists as an anion in solution and anion adsorption onto oxide surfaces is favored at low pH. This claim is supported by the fact that the curve developed for the samples containing 10 mg/L iron exhibited the same trends as for the untreated samples. Adsorptive behavior is expected in the sample containing iron, and the similarity in the shapes of the two plots suggests that adsorption was also occurring in the sample that was not dosed with iron. Thus, it was concluded from these experiments that iron treatment can result in substantial removals of arsenic from ash transport water.

Performance of Bench-Scale Reactors

pH Control

As indicated by the results presented above, pH control is paramount to the success of an intrapond treatment process, and the ability to control the pH by dosing the pond influent with a given amount of acid or base was tested using the bench scale reactors. The pH values that were measured daily in each of the three reactors are plotted in Figure 9. The plot for Reactor #3 (the reactor used to test an intrapond treatment process including both iron addition and pH adjustment) indicates that by raising the pH of the daily influent to 9.5, the pH within the reactor remained within the desired range of 8.0 to 8.5 (the range of minimum solubility for manganese). Obviously, well-controlled laboratory conditions and consistent influent quality were instrumental in achieving these results. The operating conditions and composition of the influent for a full-scale ash pond can vary, but the results of these studies indicate that, if the variations can be either minimized or predicted, it is possible to maintain the pH within the pond at a desired level by dosing the influent with the proper amount of base. The base doses used in this study were estimated from the titration and dosing experiment results for fly ash.

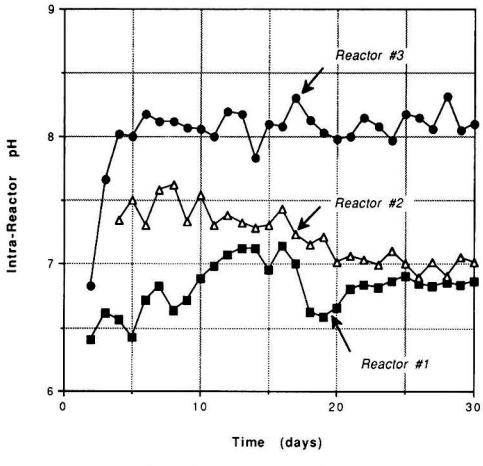

FIGURE 9. Bench-scale reactors: intra-reactor pH

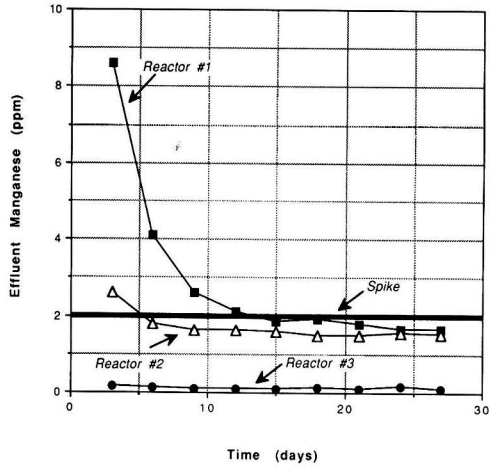

FIGURE 10. Bench-scale reactors: effluent manganese concentrations

Manganese Removal

The effectiveness of intrapond treatment for removal of manganese from solution can be estimated by comparing the manganese data for Reactor #3, the treated reactor, with the data for the other two untreated reactors. The manganese concentrations measured in 3-day composite samples of each reactor effluent are presented in Figure 10, along with the influent concentration of 2 mg/L which was the same for all three reactors. As illustrated, the manganese concentrations in the effluent from Reactor #3 were significantly lower than those in the effluents from Reactors #1 and #2 and remained close to 0.2 mg/L over the course of the 30-day experiment. There was no evidence of resolubilization of the manganese. Based on the results of the batch adsorption experiments, the reduced manganese concentrations in Reactor #3 were more likely related to the elevated pH than to the daily addition of 50 mg/L iron. Similarly, the variations in the manganese concentrations for the two untreated reactors can also be explained by the slight variations in pH that occurred within these reactors, as depicted in Figure 9. The initially high manganese concentrations in Reactor #1 effluent, which were above the spiked concentration, suggest that there may have been leaching of manganese from the ash particles in the pH range below 7.0. Thus, to achieve significant removals of manganese from solution, a pond pH greater than 7.5, and preferably closer to 8.5, must be maintained.

Fate of Iron

Although the 50 ppm iron that was added to Reactor #3 on a daily basis did not significantly enhance the removal of manganese from solution, it was included in the intrapond treatment process in order to study its fate in a flow-through system as well as its effect on the overall performance of the reactor (pH stability, etc.). The expectation was that the iron would precipitate from solution as $Fe(OH)_3(s)$ and settle with the ash particles in the reactor. However, the plot of effluent iron concentrations shown in Figure 11 indicates that the iron concentration in the effluent from Reactor #3 was consistently above 1 mg/L and exhibited an increase over time. The Reactor

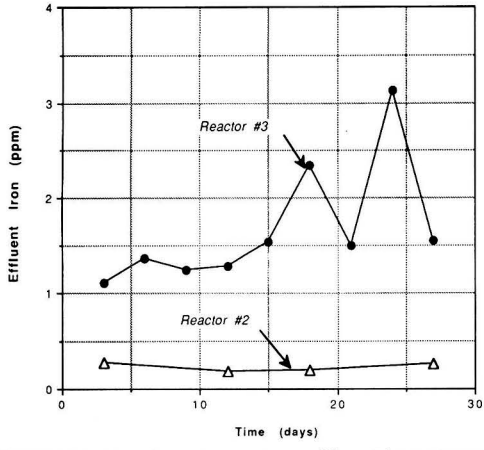

FIGURE 11. Bench-scale reactors: effluent iron concentrations

#3 effluent also contained significantly higher concentrations of suspended solids than the other two reactors. These results suggest that effective settling of the precipitated iron particles was not achieved and that some of the particles were carried out in the effluent. The inefficient sedimentation of iron oxide particles may have been related to adsorption of the cationic polymer, resulting in creation of a positive charge and hence repulsion of iron oxide particles. Thus, an intrapond treatment process that includes iron addition would require close monitoring and fine tuning of the influent chemistry, especially the polymer type and dose, to prevent the formation of a stable suspension of precipitated iron particles.

Effect of Ash Buildup

The total suspended solids concentrations detected in the effluents from Reactors #1 and #2 were approximately the same over the course of the experiment, even though Reactor #2 was half-filled with ash at the start of the test and Reactor #1 was empty. The 50% reduction in reactor volume associated with the accumulation of ash did not appear to adversely effect the sedimentation efficiency. These results are consistent with results obtained by Cullen [*10, 18*], who measured fly ash and bottom ash sedimentation rates and used these data in the combined hydraulic/sedimentation ash pond model of Farley et al. [*6*] to predict the effect of ash buildup on the effluent solids concentrations for the Cheswick ash ponds. The "ponding model" predicted a significant increase in effluent solids concentrations with accumulations of ash comprising greater than 60% of the pond volume. Mass removal of ash by sedimentation was predicted to be basically unaffected by ash buildups of less than 60% of the total volume, but to decrease significantly at ash buildups of greater than 60%. Minimization of effluent solids concentration is desirable not only to meet discharge limits for suspended solids, but also to limit total (dissolved plus suspended) effluent metal concentrations.

SUMMARY AND CONCLUSIONS

Effluents from ash sedimentation ponds at coal-fired power plants often contain metals derived from the ash particles and sometimes at concentrations that exceed discharge limits. Metal concentrations in these effluents can be reduced by promotion of metal precipitation and adsorption in the ash pond. This "intrapond treatment" approach is potentially cost effective relative to implementation of back-end treatment schemes but has been studied little.

Because metal precipitation and adsorption reactions are pH dependent, their use to reduce metal concentrations in ash transport waters requires adjustment and control of the pond pH within a certain range. Investigation of pH adjustment of ash suspensions in this study showed that the kinetics are slow because of the slow rate of proton adsorption-desorption reactions with the ash particles and mass transfer limitations under weak mixing conditions. Equilibration times on the order of days were required to attain a stable pH in the range of 7 to 9 under weak mixing conditions. Because of the acid-base properties of the ash, the amount of base required to raise the pH of ash-laden water is higher than for ash-free water.

Removal of aluminum and manganese from ash transport water was found in batch tests to be controlled primarily by solubility. Maximum removals of aluminum (probably as $Al(OH)_3(s)$) were achieved in the pH range close to 7.0, and removal of manganese (probably as $MnCO_3(s)$) was greatest at pH 8.5. The addition of ferric chloride, to promote aluminum or manganese adsorption on the iron oxyhydroxide subsequently formed, did not significantly enhance the removal of either metal, except in the pH ranges where solubility was not a controlling factor. In the case of arsenic, which exists as an anionic species in solution, the addition of 50 ppm of ferric iron consistently enhanced removals over the pH range investigated (6.5 to 8.5). From these results it is apparent that simultaneous removal of all three metals in an intrapond treatment process would require a combination of both pH adjustment and iron addition.

The ability to control pH and promote manganese removal was investigated using three bench-scale reactors operated with intermittent inflow as in full-scale ash ponds. It was found that by dosing the influent ash slurry with the proper amount of base, the pH within the reactor could be maintained within the desired range of 8.0 to 8.5. Under these conditions, the manganese concentration was consistently lowered from 2 mg/L in the influent to approximately 0.2 mg/L in the effluent. There was no evidence of resolubilization of the manganese over the course of the test. Ferric iron addition to the influent of one reactor did not influence manganese removal in the pH range studied but did result in the apparent formation of some small, slow-settling iron oxyhydroxide colloids and carry-over of these colloids in the effluent. The presence of a bed of fly ash occupying about 50% of the volume of a third reactor had little influence on effluent manganese and solids concentrations, but modeling studies indicated significant carry-over of ash solids in the effluent would occur with ash buildup greater than about 60% of the pond volume.

Overall, the results of this study indicate that further examination of the intrapond treatment approach for control of metal concentrations in ash pond effluents is warranted. The bench-scale experiments conducted here indicate that adequate pH control can be achieved in an ash pond if the composition of the influent slurry is fairly uniform. By adjustment of pH, and addition of an iron(III) salt to precipitate iron oxyhydroxide in some cases, concentrations of many metals of interest in the pond effluent can be kept low by precipitation and/or adsorption on the iron oxyhydroxide. Adequate pH control is the key to prevention of remobilization. Effective sedimentation of ash and iron oxyhydroxide is required for effective metal removal in the intrapond approach. The carry-over of ash and/or iron oxide particles in the pond effluent would adversely affect the removal efficiencies of metals which have adsorbed to the particles. Sedimentation tests [*10, 18*] indicate that effective sedimentation can be achieved readily, in some cases with the assistance of polymer addition. Ash accumulation cannot be allowed to exceed the design ash storage depth, however, as this leads to insufficient hydraulic residence time and ash carry-over in the effluent.

ACKNOWLEDGMENTS

This work was supported by Duquesne Light Company through a research contact with Carnegie Mellon University. The authors thank James Cool, the project officer at Duquesne Light, for his helpful suggestions; Lawrence Cartwright of CMU for his assistance with construction of various pieces of laboratory equipment; Scott Cullen for his help with the ash sedimentation modeling and with the field sampling; David Black and David Jackson of Duquesne Light for their assistance with the field work; and Sara Marie Baldi of Duquesne Light for the supplementary pond monitoring analyses. This paper was presented at the 1990 Fall National Meeting of the American Institute of Chemical Engineers.

LITERATURE CITED

1. TRW, Inc., "Aqueous Discharges from Steam-Electric Power Plants: Trace Metal Sampling and Analysis Reference Guide," EPRI-CS-3739, Electric Power Research Institute, Palo Alto, CA (1984).
2. Brown and Caldwell, Inc., "Trace Element Removal by Coprecipitation with Amorphous Iron Oxyhydroxide: Engineering Evaluation," EPRI-CS-4087, Electric Power Research Institute, Palo Alto, CA (1985).
3. Leckie, J. O., M. M. Benjamin, K. F. Hayes, G. Kaufman, and S. Altmann, "Adsorption/Coprecipitation of Trace Elements from Water with Iron Oxyhydroxide," EPRI-CS-1513, Electric Power Research Institute, Palo Alto, CA (1980).
4. Leckie, J. O., A. R. Appleton, N. B. Ball, K. F. Hayes, and B. D. Honeyman, "Adsorptive Removal of Trace Elements from Fly-Ash Pond Effluents onto Iron Oxyhydroxide," EPRI-RP-910-1, Electric Power Research Institute, Palo Alto, CA (1984).
5. Benjamin, M. M., K. F. Hayes, and J. O. Leckie, "Removal of Toxic Metals from Power-Generation Waste Streams by Adsorption and Coprecipitation," *J. Water Pollution Control Federation*, **54**(11), pp. 1472–1481 (1982).
6. Farley, K. J., D. R. Harleman, and F. M. M. Morel, "Ponding of Effluents from Fossil Fuel Steam Electric Power Plants," Report No. MIT-EL-84-007, MIT Energy Labortory, Massachusetts Institute of Technology, Cambridge, MA (1984).
7. Dzombak, D. A. and F. M. M. Morel, "Adsorption of Inorganic Contaminants in Ponded Effluents from Coal-Fired Power Plants," Report No. MIT-EL 85-005, MIT Energy Laboratory, Cambridge, MA (1985).
8. Brown and Caldwell, Inc., "Field Evaluation of Arsenic and Selenium Removal by Iron Coprecipitation," EPRI-CS-5187, Electric Power Research Institute, Palo Alto, CA (1987).
9. Brown and Caldwell, Inc., "Trace Metal Removal by Iron Coprecipitation: Field Evaluation," EPRI-GS-6438, Electric Power Research Institute, Palto Alto, CA (1989).
10. Lagnese, K. M., "Use of Sedimentation Ponds for Removal of Trace Elements from Ash Transport Waters," M.S. Thesis, Department of Civil Engineering, Carnegie Mellon University, Pittsburgh, PA (1990).
11. Merrill, D. T., M. A. Manzione, J. J. Peterson, D. S. Parker, W. Chow, and A. O. Hobbs, "Field Evaluation of Arsenic and Selenium Removal by Iron Coprecipitation," *J. Water Pollution Control Federation*, **58**(1), pp. 18–26 (1986).
12. Merrill, D. T., M. A. Manzione, D. S. Parker, J. S. Peterson, W. Chow, and A. O. Hobbs, "Field Evaluation of Arsenic and Selenium Removal by Iron Coprecipitation," *Environmental Progress*, **6**(2), pp. 82–90 (1986).
13. Patterson, J. W., *Industrial Wastewater Treatment Technology*, 2nd Edition, Butterworth, Boston (1986).
14. Cushnie, G. C., Jr., *Removal of Metals from Wastewater*, Noyes Publications, Park Ridge, NJ (1984).
15. Dzombak, D. A., and F. M. M. Morel, "Adsorption of Inorganic Pollutants in Aquatic Systems," *J. Hydraulic Engineering*, **113**(4), pp. 430–475 (1987).
16. Benjamin, M. M., and J. O. Leckie, "Multiple-Site Adsorption of Cd, Cu, Zn, and Pb on Amorphous Iron Oxyhydroxide," *J. Colloid Interface Science*, **79**(1), pp. 183–217 (1980).
17. Farley, K. J., and F. M. M. Morel, "Role of Coagulation in the Kinetics of Sedimentation," *Environ. Sci. Technol.*, **20**(2), pp. 187–195 (1986).
18. Lagnese, K. M., D. A. Dzombak, and S. C. Cullen, "Use of Sedimentation Ponds for Removal of Trace Elements from Ash Transport Waters," Final Report submitted to Duquesne Light Company, Department of Civil Engineering, Carnegie Mellon University, Pittsburgh, PA (1991).
19. Onoda, G. Y., and P. L. DeBruyn, "Proton Adsorption at the Ferric Oxide/Aqueous Solution Interface, I. A Kinetic Study of Adsorption," *Surface Science*, **4**, pp. 48–63 (1966).

Rate Controlling Model for Bioremediation of Oil Contaminated Soil

K. Y. Li, S. N. Annamalai and J. R. Hopper

Chemical Engineering Department, Lamar University, Beaumont, Texas 77710

A mathematical model of bio-remediation of hydrocarbons in a soil matrix has been developed to predict the rate controlling step and the remediation rate during the bioremediation of a contaminated soil. The model is based on mass transfer of oxygen and oil into the aqueous solution in the soil matrix and the biodegradation of the hydrocarbons in the aqueous solution. Monod's equation was used to describe the biodegradation rate in aqueous solution while the mass transfer equations were used to describe the mass transfer rates of oxygen and oil in the soil matrix. Results from model calculations indicate that the bio-remediation rate increases and approaches a limiting value when one of the rates becomes controlling. When the parameters of the site soil samples are measured and the solubilities of oxygen and oil in aqueous solution are obtained, the bioremediation rate can be predicted by this model. The rate controlling step of the bioremediation site may be identified quickly and steps to improve the bioremediation rate can be recommended.

INTRODUCTION

Biological processes have been used successfully to remediate petroleum hydrocarbons and their derivatives in soil matrices [*1–3*]. Bioremediation is the use of microbes in natural systems to destroy contaminants to an environmentally acceptable level without producing adverse by-products. When microbes are acclimated, the bioremediation rate depends on the supply of oxygen and nutrients, and also on the mass transfer of contaminants (desorption and diffusion) to the right environment. The engineer's major job is to optimize the conditions for bioremediation.

This rate controlling concept is illustrated by a case study of bioremediation of a petroleum contaminated soil [*2*]. In the study, it was reported that the maximum bioremediation rate occurs at approximately 40 to 50 percent of the maximum field holding capacity of water. This observation is due to the fact that at the maximum field holding capacity of water the transfer rate of oxygen inside the soil is inhibited; but on the other hand, low humidity hinders the microbial activity in soil matrices.

Correspondence concerning this paper should be addressed to K. Y. Li.

The conceptual model to qualitatively describe the biodegradation of hydrocarbons in porous soils have been introduced [*3*]. As depicted in Figure 1, the porous soil matrix is composed of mixtures of sands, aggregates of silt, natural organics, non-aqueous phase liquid (NAPL), pores filled with water and pores filled with air. An enlarged view of each of the components; hydrocarbons (NAPL), sand grains, and fine aggregates; in Figure 1 shows that a biofilm exists around each of them. A biofilm is simply a layer of bacterial cells and other soil microorganisms which adhere to the exterior surface. Biodegradable organics diffuse through water or soil moisture into the biofilm where they are degraded by the microorganisms [*4*]. Microbial activity will not occur in the interior pocket of the hydrocarbons because of the physical-chemical characteristics of hydrocarbons. In addition, small pore diameters prevent micro-organisms from going into the micropore structure of both sand and fine aggregate. Hence, active biodegradation only occurs in the biofilms surrounding the surfaces of these materials.

Despite the availability of a conceptual model, no mathematical analysis has been developed which will quantitatively predict the remediation rate during soil bioremediation. This paper develops a mathematical model which can be used to

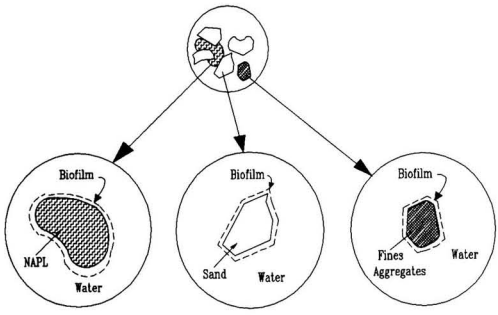

FIGURE 1. A conceptual model of soil matrix.

predict the bioremediation rate and the rate controlling steps, such as oxygen transfer, the movement of hydrocarbons, and the bioreaction in soil matrices.

DEVELOPMENT OF A MATHEMATICAL MODEL

One of the basic premises of the conceptual model is that soil bioremediation is a water-based process. In the aqueous solution, hydrocarbons can diffuse or move to a location where microorganisms can degrade them in the presence of nutrients and oxygen. The bioremediation rate in an aqueous solution may be controlled by the transfer rate of the organic contaminants, the transfer rate of oxygen or the biochemical reaction rate. The step, which has the highest resistance in the rate equation, will be the rate controlling step for the bioremediation process.

Although the biodegradation rate may be affected by the concentration of nutrients such as nitrogen and phosphorous, these concentrations are usually not critical in the bioremediation of a contaminated soil. The concentrations are not critical either because the solubilities of ammonium and phosphate ions are large compared to those of organic contaminants or the concentrations of ammonium and phosphate ions in the soil are already high.

Mass transfer of hydrocarbons in a soil matrix is a complicated process, often involving molecular diffusion and adsorption/desorption of the organic contaminants [5]. The hydrocarbon mass transfer rate, R_c, may be expressed in a simple formula [6]:

$$R_c = A_c k_s (C_{cs} - C_c) \tag{1}$$

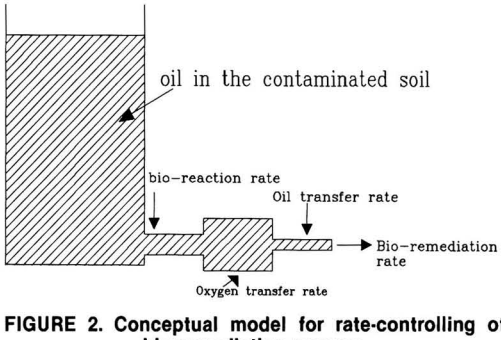

FIGURE 2. Conceptual model for rate-controlling of bio-remediation process

where

R_c = hydrocarbon mass transfer rate, mg BOD/sec,
A_c = total area for mass transfer of hydrocarbons, cm^2,
k_c = hydrocarbons mass transfer constant, cm/sec,
C_{cs} = solubility of hydrocarbons in water, mg BOD/cm^3, and
C_c = bulk concentration of hydrocarbons in water, mg BOD/cm^3.

The effect of adsorption and desorption on mass transfer may be represented by the value of k_c, which is an experimentally measured quantity.

The other important factor for bioremediation is the availability of oxygen to the biochemical reaction, because oxygen supply is vital for the growth of bacteria. The mass transfer rate of oxygen from the air which is in the pores of the soil is also a very complicated process. The transfer rate of oxygen in pores filled with air is much faster than in the pores filled with water [7]. The oxygen mass transfer rate in water pores is described by:

$$R_o = A_o k_o (C_{os} - C_o) \tag{2}$$

where

R_o = oxygen mass transfer rate, mg BOD/sec,
A_o = total area for mass transfer of hydrocarbons, cm^2,
k_o = oxygen mass transfer constant, cm/sec,
C_{os} = solubility of oxygen in water, mg BOD/cm^3, and
C_o = bulk concentration of oxygen in water, mg BOD/cm^3.

The biochemical reaction rate in an aqueous solution is described by a modification of Monod's equation:

$$R_b = V \frac{(k_s X C_c C_o)}{(K_m + C_c)} \tag{3}$$

where

R_b = oxygen mass transfer rate, mg BOD/sec,
k_s = biodegradation rate constant of the substrate, l/(mg VSS.sec)
K_m = Substrate concentration when the biodegradation rate is half of the maximum rate, mg BOD/l,
X = concentration of the microbes, mg VSS/l, and
V = Volume of the water in the soil, l.

In the porous soil matrix these three rates (equations (1), (2) and (3)) are not independent. In fact, the bioremediation process in a contaminated soil is simulated by a series process, depicted in Figure 2. This relationship may be expressed mathematically as,

$$R_c = R_b = R_o \tag{4}$$

The equality is in these three rates is true only when the rate is expressed in the units of mg BOD/sec. The step which has the highest resistance will be the rate controlling step for the entire bioremediation process.

Assuming that K_m is much larger than C_c, (in most of the cases the dissolved hydrocarbon concentration, C_c, is small) equations (1) through (4) may be solved for the concentrations of organics, C_c, and oxygen, C_o. The bioremediation rate can be calculated using,

$$R_b = (k_s/K_m) X C_c C_o \tag{5}$$

When values of the constants, $A_c k_c$, $A_o k_o$, k_s, K_m, and X are measured, and the solubility concentrations, C_{cs} and C_{os} are available, the bioremediation rate may be calculated. Results of these calculations are shown in Figures 3 through 7.

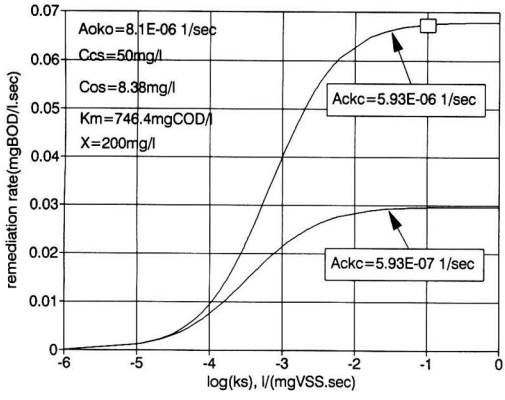

FIGURE 3. Effect of biodegradation rate constant on remediation rate

PARAMETER SELECTION FOR MODEL PREDICTION

Measurement of biodegradation rates of petroleum hydrocarbons in an aqueous solution have been reported by Li et al [8]. These data were obtained using a computer controlled respirometer. Kinetic data were analyzed successfully by Monod's equation which may be expressed as:

$$\frac{dC_c}{dt} = -\frac{k_s' X C_c}{K_m + C_c} \tag{6}$$

where $k_s' = k_s C_o$.

The value of k_s' and K_m, were estimated to be 3.82×10^{-2} mg BOD/(mg VSS•hr) and 746.4 mg BOD/l, respectively. Since the value of k_s' was measured at the condition of saturated oxygen (in the respirometer), the k_s value is obtained after dividing k_s' by the oxygen solubility, C_o. The calculated value of k_s is 1.27×10^{-6} l/(mg VSS.sec).

The mass transfer coefficient of petroleum hydrocarbons in a soil matrix was measured. The value of k_c is estimated to be 5.93×10^{-5}cm/sec for the transfer of petroleum in a sand/clay soil matrix. Details of the experiment and result will be published in the near future.

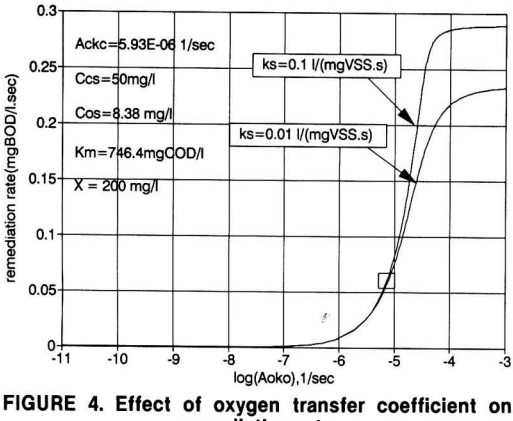

FIGURE 4. Effect of oxygen transfer coefficient on remediation rate

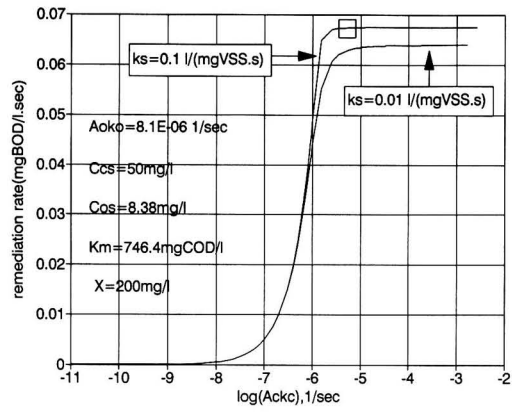

FIGURE 5. Effect of oil transfer coefficient on remediation rate

Mass transfer of oxygen in a soil matrix is complicated because the soil matrix consists of sand, pores of water, and pores of air. Moreover, the process of tilling the soil will enhance the oxygen transfer rate in the soil matrix. The enhancement factor of oxygen transfer due to tillage has not been considered in this study or any other published study. The mass transfer coefficient of oxygen in a saturated soil matrix was measured to be $k_o = 0.29$ cm/hr. Details of the experiment and the results will be published later. The oxygen mass transfer coefficient for a soil matrix containing air pores is higher than that for water saturated soil matrix.

The other properties and parameters selected for the calculations are shown below,

$C_{os} = 8.38$ mg/l.

$C_{cs} = 50$ mg/l.

$A_o = A_c = 100$ cm^2/l.

RESULT FROM MODEL PREDICTION

Effect of Biochemical Reaction on Bioremediation Rate

The effect of the biochemical reaction constant, k_s, on the bioremediation rate is shown in Figure 3. At low values of k_s,

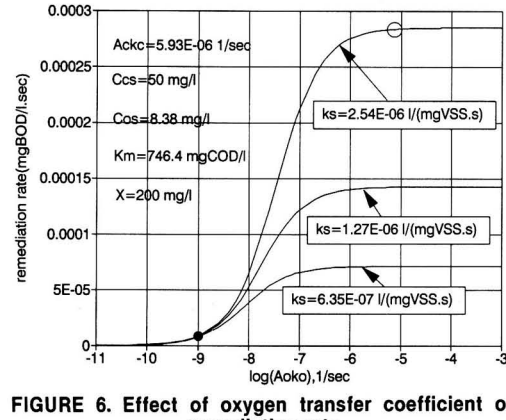

FIGURE 6. Effect of oxygen transfer coefficient on remediation rate

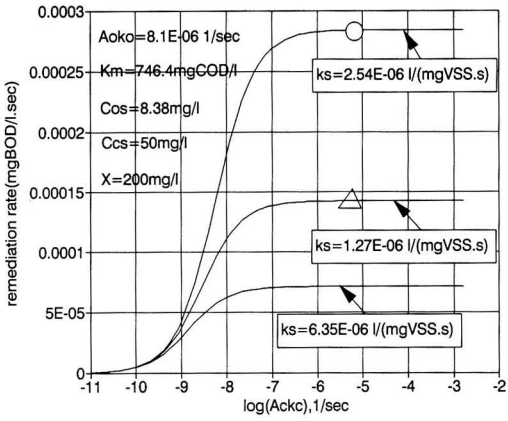

FIGURE 7. Effect of oil transfer coefficient on remediation rate

the bioremediation rate increases slowly with k_s. As k_s increases, bioremediation becomes a linear function of the k_s value. At high values of k_s, the bioremediation rate approaches a constant level and is independent of the value of k_s. At this limiting condition of large k_s, the bioremediation rate is controlled by mass transfer. The mass transfer controlling step could be either oxygen transfer or organic contaminants transfer.

A case where the bioremediation rate is independent of biochemical reaction rate but is oxygen mass transfer limited is shown in Figure 3 (as indicated by the □ sign on Figure 3). For this case, $k_s = 0.1$ l/(mg VSS sec), $A_o k_o = 8.1 \times 10^{-6}$ sec^{-1}, and $A_c k_c = 5.93 \times 10^{-6}$ sec^{-1}, the rate controlling step is mass transfer of oxygen. This may be visualized from the □ sign in Figure 4 which depicts a pattern of significant increase in the bioremediation rate with an increase of $A_o k_o$. However, the bioremediation rate will not increase significantly with an increase in $A_c k_c$ value, as can be seen from Figure 5.

EFFECT OF OXYGEN TRANSFER ON BIOREMEDIATION RATE

The effect of the oxygen transfer constant, $A_o k_o$, on the bioremediation rate is shown in Figure 6. When the $A_o k_o$ values are in the range of 1×10^{-9} to 1×10^{-7} sec^{-1}, the bioremediation rate increases linearly with $A_o k_o$. When the $A_o k_o$ value is relatively high, the bioremediation rate is independent of the value of $A_o k_o$ and depends on either the k_s value (as shown by the ○ sign in Figure 6) or the $A_c k_c$ value. The former case is illustrated in Figure 7. For this case the value of $A_o k_o$ is 8.1×10^{-6} and the value of $A_c k_c = 5.93 \times 10^{-6}$ sec^{-1}. The bioremediation rate is already in the plateau range and the increase of $A_c k_c$ will not increase the bioremediation rate.

At this condition, the bioremediation rate could be increased from 0.00015 to 0.00028 mg BOD/(l sec) when the k_s value increases from 1.27×10^{-6} to 2.54×10^{-6} l/(mg VSS sec) as can be visualized from Figure 7.

Effect of Oil Transfer on Bioremediation Rate

The effect of $A_c k_c$ on the bioremediation rate is similar to that of $A_o k_o$ as may be visualized from Figure 7. When the $A_c k_c$ values are in between 1×10^{-10} and 1×10^{-8} sec^{-1}, the bioremediation rate increases linearly with $A_c k_c$. When the $A_c k_c$ value is relatively high, the bioremediation rate depends on either the k_s value (as shown in this figure) or the $A_o k_o$ value. However, at the value of $A_o k_o = 8.1 \times 10^{-6}$ sec^{-1} the bioremediation rate is already in the plateau region and the increase of $A_o k_o$ will not increase the bioremediation rate, as can be seen from Figure 6.

It should be noted that the k_c value is relatively small due to the slow mass transfer rate of organic contaminants in the soil matrix. An increase in the value of k_c may be accomplished by using surfactants or by tillage of the soil. However in reality the magnitude of an increase in the value of k_c is quite limited.

Application

Pragmatic application of this rate controlling model involves a two-step approach. The first step is to measure the bioremediation parameters, i.e., k_s, $A_o k_o$, and $A_c k_c$. This can be accomplished by a laboratory measurement of the contaminated soil. The second step is to identify the rate controlling steps of the bioremediation process by using the measured parameters with the model prediction chart. The following two examples will illustrate the procedure.

Case 1 The following parameters were obtained from a laboratory test of soil samples from the field:

$k_s = 1.27 \times 10^{-6}$ l/(mg VSS·sec),
$K_m = 746.4$ mg BOD/l,
$A_c k_c = 5.93 \times 10^{-6}$ l/sec,
$A_o k_o = 8.1 \times 10^{-6}$ l/sec,
$C_{cs} = 50$ mg/l, and,
$C_{os} = 8.38$ mg/l.

For this case, what is the bioremediation rate? How can we improve the bioremediation rate?

The above parameters are used to determine the condition of this system. The condition is located by a ▵ mark in Figure 7. The bioremediation rate for this condition is 1.4×10^{-4} mg BOD/(l·sec). Under this condition the bioremediation rate may be improved by increasing the value of k_s, as can be seen from Figures 6 and 7. The bioremediation rate will increase with an increase of k_s, until a value of k_s value greater than 0.01 l/(mg VSS·sec). An increase in value of k_s can be accomplished by: optimizing nutrients supply (N and P), proper control of temperature and pH, and optimum aeration and irrigation of the soil.

Case 2 The following parameters were obtained from a laboratory test of soil samples from the field:

$k_s = 1.27 \times 10^{-6}$ l/(mg VSS·sec),
$K_m = 746.4$ mg BOD/l,
$A_c k_c = 5.93 \times 10^{-6}$ l/sec,
$A_o k_o = 1 \times 10^{-9}$ l/sec,
$C_{cs} = 50$ mg/l, and,
$C_{os} = 8.38$ mg/l.

For this case, what is the bioremediation rate? How can we improve the bioremediation rate?

The above condition is represented by a ● mark in Figure 6. The bioremediation rate for this situation is 1.1×10^{-5} mg BOD/(l·sec). This bioremediation rate may be improved by increasing the value of $A_o k_o$, as can be seen from Figure 6. The bioremediation rate can be increased with an increase of $A_o k_o$, until an $A_o k_o$ limiting value of 1.4×10^{-4} mg BOD/(l·sec) is reached. Increase in $A_o k_o$ values can be accomplished by tillage of the soil and control of the humidity in the soil.

CONCLUSION

A simple rate controlling model has been used to predict the bioremediation rate and also the rate controlling step for soil remediation. When the parameters of the site soil samples are

measured, the bioremediation rate can be estimated. The rate controlling conditions of the site may be identified quickly and the steps to improve the bioremediation rate can be recommended.

ACKNOWLEDGMENT

The authors wish to express their appreciation for a financial support from the Gulf Coast Hazardous Substance Research Center (GCHSRC)—Beaumont, Texas.

LITERATURE CITED

1. Newton, J., "Remediation of Petroleum Contaminated Soils," *Pollution Engineering*, December, pp. 46–52 (1990).
2. Cioffi, J. C., W. R. Mahaffey, and T. M. Whitlock, "Successful Solid-Phase Bioremediation of Petroleum-Contaminated Soil," Remediation Vol. 1, No. 4, p. 373 (1991).
3. Middleton, A. C., D. V. Nakles, and D. G. Linz, "The Influence of Soil Composition on the Bioremediation of PAH-Contaminated Soils," Remediation Vol. 1, No. 4, p. 391 (1991).
4. Rittman, B. E., A. J. Balochi, and P. Bareye, "Fundamental Quantitative Analysis of Microbial Activity in Aquifier Bioremediation," *Progress Report*, DOE/ER/60-773-1 (1990).
5. Richter, J., "The Soil As A Reactor—Modeling Processes in the Soil," CATENA VERLAG, (1987).
6. Treybal, R. E., "Mass-Transfer Operations," 3rd edition McGraw-Hill Book Company, New York (1980).
7. Currie, J. A., Soil Respiration, in: *Soil Physical Conditions and Crop Production.—MAFF Bulletin*, **29**, pp. 461–468 (1975).
8. Li, K. Y., A. Kane, W. A. Cawley, and J. J. Wang, "Measurement of Biodegradation Rate Constants on An Water Extract from Oil Contaminated Soil," paper in printing, Waste Management.

RBC Nitrification Design Using Zero-Order Kinetics

Edward J. Opatken

U.S. Environmental Protection Agency, Risk Reduction Engineering Laboratory, Cincinnati, Ohio 45268

INTRODUCTION

The design of rotating biological contactor (RBC) systems for nitrifying municipal wastewater or leachates from hazardous waste landfills is based on empirical curves developed by the various manufacturers of RBCs. User communities have relied heavily on RBC manufacturers to provide design assistance and to specify the number of RBC units as well as their arrangements in stages and trains. User communities normally include a performance clause in their design specifications to ensure that the process will produce the desired effluent quality at a specified design flow, concentration, and temperature. The applicability of zero-order nitrification kinetics to the rate of oxidation or disappearance of ammonia nitrogen (NH_3-N) in RBCs has been previously established [*9*].

DESIGN PROCEDURE USING ZERO-ORDER KINETICS

The purpose of this paper is to illustrate the use of zero-order kinetics to incorporate nitrification in the design of an RBC treatment facility, illustrate the effect of temperature on the number of RBC units required, and define the rationale behind the steps employed in the design process. A step-by-step design procedure is presented below for an example design problem.

Step 1. Define Design Conditions (Assumed)

- Average influent flow rate = 5 mgd = 19,000 m^3/d = 210,000 gal/h = 800,000 L/h.
- Minimum wastewater temperature = 13°C = 55°F
- Maximum wastewater temperautre = 29°C = 85°F
- Average influent NH_3-N = 20 mg/L
- k_N = zero-order reaction rate constant for NH_3-N oxidation at 13°C = 5.8 mg/L h (see Figure 1).
- k_N = zero-order reaction rate constant for NH_3-N oxidation at 29°C is 13.2 mg/L h (see Figure 1).

Step 2. Established Final Effluent Quality Requirements

- NH_3-N ≤ 2 mg/L

Step 3. General RBC Design Conditions

RBCs are available in two sizes. A standard (STD) 25-ft (7.6-m) long RBC shaft contains 100,000 sq ft (9100 m^2) of media surface area, whereas a 25-ft (7.6-m) long high density (HD) RBC shaft contains 150,000 sq ft (14,000 m^2) of media surface area [*1*]. Normally, STD RBCs are located in the first two stages of a train where organic loadings are heaviest. HD RBCs are generally located in the rear stages of a train at a point where most of the incoming organics have been removed and nitrification can proceed. Use of HD RBCs in the first two stages would likely result in structurally overloaded shafts and media due to heavy bio mass growth. Since this paper is limited to only nitrification, HD RBCs are specified for all stages.

Step 4. Calculate the Hydraulic Residence Time (HRT) for One HD RBC Shaft

A design standard established by RBC manufacturers is a volume-to-surface area ratio of 0.12 gal/sq ft (5.0 L/m^2) [*2*].

$$\text{HD RBC Volume} = 0.12 \text{ gal/sq ft} \times 150{,}000 \text{ sq ft/shaft}$$

$$= 18{,}000 \text{ gal/shaft}$$

$$= 5 \text{ L/m}^2 \times 14{,}000 \text{ m}_2 \text{ shaft} = 70{,}000 \text{ L/shaft}$$

$$\text{HD RBC HRT} = \frac{V}{Q} = \frac{18{,}000 \text{ gal/shaft}}{210{,}000 \text{ gal/h}}$$

$$= 0.086 \text{ h/shaft} = 5.1 \text{ min/shaft}$$

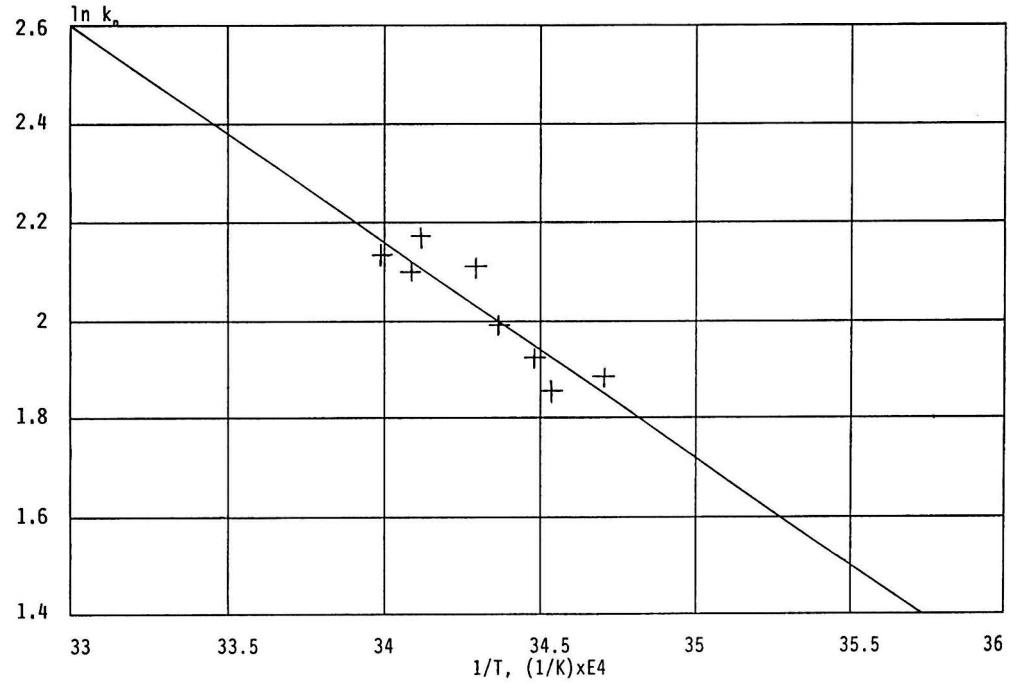

FIGURE 1. Effect of temperature on ammonia nitrogen rate constant (K) [5].

Step 5. Determine The Total Number of RBCs

The positioning of the RBC shafts in parallel or series arrangement is immaterial relative to its effect on the reaction volume needed to obtain a specific effluent NH_3-N level because of the zero-order relationship. The major factors that need to be addressed for ammonia nitrogen conversion are time, temperature, and ensuring a pH above 6. Other parameters, such as biomass concentration and oxygen transfer, must be adequate and not rate limiting. However, if carbonaceous soluble BOD (SBOD) removal is also specified, there is a decided advantage for positioning the RBC shafts in a series mode. Reaction kinetics for SBOD removal follow a second-order relationship [6], and a series arrangement will yield a significant reduction in surface area. This can be translated into a reduction in the capital costs when compared with placing RBC shafts in a parallel arrangement.

The total reaction time for nitrification can be calculated using a zero-order reaction rate constant. The reaction rate constant, k_n, at 13°C is obtained from the curve in Figure 1.

$$T = 273°K + 13°C = 286°K$$

$$1/T = 1/286 = 0.00349 = 34.9 \times 10^{-4}$$

From Figure 1, when $1/T = 34.9 \times 10^{-4}$, ln $k_n = 1.75$ and $k_n \approx 5.8$ mg/L h

The zero-order kinetic relationship for converting NH_3-N to NO_3-N is expressed by:

$$dC = k_n dt$$

where:

Table 1 Arrangement of RBC Shafts into Trains

RBC Array	No. of Trains	No. of RBC Shafts (Stages) per Train	Q/Train (gph)	HRT/RBC Stage (min)	Remarks
1×36	1	36	210,000	5.1	HRT <15 min
2×18	2	18	105,000	10.3	HRT <15 min
3×12	3	12	70,000	15.4	
4×9	4	9	52,000	20.8	
6×6	6	6	35,000	31.0	
9×4	9	4	23,000	47.0	
12×3	12	3	18,000	60.0	
18×2	18	2	12,000	90.0	
36×1	36	1	5,800	186.0	

Table 2 Ammonia Nitrogen Concentration for Each Stage at 13° (55°F)

Stage No.	NH_3-N (mg/L)
Influent	20
1	17
2	14
3	11
4	8
5	5
6	2

Table 3 Ammonia Nitrogen Concentration for Each Stage at 29°C (85°F)

Stage No.	NH_3-N (mg/L)
Influent	20.0
1	13.1
2	6.3
3	<1.0
4	<1.0
5	<1.0
6	<1.0

$dC = \Delta C = C_i - C_e$

C_i = influent NH_3-N concentration = 20 mg/L

C_e = final effluent NH_3-N concentration = 2 mg/L

k_n = zero-order reaction rate constant at 13°C = 5.8 mg/L h

$dt = \Delta t = \text{HRT} = C_i - C_e/kn = (20\text{-}2)/5.8 = 3.1$ h

The HRT required to nitrify the total volume of wastewater (5 mgd) for NH_3-N conversion is 3.1 h. The entire volume of wastewater will flow through one HD RBC shaft in 0.087 h or 5.2 min. The total number of HD RBC shafts required to obtain an HRT of 3.1 h is:

$$\text{Total No. of RBC Shafts} = \frac{3.1 \text{ h}}{0.087 \text{ h}} = 36$$

Step 6. Determine the RBC Shaft Arrangement

RBC shaft should be arranged in a configuration that will provide a minimum HRT of 15 min. per shaft or stage to ensure that each RBC shaft is completely mixed. The shorter the HRT the greater the probability that short circuiting of influent can occur. Dividing RBC units into parallel trains results in a greater HRT per shaft or stage because of the reduced volumetric flow to each RBC train. This is illustrated in Table 1 where one train with 36 shafts in series treats 210,000 gph and 36 trains in parallel with one shaft per train treat 5,800 gph per train.

With the exception of the 1×36 and 2×18 arrays, any of the other arrangements will meet the 15 min minimum HRT per shaft or stage. The 6×6 array is a compact layout plan with twice the required minimum HRT per shaft and is the preferred arrangement selected for this example design problem. A 6×6 array consists of six trains and six stages. Each stage is composed of six parallel shafts, such that each stage has $150{,}000 \times 6 = 900{,}000$ sq ft (84,000 m^2) of HD RBC media surface area.

Step 7. Determine the Ammonia Nitrogen Concentration in Each Stage

Influent flow to each of the six trains is 35,000 gph. The HRT in each of the six stages is 31 min or 0.52 h. The reaction rate constant, k_n, at 13°C (55°F) obtained from Figure 1 is 5.8 mg/L h. The concentration of NH_3-N in Stage 1 is obtained using the zero-order relationship.

$$\Delta C = k_n \Delta t$$

$$C_i - C_e = k_n \text{ HRT}$$

$$20 - C_e = 5.8 \text{ mg/L h} \times 0.52 \text{ h}$$

$$C_i = 17 \text{ mg/L}$$

The above calculation is repeated for Stages 2 through 6 to obtain the NH_3-N concentration in each stage. The NH_3-N concentration entering Stage 2 is the same as the concentration in Stage 1 = 17 mg/L. The results obtained from applying a zero-order reaction rate of 5.8 mg/L h in each stage are summarized in Table 2.

Step 8. Determine the No. of RBC Shafts Required at a Temperature of 85°F

Temperature has a significant effect on the NH_3-N oxidation or conversion rate and is best illustrated by comparing the number of RBC shafts required at the anticipated minimum operating temperature of 13°C (55°F) with the number required when operating at the anticipated maximum temperature of 29°C (85°F).

$$°K = 273 + 29°C = 302$$

$$1/T = 1/302 = .00331 = 33.1 \times 10^{-4}$$

From Fig. 1;

$$\ln k_n = 2.58$$

$$k_N = 13.2 \text{ mg/L h}$$

$$\Delta t_1 = 0.52 \text{ h}$$

Using $k_n = 13.2$, the concentration of NH_3-N in Stage 1 is calculated as:

Table 4 Effect of Temperature on RBC Media Surface Area Requirements

T °F	T °C	k_n (mg/L h)	HD RBC Shafts Required (No.)	HD RBC Media Surface Area Required (sq ft)
55	13.0	5.8	36	5.4×10^6
60	15.5	6.6	36	5.4×10^6
65	18.3	7.6	30	4.5×10^6
70	21.1	8.7	24	3.6×10^6
75	23.9	10.2	24	3.6×10^6
80	26.7	11.6	18	2.7×10^6
85	29.0	13.2	18	2.7×10^6

$$C_i - C_1 = k_n \Delta t_1$$
$$20 - C_1 = 13.2 \times 0.52$$
$$C_1 = 13.1^\circ \text{ mg/L}$$

This calculation is repeated using the zero-order kinetic equation until the NH_3-N concentration drops below 2 mg/L. The NH_3-N concentrations for all six stages are shown in Table 3.

Table 3 indicates that only three stages per train or a total of 18 RBC shafts are required to achieve an effluent NH_3-N below 2.0 mg/L when the system operates at 29°C (85°F). A capital savings of 18 HD RBCs would be realized if the system always operates at a temperature of 85°F (29°C). Only 45% of the NH_3-N would be removed with a three-stage RBC train during cold weather conditions when the wastewater temperaure is 13°C (55°F), whereas 95+% of the NH_3-N would be removed during warm weather with the same three-stage RBC train.

To illustrate the effect of temperature on RBC media surface area requirements, a summary of the number of RBC shafts required at various temperatures is displayed in Table 4. The table clearly shows that operating temperature has a significant effect on RBC media surface area requirements.

SUMMARY

The zero-order kinetic design procedure was used to illustrate an alternative approach for specifying the number of RBC shafts required to achieve a final effluent NH_3-N concentration. The arrangement of RBC shafts into stages is independent of parallel or series configuration when kinetics are zero-order. The effect of temperature on the NH_3-N reaction rate constant has a significant effect on the number of RBC shafts required to achieve a final effluent NH_3-N level.

LITERATURE CITED

1. "Envirodisc Rotating Biological Contactor System," Clow Corporation, WTD 880-0510.
2. Brenner, R. C, J. A. Heidman, E. J. Opatken, and A. C. Petrasek, "Design Information on Rotating Biological Contactors," EPA-600/2-84-106, June 1984.
3. "Process Design Manual for Nitrogen Control," U.S. Environmental Protection Agency, October 1975.
4. Antonie, R. L., *Fixed Biological Surfaces—Wastewater Treatment*, CRC Press, 1976.
5. Perry, R. H., D. W. Green, *Perry's Chemical Engineering Handbook*, McGraw Hill Book Company, Sixth Edition, 1984.
6. *Wastewater Engineering: Treatment Disposal Reuse*, Metcalf & Eddy, Inc., Second Edition, 1979.
7. Knox, K., "Leachate Treatment with Nitrification of Ammonia," *Water Resources*, Volume 19, No. 7, 1985.
8. Steiner, L., et al., "Demonstrating Leachate Treatment," U.S. Environmental Protection Agency, Solid Waste Management Series, Report SW-758, 1979.
9. Opatken, E. J., and J. J. Bond, "RBC Nitrification of High Ammonia Leachate," *Environmental Progress*, **10**, No. 1.

Developing Strategies for Compliance with OCPSF Regulations

Ralph L. Stephenson, Annette J. Kikta, Gary L. Clark, and Hassan M. Gomaa

The M. W. Kellogg Company, Houston, TX 77210

This paper presents a brief summary of the Organic Chemical, Plastics, and Synthetic Fibers (OCPSF) regulations and a 10 point plan for compliance with the regulations. Several practical examples are discussed concerning the application of this plan to actual facilities with emphasis placed on waste minimization methods.

INTRODUCTION

This paper presents a brief summary of the Organic Chemical, Plastics, and Synthetic Fibers (OCPSF) regulations and a 10 point plan for compliance with the regulations. Several practical examples are discussed concerning the application of this plan to actual facilities with emphasis placed on waste minimization methods. The following section contains the OCPSF regulation summary.

REVIEW OF THE OCPSF REGULATIONS

On 5 November 1987 the final ruling for 40 CFR 414, Effluent Guidelines and Standards for (OCPSF) was published in the federal register. These regulations define the effluent limitations and pretreatment standards for all applicable process wastewaters. The standards are divided into categories by products manufactured; Subpart B—Rayon Fibers; Subpart C—Other Fibers; Subpart D—Thermoplastic Resins; Subpart E—Thermosetting Resins; Subpart F—Commodity Organic Chemicals; Subpart G—Bulk Organic Chemicals; and Subpart H—Specialty Organic Chemicals. Within each category, standards for meeting best practicable control technology currently available (BPT), best available technology economically achievable (BAT), new source performance standards (NSPS), pretreatment standards for existing sources (PSES), and pretreatment standards for new sources (PSNS) are identified.

Determination of the relevant standards is dependent upon the source type and treatment method. Figure 1 is a flow chart identifying the steps required to determine applicable standards. The flow chart is applicable for every category of wastes regulated under 40 CFR 414.

For all categories, BAT is defined as the same level of treatment as BPT when the production is less than or equal to 5 MM lbs/yr. BPT effluent limitations for each of the subcategories are listed in Table 1. Pretreatment standards for existing and new sources for all categories are identical and are listed in Table 2. Direct discharge limitations for point sources that do and do not use end-of-pipe biological treatment are listed in Tables 3 and 4, respectively. Table 4 includes 2 organic compounds (acrylonitrile and 2,4-dinitrophenol) and 3 metals (chromium, copper, and nickel) not found in Table 2.

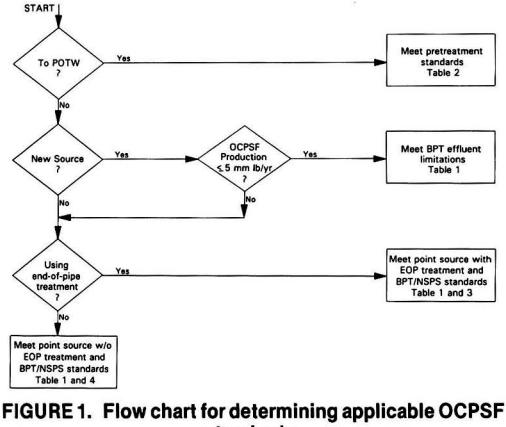

FIGURE 1. Flow chart for determining applicable OCPSF standards.

Table 1 BPT/NSPS Effluent Limitations for OCPSF Regulations

	BOD_5		TSS		pH
	Monthly[1] Average mg/L	Daily[2] Maximum mg/L	Monthly[1] Average mg/L	Daily[2] Maximum mg/L	
Subpart B Rayon Fibers	24	64	40	130	6–9
Subpart C Other Fibers	18	48	36	115	6–9
Subpart D Thermoplastic Resins	24	64	40	130	6–9
Subpart E Thermosetting Resins	61	163	67	216	6–9
Subpart F Commodity Organic Chemicals	30	80	46	149	6–9
Subpart G Bulk Organic Chemicals	34	92	49	159	6–9
Subpart H Specialty Organic Chemicals	45	120	57	183	6–9

(1) Maximum for monthly average
(2) Maximum for any one day

Table 2 Pretreatment Standards for Existing and New Sources for OCPSF Regulations

	Daily[1] Maximum μg/L	Monthly Average[2] Maximum μg/L
Benzene	134	57
Carbon Tetrachloride	380	142
Chlorobenzene	380	142
1,2,4-Trichlorobenzene	794	196
Hexachlorobenzene	794	196
1,2-Dichloroethane	574	180
1,1,1-Trichloroethane	59	22
Hexachloroethane	794	196
1,1-Dichloroethane	59	22
1,1,2-Trichloroethane	127	32
Chloroethane	295	110
Chloroform	325	111
1,2-Dichlorobenzene	794	196
1,3-Dichlorobenzene	380	142
1,4-Dichlorobenzene	380	142
1,1-Dichloroethylene	60	22
1,1-Trans-dichloroethylene	66	25
1,2-Dichloropropane	794	196
1,3-Dichloropropylene	794	196
Ethylbenzene	380	142
Methylene Chloride	170	36
Methyl Chloride	295	110
Hexachlorobutadiene	380	142
Nitrobenzene	6402	2237
2-Nitrophenol	231	65
4-Nitrophenol	576	162
4,6-Dinitro-o-cresol	277	78
Tetrachloroethylene	164	52
Toluene	74	28
Trichloroethylene	69	26
Vinyl Chloride	172	97
Total Cyanide	1200	420
Total Lead	690	320
Total Zinc	2610	1050

(1) Maximum for any one day
(2) Maximum for monthly average

Treatment plants placed in operation after 5 November 1987 were required to meet the OCPSF regulations. Facilities holding valid permits on that date were allowed to continue operation under their existing permits until the permits expiration date. As National Pollutant Discharge Elimination System (NPDES) permits are renewed, OCPSF regulations are incorporated. Plants will be required to re-evaluate their existing wastewater treatment systems and, if necessary, to upgrade their facilities to meet the new standards.

Existing facilities with OCPSF production of less than 5 MM lbs/yr of product will be required to meet only the BPT effluent limitations. These facilities must evaluate their current wastewater treatment with the new biochemical oxygen demand (BOD_5) and total suspended solids (TSS) standards. If the existing treatment processes are capable of meeting the limitations, but are not doing so currently, modifications to the operating parameters may be sufficient to meet the new guidelines. If the current treatment technology is not adequate, new treatment facilities will be required.

More stringent effluent guidelines for BOD_5, TSS, and priority pollutants will dictate improved performance from existing wastewater treatment plants (WWTP), modifications to existing WWTP, or replacements with new wastewater treatment facilities. All OCPSF manufacturers will need to review their existing treatment facilities and evaluate the ability or inability to meet the effluent guidelines. This will require a full characterization of the plant effluent including conventional parameters such as BOD, chemical oxygen demand (COD), pH, organics, and metals. In some cases, this will require effluent testing programs *not* currently underway. Once a characterization is completed, the manufacturer will need to determine the additional treatment facilities required to meet the limitations. In many cases, physical/chemical treatment will be insufficient to meet the new regulations. It is likely that biological treatment or activated carbon treatment will be required.

Recently promulgated rules under the Resource Conservation and Recovery Act (RCRA) as well as further modifications to the Clean Water Act (CWA) must be incorporated into plans for treatment plant upgrades. Construction of new wastewater treatment facilities also involves decommissioning and/or closure of existing facilities. Many existing facilities use unlined surface impoundments as part of their wastewater treatment plant. These impoundments fall within the jurisdic-

Table 3 Effluent Standards for Point Sources that Utilize End-of-Pipe Biological Treatment

	Daily[1] Maximum μg/L	Monthly Average[2] Maximum μg/L
Acenaphthene	59	22
Acrylonitrile	242	96
Benzene	136	37
Carbon Tetrachloride	38	18
Chlorobenzene	28	15
1,2,4-Trichlorobenzene	140	68
Hexachlorobenzene	28	15
1,2-Dichloroethane	211	68
1,1,1-Trichloroethane	54	21
Hexachloroethane	54	21
1,1-Dichloroethane	59	22
1,1,2-Trichloroethane	54	21
Chloroethane	268	104
Chloroform	46	21
2-Chlorophenol	98	31
1,2-Dichlorobenzene	163	77
1,3-Dichlorobenzene	44	31
1,4-Dichlorobenzene	28	15
1,1-Dichloroethylene	25	16
1,1-Trans-dichloroethylene	54	21
2,4-Dichlorophenol	112	39
1,2-Dichloropropane	230	153
1,3-Dichloropropylene	44	29
2,4-Dimethylphenol	36	18
2,4-Dinitrotoluene	285	113
2,6-Dinitrotoluene	641	255
Ethylbenzene	108	32
Fluoranthene	68	25
Methylene Chloride	89	40
Methyl Chloride	190	86
Hexachlorobutadiene	49	20
Naphthalene	59	22
Nitrobenzene	68	27
2-Nitrophenol	69	41
4-Nitrophenol	124	72
2,4-Dinitrophenol	123	71
4,6-Dinitro-o-cresol	277	78
Phenol	26	15
Bis(2-ethylhexyl) phthalate	279	103
Di-n-butyl phthalate	57	27
Diethyl phthalate	203	81
Dimethyl phthalate	47	19
Benzo(a)anthracene	59	22
Benzo(a)pyrene	61	23
3,4-Benzofluoranthene	61	23
Benzo(k)fluoranthene	59	22
Chrysene	59	22
Acenaphthylene	59	22
Anthracene	59	22
Fluorene	59	22
Phenanthrene	59	22
Pyrene	67	25
Tetrachloroethylene	56	22
Toluene	80	26
Trichloroethylene	54	21
Vinyl Chloride	268	104
Total Chromium	2770	1110
Total Copper	3380	1450
Total Cyanide	1200	420
Total Lead	690	320
Total Nickel	3980	1690

(1) Maximum for any one day
(2) Maximum for monthly average

Table 4 Effluent Standards for Point Sources that Do Not Utilize End-of-Pipe Biological Treatment

	Daily[1] Maximum μg/L	Monthly Average[2] Maximum μg/L
Acrylonitrile	232	94
Benzene	134	57
Carbon Tetrachloride	380	142
Chlorobenzene	380	142
1,2,4-Trichlorobenzene	794	196
Hexachlorobenzene	794	196
1,2-Dichloroethane	574	180
1,1,1-Trichloroethane	59	22
Hexachloroethane	794	196
1,1-Dichloroethane	59	22
1,1,2-Trichloroethane	127	32
Chloroethane	295	110
Chloroform	325	111
1,2-Dichlorobenzene	794	196
1,3-Dichlorobenzene	380	142
1,4-Dichlorobenzene	380	142
1,1-Dichloroethylene	60	22
1,1-Trans-dichloroethylene	66	25
1,2-Dichloropropane	794	196
1,3-Dichloropropylene	794	196
Ethylbenzene	380	142
Methylene Chloride	170	36
Methyl Chloride	295	110
Hexachlorobutadiene	380	142
Nitrobenzene	6402	2237
2-Nitrophenol	231	65
4-Nitrophenol	576	162
2,4-Dinitrophenol	4291	1207
4,6-Dinitro-o-cresol	277	78
Tetrachloroethylene	164	52
Toluene	74	28
Trichloroethylene	69	26
Vinyl Chloride	172	97
Total Chromium	2770	1110
Total Copper	3380	1450
Total Cyanide	1200	420
Total Lead	690	320
Total Nickel	3980	1690
Total Zinc	2610	1050

(1) Maximum for any one day
(2) Maximum for monthly average

tion of the RCRA. Under RCRA authority, a number of regulatory issues apply. Depending upon waste characteristics, closure of impoundments could involve; (1) RCRA Corrective Action, (2) the Toxicity Characteristic Rule, (3) Land Disposal Restrictions, and (4) RCRA Closure and Postclosure Requirements. As new NPDES permits are issued, state regulators also will incorporate requirements for water quality standards and effluent toxicity testing. These requirements also must be included in the development of the overall plan for the new wastewater treatment facilities. Construction schedules will need to be prepared which incorporate compliance deadlines for all the regulations involved.

THE TEN POINT WASTEWATER COMPLIANCE MASTER PLAN

The development of a cost-effective approach to compliance with OCPSF regulations requires a well-planned strategy. The M. W. Kellogg Company has developed a ten point master

plan which is applicable for the development of chemical plant wastewater compliance programs. This plan is designed to define correctly the most cost effective means of compliance with wastewater regulations. Steps required to develop this plan are as follows:

Comprehensive Flow Diagram and Description of Existing System

The first step is to gather a database of all relevant engineering, design, and analytical data information on existing wastewater collection and treatment systems. This database consists of the following types of information:

- Process Flow Diagrams
- Piping and Instrument or Mechanical Flow Diagrams
- Design Basis for Facilities
- Operating Manuals
- NPDES Analytical Data
- Operating Records and Analytical Data
- Copies of all permits (NPDES, RCRA, Clean Air Act (CAA), etc.)
- Plans of Conveyance Facilities
- Plans of Wastewater Treatment Facilities
- Engineering Files
- Metering Data (Water and Wastewater)

Included in this database is a comprehensive flow diagram which shows in block form all sources of wastewater, all conveyance facilities, and all wastewater process units. This block flow diagram (BFD) is generated through analysis of the above listed information.

Source Database

A source database then is created showing sources of wastewater and their composition. The method to accomplish this is to develop a water and mass (pollutants) balance for the entire facility, starting with water treatment facilities, then develop water and mass balances for each process unit, and finally combine all the information into an overall water and mass balance for the facility.

The water and mass balance is generated by first analyzing information found in Step 1, then interviewing unit process engineers and operating personnel to determine the flow rates, pollutant concentrations, locations, and frequencies of wastewater entering sewer systems. Exact, or even approximate, analyses of many wastewater streams are unknown. Flow rates for wastewater streams may be accurate to + or − 10%, but the pollutant concentrations in the wastewater will not be known with sufficient accuracy.

If the quality and/or quantity of wastewater cannot be determined by process knowledge, then a sampling and flow measurement plan may be required. Such a plan should contain, as a minimum, the following elements:

- Goals and objectives of the plan
- Sampling locations and rationale for selection
- Procedures for sampling and flow measurement
- Analytical requirements
- Chain of custody procedures

Upon completion of the sampling plan, a final water flow and mass balance is generated, and all regulated wastewater streams will have been identified properly.

Document Planned and Potential Facility Expansions

Any planned expansions of the facility and/or modifications to existing process units should be identified so projections of future wastewater discharge loads can be determined. Projections could be made from knowledge of the process, from data of similar operating units, or from process design calculations. Estimates of flow and quantity will be used with information obtained in the previous step to project expected wastewater flow and quantity.

Evaluate Regulatory Requirements

A key to developing a cost-effective wastewater compliance progam is to identify and analyze applicable regulatory issues affecting collection, treatment, and discharge of wastewater. A projection of anticipated future regulatory requirements must be made so that today's facility design will not become obsolete. Objectives of this step are:

- Define current regulatory requirements
- Identify a schedule for regulatory promulgation (future regulations)
- Identify regulatory compliance dates applicable to the plant
- Project requirements of any proposed regulations
- Forecast the direction of regulations

Laws and regulations that impact wastewater systems have expanded greatly in the past few years, and there is an increasing overlap of regulations from other areas that impact wastewater systems. Wastewater was and still is regulated primarily by the CWA. However, in the past few years, CAA, RCRA, and other acts have evolved many regulations that directly impact wastewater systems. Some examples are regulation of emissions of volatile organic compounds (VOCs) and hazardous air pollutants from wastewater by the CAA; and phased elimination of certain types of waste treatment facilities and design standards for other facilities required by RCRA. Further, projections of future regulations can be made on the basis of laws passed that require promulgation of regulations yet to be written. A plant master compliance plan must be developed with predictions of future environmental laws and regulations based upon known regulatory trends. Of all the steps contained in this plan, there undoubtedly are none that will have a greater economic impact than correctly determining the impact of present and projected future regulations.

Determine if Conveyance and/or Treatment Improvements are Required

Information found in Steps 1 through 3 must be analyzed, using the requirements in Step 4, to determine if improvements to the conveyance and/or treatment systems are required. This study will identify:

- What parts or units of the conveyance and treatment facilities require improvements for compliance
- Objectives of the improvements
- Date by which improvements must be operational
- Regulatory exemptions or extensions that can be applied
- Determination if regulatory noncompliance is a global (plant wide) or isolated (few streams) problem

Existing facilities may be in compliance with current regulations, but may not be with future regulations. If an existing facility is in compliance with existing and anticipated future regulations, then the analysis can be ended. If not, then proceed to the next steps in the plan.

Frequently, waste minimization and at-source treatment opportunities are identified in Steps 1 through 3. Note that waste minimization and at-source treatment often can be cost-effective even when a facility already is in compliance with regulations.

Develop and Evaluate Options for Waste Prevention/ Minimization, System Modifications, and New Construction

If it is determined from Step 5 that improvements must be made to comply with regulations, then alternatives for compliance can be developed using information gathered in Steps 1 through 4. Alternatives are best organized and ranked, from an pollution elimination effectiveness standpoint, using the waste management hierarchy shown as follows:

- Eliminate waste by process modifications, changing processes, operational changes.
- Recycle wastes to other processes, off-site facilities.
- Reduce amount of wastes produced by process modifications, changing processes, operational changes.
- Treat wastes at-source where they are more concentrated and easier to treat. This also eliminates conveyance problems.
- Treat wastes at the end-of-pipe.

Brainstorming sessions are held to generate a complete list of alternatives. All alternatives that can be imagined should be listed, then the obviously impractical alternatives can be eliminated. Alternatives considered impractical sometimes can become practical when all factors are considered, and impractical alternative generation frequently stimulates thinking so that more practical, but unconventional, alternatives can be generated. Remaining alternatives are evaluated carefully for risk of noncompliance, capital and operating costs, operability, and schedule impacts.

Risk of noncompliance is an issue that deserves careful study. Most alternatives present some risk of noncompliance, and the potential economic impact, potential publicity, and potential criminal actions must be considered carefully for each alternative. Again, the waste management hierarchy previously mentioned is, in general, hierarchy of least to greatest risk. Not producing a waste or minimizing production of wastes is far less risky than storing, conveying, and treating it.

Develop an Integrated Conceptual Plan of Upgrades, Schedules, and Cost Estimates

Once viable alternatives are identified from the preceding step, an integrated conceptual plan for upgrades, including schedules and cost estimates, can be made. The chosen alternatives are developed conceptually into designs by creating process flow diagrams, major equipment lists, and equipment layouts. Equipment costs and delivery times are obtained so that order of magnitude cost estimates and construction schedules can be made. Using this data, order of magnitude cost estimates for various alternatives can be developed, evaluated, and ranked for cost-effectiveness.

Check for Constructability, Safety, and Schedule

Construction and safety experts should be consulted on the constructability and safety issues of proposed modification(s) to the facilities. Constructability issues include type of materials, machinery usage (type and manuverability), foundation design techniques, layout of equipment, sequence (staging) of installation, safety, permitting (in plant), work space access, and obstructions. In validating constructability aspects associated with modifications, the following general considerations should be addressed for each equipment item affected:

- Safety
- Permitting
- Staging and Storage Areas
- Site Access
  - —Oversize Loads
  - —Working Clearances
- Construction Utilities
- Obstructions
- Construction Schedule
  - —Equipment Shutdowns
  - —Material Deliveries
  - —Coordination and Sequencing
  - —Process Disruptions

Potential scheduling conflicts with other projects, turnarounds, and regulatory deadlines should be evaluated. Frequently, costs can be reduced with a constructability review. Scheduling conflicts can be a source of increased costs that can be avoided if correctly ascertained at this point.

Comprehensive Facility Group Review

The proposed compliance plan should be reviewed by all concerned in the facility, including environmental, engineering, operating, and safety personnel, as well as management and legal. This review will allow suggestions for improvements to be made.

Implementation of the Compliance Plan

The compliance plan is divided into specific projects at this time, if not already done, and the various identified projects can be prioritized. Schedules and deadlines for each project should be developed, and the engineering, procurement, and construction costs can be estimated, together with projections of cash flows.

CASE HISTORIES

The use of the Ten Point Wastewater Compliance plan can be illustrated by the following case histories.

Case History 1—Synthetic Pulp and Reaction Molding Resins Plant

The plant contained two distinct operating units, a synthetic pulp (fibers) production unit and a reaction molding resins unit. The synthetic pulp plant had to meet Subpart C and the resins unit had to meet Subpart D for BOD and TSS requirements. Combined flow from both units had to meet section 414.101, Subpart J requirements. Facility permits for the combined discharge had NPDES requirements for BOD and TSS which were more stringent than the OCPSF requirements. The OCPSF pH requirement of 6–9 was the same as the NPDES requirement which was met easily.

The synthetic pulp unit produced fibers from polyethylene and polypropylene fluff. The fluff was dissolved in a solvent from which fibers were flash spun into a treated water bath. Fibers were processed similarly to wood pulp and dewatered into sheets of pulp. Water from the synthetic fiber plant was treated by pH adjustment, solids separation, and carbon adsorption before being discharged.

The base plastic and wetting agents added to the water bath are not toxic; they typically are used in food wraps and contact lens solutions. However, chemical additives and biocides used for fiber property enhancement and product preservation were suspected as potential contributors to OCPSF chemicals in the wastewater. By-products from biocide and chemical additive interaction and their reactions with microbes were not known. Some of these chemicals additives and biocides were ethylene acrylic acid, maleic anhydride, cellulose from the Kraft process, methylene bis thiocyanate, and thiocyanomethylthiobenzothiazole, epicholorhydrin, toponal, and sodium hypochlorite.

The resins unit produced two components for reaction in-

jection molding into large structural composites at customers' locations. Process wastewater was treated by a simple gravity separator and discharged to combine with treated wastewater from the synthetic pulp unit. The resins unit was designed with dikes around intermediate, off-specification, and raw material storage tanks and curbing around the paved process unit. Wastewater was comprised of cooling tower blowdown, steam-outs and flushing waters, and first flush stormwater. When sufficient rain fell, hubs were removed manually in the curbed process area to permit remaining stormwater to flow with nonprocess stormwater into the synthetic pulp plant stormwater basin.

The resins unit blended many ingredients including dicyclic hydrocarbon monomers, catalysts, co-catalysts, odorants, emulsifiers, additives, and stabilizers into unreacted monomer formulations. Active ingredients in the raw materials were identified, but trace components were not known. All chemicals in the resins unit were suspect for containing OCPSF chemicals, but because the process was closed and blended resins froze at ambient temperatures, the wastewater was not expected to show significant quantities of any OCPSF chemicals.

Utilization of the 10 point master plan organized the approach for sampling and analysis to determine whether or not the plant was in compliance with OCPSF regulations. The first five points of the master plan were used and these points are referenced by number in the following discussion.

Point 1

The database of process flow drawings, piping and instrumentation diagrams (P&IDs), material balances differentiated by product manufacture, actual effluent flow data, and known contaminants in the effluent were compiled. This information was used to create a database of the known composition of wastewater streams from each unit for each product. This included identifying for each product formulation, raw materials used and streams which contribute to the unit wastewater flow.

Point 2

A sampling plan was developed to take samples from the pulp unit after treatment and from the resins unit at the sewer collection point. In accordance with the plan, samples were to be taken further upstream in the sewer system if warranted by analyses of the collection point samples (see Figure 2). Additionally, the database was expanded to include infrequent sources of wastewater. From the synthetic pulp unit, infrequent flows included equipment flushing for microbial decontamination, additive drum flushing, maintenance procedures, and backflushing the carbon bed. From the resin unit, infrequent flows resulted from line steaming and from unit washdown. By the sampling plan, samples were to be collected from flushing procedures only if OCPSF chemicals were found in wastewater collection point samples because flushing and maintenance procedures did not introduce any new chemicals.

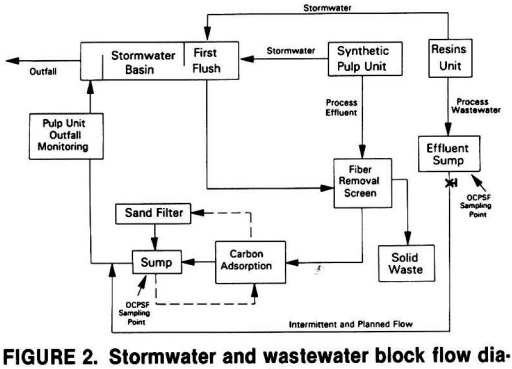

FIGURE 2. Stormwater and wastewater block flow diagram for Case 1

Point 3

Planned facility expansions were well into the future so future pollutant loads were not of concern. Possibilities of producing new grades of resins and synthetic pulp were anticipated, but the decision was made to address impacts to wastewater quality with OCPFS chemicals on a case by case basis. The cost to prevent OCPSF pollution or remove a OCPSF chemical from wastewater was to be considered in the manufacturing cost of the future grade of resin or pulp.

Point 4

Because each production unit produced "wild card" products, they would be in operation only seven to ten years unless the products were a success. Capital investment was limited to necessities and high return on investment projects. Planning for a 5 or 10 year regulatory window was not accepted, however compliance with current law and regulations 1 to 2 years into the future was given high priority.

Point 5

To determine if conveyance or treatment improvements were required, more information was needed. An outside laboratory was contracted to analyze samples. Within the limited budget for analyses, sufficient samples were taken to determine if OCPSF contaminants existed in manufacturing the normal product grades. The laboratory was required to run quality checks and to report these findings along with the analyses. Prior to determining whether a contaminant was at a level for concern, quality control documentation was reviewed thoroughly to ensure analytical accuracy.

All chemicals listed in Table 4 were run on the samples taken from each unit. Results of analyses are reported on Tables 5 and 6 for those organic chemicals showing levels greater than the Method Quantification Level. The analyses did not show that any significant chemical levels could be found in wastewater discharging from the synthetic pulp unit. From the reaction molding resins unit, the only analytical result which exceeded the daily maximum limit was the value for methylene chloride obtained from the 15 September sample. From the process chemistry, presence of this chemical was not evident and without finding the chemical in subsequent samples, it was decided that this analysis was not of concern.

The analysis showed facility units met stringent requirements for OCPSF chemicals in the wastewater (this included the manufacture of all grades of pulp and resins). The company informed the Environmental Protection Agency (EPA) and the state regulatory agency that both units met the OCPSF regulations. Analytical results were maintained for proof of compliance.

The approach for identifying OCPSF chemicals from the facility using the 10 point plan were included as a guidance documentation in the Environmental Compliance Manual which was maintained at the facility. The document provided a consistent approach for identifying wastewater chemical contaminants and evaluating prevention and treatment options. The application could be applied to future expansions, introduction of new chemicals, and development of new products.

Table 5 Synthetic Pulp Unit

	MQL µg/L	NOV 2 S/B µg/L	OCT 21 S/B µg/L	OCT 13 S/B µg/L	OCT 7 S/B µg/L	SEP 6 S/B µg/L
Gas Chromatography/Mass Spectrometry Analysis						
Chloroform	1.7	2/ND	<MQL/ND	2/ND	<MQL/N	7/ND
Toluene	1.7	4/6	4/6	4/6	4/6	<MQL/<MQL
Bis(2-ethylhexyl) phthalate	4	24/<MQL	10/15	ND/60	<MQL/60	<MQL/ND
EPA and SW846 Analyses						
Total Chromium		<0.01	<0.01		<0.01	0.01
Total Copper		<0.01	<0.01		<0.01	<0.01
Total Cyanide		<0.01	<0.1		<0.1	<0.1
Total Lead		<0.05	<0.05		<0.05	<0.05
Total Nickel		<0.01	<0.01		0.01	0.02
Total Zinc		0.04	0.02		<0.01	0.02

MQL: Method Quantitation Limit
ND: Not Detected
S: Sample
B: Blank

Case History 2—Gasoline Additives Plant

A gasoline additives manufacturing facility had a primary treatment facility that consisted of an old American Petroleum Institute (API) separator followed by lagoons. The plant discharged effluent from lagoons into a refinery wastewater plant. Lagoons were RCRA waste management units and were required to be closed. A flow diagram of these facilities is shown as Figure 3.

Utilization of the 10 point master plan organized the approach for solution of anticipated regulatory noncompliance problems.

Points 1 and 2

Management had performed a number of studies which conformed to the first five points of the master compliance plan. During development of the first two points, namely development of a comprehensive flow diagram, and generation of a source database, it was determined that 8 OCPSF chemicals were in the wastewater, as well as RCRA regulated compounds.

Table 6 Reaction Molding Resins Unit

	MQL µg/L	DEC 13 S/B µg/L	OCT 27 S/B µg/L	SEP 15 S/B µg/L
Gas Chromatography/Mass Spectrometry Analysis				
Diethyl Phthalate	1		2/ND	
Bis(2-ethylhexyl) phthalate	3	9/21		
Methylene Chloride	3.3			3400/ND
Phenol	2	5/<MQL		
EPA and SW846 Analyses				
Total Chromium		<0.01	<0.01	
Total Copper		0.01	0.02	
Total Cyanide		<0.1	<0.01	
Total Lead		0.08	<0.05	
Total Nickel		0.02	<0.01	
Total Zinc		0.3	0.04	

MQL: Method Quantitation Limit
ND: Not Detected
S: Sample
B: Blank

Point 3

There were no plans then for any expansions or deletions at the facility, so the source database was accepted as influent for future facilities.

Point 4

The regulatory review performed by plant staff revealed that RCRA facilities would have to be closed and replaced. The API separator was old and cracked and it was decided to replace it to comply with anticipated future regulations. In addition, management had decided ultimately to build their own wastewater plant which would be required to meet OCPSF and NPDES requirements. Thus, phased construction of a complete new treatment facility was determined to be necessary to meet future regulations.

Point 5

The regulatory review had determined what treatment improvements would be required. It was decided that the first phase would be closure of RCRA lagoons and replacement of all primary facilities. Future phases would complete the construction of the wastewater treatment plant. Conveyance facilities were examined and found to be not in compliance with RCRA and VOC regulations which were to become effective within about two years, so conveyance improvements also were planned. These consisted of replacement of a ditch and un-

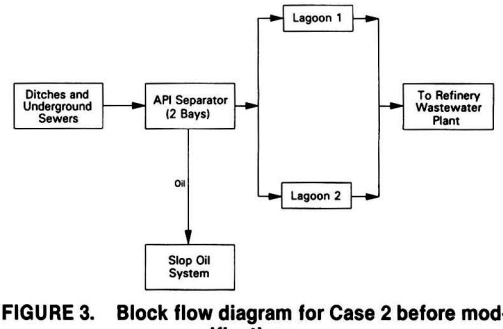

FIGURE 3. Block flow diagram for Case 2 before modifications

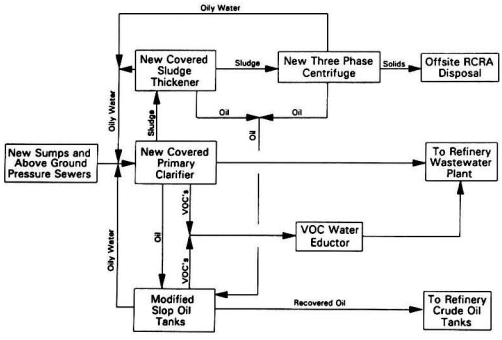

FIGURE 4. Block flow diagram for Case 2 after modifications

derground sewer system with a pumped above ground pressure sewer system to meet RCRA minimum technology requirements (MTR) and VOC requirements. It also was decided that new primary facilities would include flow equalization, primary clarification, sludge thickening and dewatering, and slop oil treatment. All facilities would be designed ultimately to meet VOC and MTR standards in a phased manner, and meet OCPSF and NPDES treatment standards.

Point 6

An engineering and construction (E&C) company was hired to develop and evaluate options for system modifications described above. Management of the chemical company did not feel that waste prevention/minimization steps were feasible after a preliminary review so these activities were not in the scope of work for the E&C company. Further examination of the data by the E&C company led to recommendation for combining primary treatment and flow equalization steps by building a larger primary clarifier to handle surges in flow. Modifications to existing slop oil tanks were investigated and it was found that they could be modified to meet new regulations by internal modifications, by adding VOC facilities, and by adding secondary containment. Note that the VOC's included both OCPSF compounds and RCRA compounds. The final configuration decided upon is illustrated in Figure 4 and consisted of a new closed sump and header system for wastewater conveyance, a covered vapor tight primary clarifier, a covered but not vapor tight sludge thickener, three modified slop oil tanks to be made vapor tight, a three phase centrifuge for dewatering and deoiling, a VOC system which removed VOC's from the clarifier and slop oil tanks and sent the VOC's to refinery wastewater plant in a separate stream for treatment. It was planned in future phases to treat the VOC's on site.

Point 7

Then the E&C company conceptually designed the facilities, developed schedules for construction, and generated a cost estimate. Equipment vendors were contacted and information on available equipment was obtained, including costs. The BFD for these facilities is illustrated in Figure 4. Equipment layouts, BFD's, P&ID's, and equipment lists were prepared.

Point 8

A constructability, safety, and schedule review was performed with participation by both the E&C and chemical companies experts. Tanks were found to be too close together for effective construction, and severe foundation problems were discovered. The tanks were placed further apart, and foundation and piping designs were changed to allow more settlement.

Point 9

The comprehensive facility group review resulted in minor changes in the design to improve operability. The centrifuge platform was expanded and a monorail was added for maintenance. Other minor modifications were made to improve accessability for operating personnel.

Point 10

The E&C company prepared bid packages for various components, in this case divided into construction specialty packages, received bids, and awarded contracts. The facility was built within budget and was operational on schedule. It should be noted that the chemical company previously had awarded contracts for closure of RCRA facilities, so these facilities were closed by the time construction started on their replacements. Flow was diverted to the refinery wastewater plant during this interim period, with no permit violations. Most of the OCPSF compounds were removed as VOC's by the facility, and future additions planned included biological treatment and VOC destruction facilities for complete removal of OCPSF compounds.

SUMMARY AND CONCLUSIONS

Many facilities will require upgrading to meet new limits defined in the standards. The 10 point plan provides an organized approach to identify contaminants, their sources, and cost-effective treatment alternatives. Wastewater volume and contaminant load reduction should be considered first, with at-source treatment considered second, and end-of-pipe treatment considered last, i.e., the waste management hierarchy should be followed as this is the route toward the greatest cost effectiveness.

Some of the processes that can be considered for both at-source treatment and end-of-pipe treatment are activated sludge treatment, granular activated carbon treatment, powdered activated carbon treatment, steam and air stripping, chemical and ultraviolet light oxidation, and metals precipitation or ion exchange. Treatment process evaluations have shown that OCPSF regulations can be met by using one or more of these treatment systems. The choice of process depends upon the characteristics of the wastewater stream.

Compliance with OCPSF regulations certainly will have a significant cost impact on the OCPSF industry. New treatment systems costs easily can go into the millions and do not increase the plant profitability. Only fines for noncompliance can be considered as money saved by utilization of the new system.

ACRONYM LIST

API	American Petroleum Institute
BAT	Best Available Technology
BFD	Block Flow Diagram
BOD	Biochemical Oxygen Demand
BPT	Best Practicable Technology
CAA	Clean Air Act
COD	Chemical Oxygen Demand
CWA	Clean Water Act
E&C	Engineering and Construction
EPA	Environmental Protection Agency

MTR	Minimum Technology Requirements (RCRA)
NPDES	National Pollutant Discharge Elimination System
NSPS	New Source Performance Standards
OCPSF	Organic Chemical, Plastics, and Synthetic Fibers
P&ID	Piping and Instrumentation Diagram
PSES	Pretreatment Standards for Existing Sources
PSNS	Pretreatment Standards for New Sources
RCRA	Resource Conservation and Recovery Act
TSS	Total Suspended Solids
VOC	Volatile Organic Compound
WWTP	Wastewater Treatment Plant

LITERATURE CITED

1. U.S. E.P.A. "Effluent Guidelines and Standards for Organic Chemicals, Plastics, and Synthetic Fibers," *40 CFR 414*, (1992).
2. Ballard, R. W., et al., "Micronutrient Addition and Its Impact on WWTP Performance," *Environmental Progress*, **11**(1), pp. 80–83 (1992).
3. Cooper, A. M., K. D. Torrens, and J. L. Musterman, "On-Site Evaluation of Treatment System Requirements to Satisfy Direct and Indirect Discharge Limits for a Complex Industrial Wastewater: A Case Study," *Environmental Progress*, **11**(1), pp. 18–26 (1992).
4. Friday, T. L., and Rakesh Gupta, "Selection of Treatment Process to Meet OCPSF Limitations," *Environmental Progress*, **10**(3), pp. 218–224 (1991).
5. Cable, J. K., et al., "Integration of RCRA Corrective Action with Clean Water Act," *Environmental Progress*, **11**(2), pp. 85–90 (1992).

Wet Oxidation System— Process Concept to Design

John E. Sawicki and Baldomero Casas

Air Products and Chemicals, Inc., 7201 Hamilton Boulevard, Allentown, PA 18195

A wet oxidation process was developed to treat waste water from an organic nitration process. The waste water contained EPA listed priority pollutants including dinitrotoluene, 2-nitrophenol, 4-nitrophenol, 2,4-dinitrophenol, 4,6-dinitro-ortho-cresol and phenol. The process design was based on experimental data generated in both batch and continuous laboratory and pilot scale reactors and in cooperation with university researchers, a private development company and an engineering company. Process variables included temperatures between 250 and 500 C, pressures in the 23,000–28,000 kPa (3,450–4,000 psi) range and residence times between 1 and 7 minutes.

The final design was a tubular reactor operating at temperatures slightly below the critical temperature for water and short residence times. Destruction efficiencies for most of the priority pollutants were greater than 99% and final concentrations were below those specified by EPA regulations.

INTRODUCTION

The Environmental Protection Agency (EPA) issued categorical effluent limitations for the organic chemicals, plastics, and synthetic fiber (OCPSF) industries to control specific priority pollutants on November 5, 1987. Indirect dischargers to publicly-owned treatment works (POTW) are subject to discharge limitations under the Pre-treatment Standards for Existing Sources (PSES) section of the regulations. These limits must be met at the discharge point of the chemical production facility before reaching the POTW. These limits are given in Table 1 for those regulated compounds typically found in the effluents from an aromatic nitration process, specifically, the nitration of toluene to dinitrotoluene.

To meet the regulation's standards, several environmental technologies were investigated. Among the considered options were:

- Deep well injection
- Biological treatment/carbon adsorption
- Carbon adsorption
- Wet air oxidation

Deep well injection was eliminated from consideration because of potential future regulations and long term liabilities while the combined biological treatment/carbon adsorption process required more surface area than available in the process area. It was evident that capital investment would be substantial regardless of the technology since the waste water flow rate varies between 150 and 300 gallons per minute.

Contacts were made with The University of Texas at Austin (Center for Energy Studies), Modar, Inc., and ABB Lummus Crest. All three were currently active in wet oxidation and the overall purpose was to compress the schedule for developing a wet oxidation process specifically designed to treat the aqueous waste generated in a toluene nitration process. The University of Texas at Austin would provide feasibility information and interact with the EPA as expert consultants. Modar and Lummus Crest would assist in developing the process based on the information generated in the feasibility studies. The organizational interactions are depicted in Figure 1.

Table 1 Limits on Priority Pollutants

Compound	Monthly Average (ppb)	Typical (ppb)	Required Removal (%)
2,4-Dinitrotoluene	113	630000	99.98
2,6-Dinitrotoluene	155	250000	99.90
Nitrobenzene	27	0	0
2-Nitrophenol	41	250	83.60
4-Nitrophenol	72	350	79.43
2,4-Dinitrophenol	71	2000	96.45
4,6-Dinitrocresol	78	9000	99.13
Phenol	15	20000	99.93
Toluene	26	0	0
Total Cyanide	420	55000	99.24

WET AIR OXIDATION BACKGROUND

Wet air oxidation is a process which oxidizes material in the liquid (or dense fluid) phase. Material capable of combustion under normal conditions (i.e. incineration) is also capable of undergoing wet oxidation. Unlike incineration, however, the temperatures are lower and residence times longer, and, as the process occurs "under water", vapor emissions are less than expected for a typical incinerator. The products of wet oxidation of organics are usually ammonia and a variety of low molecular weight organic compounds (mostly acetic acid), plus carbon dioxide and water [*1*]. Some literature states that oxidation cannot occur at temperatures above the fluid's critical point because liquid water is necessary for the chemistry to proceed [*2, 3*].

Most applications for this type of process are municipal and industrial sludge treatment [*4–11*], several deal with treatment of organics in industrial aqueous waste streams [*12–19*]. The two reactor configurations are; conventional, or above ground, and vertical, or below ground. Conventional reactors can be classified as "vessels" or tubular [*2, 3*]. The advantages of a vertical reactor (below ground level) are in energy conservation due to efficient counter current heat transfer and lower capital costs for pumping equipment; high pressures are achieved by the hydrostatic pressure of the liquid column.

In concept, a vertical reactor is relatively simple (Figure 2). A set of concentric tubes is placed in a deep "well" which is suitably encased to protect the surrounding environment. Aqueous waste is introduced into the center tube with a oxidizing agent. The oxidation of organics takes place as the pressure increases near the bottom of the tube. As the oxidized waste water flows up the annulus, heat is exchanged with the down-flowing feed stream. At steady state, fuels may be added to generate the necessary temperature. Typical, well depths for below ground system are between 1,200 and 1,800 meters (4,000–6,000 feet). At these depths, pressures between 9,700 and 13,800 kPa (1,400–2,000 psi) are achieved.

In a conventional reactor, location and physical area become problems. At high pressures, safety precautions become a primary concern. But maintenance is simplified and reactor flexibility is improved; multiple injection points for the oxidant are possible.

The oxidizing gas can be either air or oxygen. The advantage of using air is the elimination of oxygen generation and/or storage of liquid oxygen and its associated equipment (e.g. evaporators, metering devices, loading/unloading stations). Air is also readily available. But the oxygen in air is nominally 20 vol %, the remainder (nitrogen) is an unreactive diluent which requires that large volumes of the gas be delivered to the reactor. This results in larger compressors and reactor volumes. In general, oxygen's advantages out-weigh its disadvantages and it is the preferred oxidizing medium.

As temperatures and pressures exceed the critical point of water, the system is said to be in the supercritical regime. Under this condition, the following properties become evident:

- The solubility of organics in supercritical water increases dramatically to the point where normally

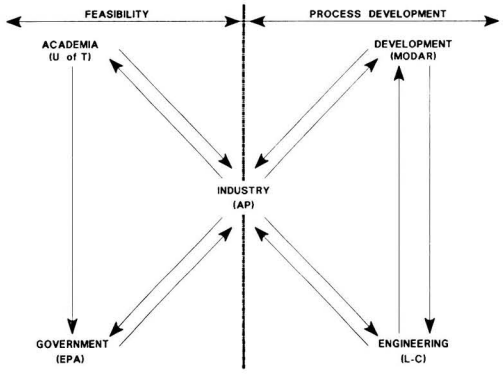

FIGURE 1. Organizational interaction.

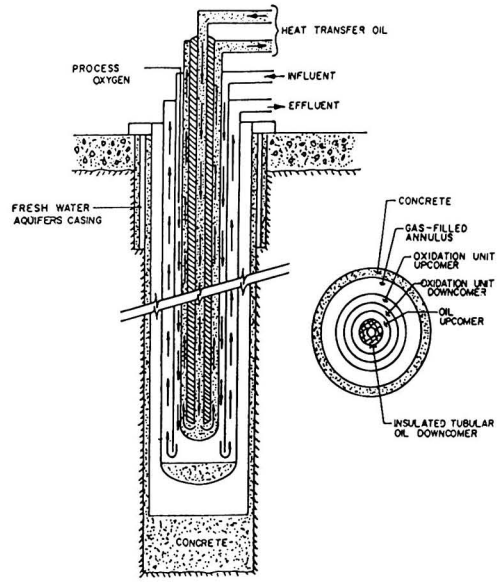

FIGURE 2. Vertical reactor.

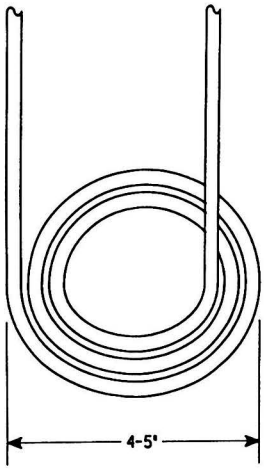

COIL HALF FILLED WITH LIQUID
FOR MAXIMUM INTERFACIAL AREA

FIGURE 3. Batch reactor design.

immiscible compounds form homogeneous mixtures.

- The solubility of gases increases to form homogeneous mixtures.
- Inorganic materials (e.g. salts) which are normally soluble in water are virtually insoluble in the supercritical regime.
- The viscosity of the fluid decreases.
- The surface tension of supercritical water is negligible.
- The density of supercritical water decreases.

Many of these properties contribute to the efficiency of oxidation. The system will operate homogeneously, thus eliminating mass transfer considerations, negligible surface tension permits penetration of the supercritical fluid into the micropore structure of solids to accelerate decomposition, and the density of the fluid can be manipulated to increase its solvating power near the critical temperature.

However, there are some costs associated with operating in the supercritical regime, and, if acceptable organic destruction efficiencies can be achieved under subcritical conditions, the system should be designed to operate in the subcritical regime.

FEASIBILITY STUDIES

Experiments were conducted at the Center for Energy Studies, The University of Texas at Austin, Balcones Research Center. This research group had been investigating wet oxidation waste treatment for several years and had the equipment, reactors and expertise to conduct high temperature/pressure oxidation reactions. The experimental program used a small batch reactor (Figure 3) and a statistically designed set of conditions was specified to explore both the subcritical and supercritical regimes. Also of interest was the effect of solid

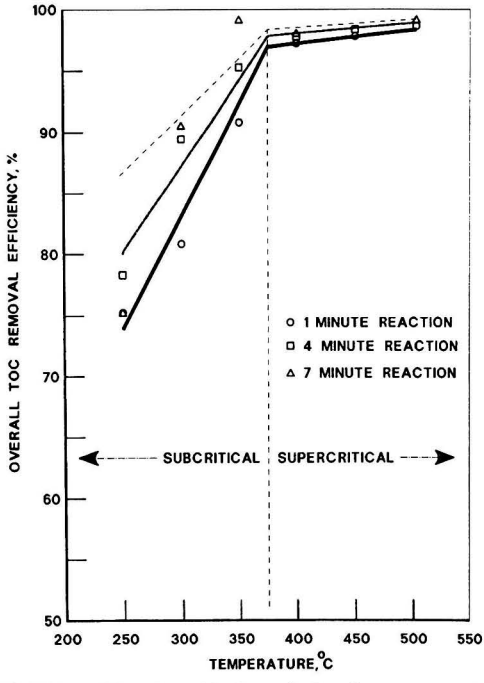

FIGURE 4. Wet air oxidation of nitration wastewater batch reactions.

fuel additions, in this case, municipal sludge. All experiments were conducted at 27,600 kPa (4,000 psi) and residence times were 1, 4, and 7 minutes.

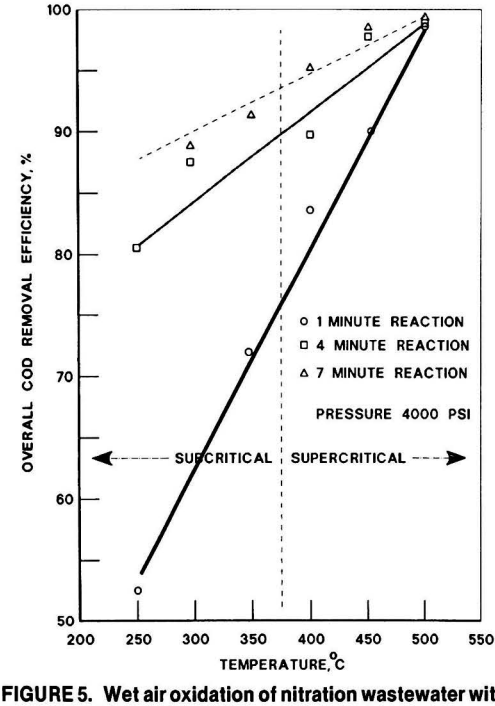

FIGURE 5. Wet air oxidation of nitration wastewater with 3% sludge solids batch reactions.

Table 2 Subcritical Wet Oxidation Without Added Sludge

Temperature (C)	Time (min)	TOC In (ppm)	TOC Out (ppm)	Removal (%)
250	1	1,840	460	74.9
250	4	1,840	400	78.5
250	7	1,840	460	74.9
300	1	1,840	330	82.2
300	4	1,840	200	89.1
300	4	1,840	230	87.7
300	4	1,840	140	92.3
300	7	1,840	140	92.3
300	7	1,840	180	90.4
350	1	1,840	140	92.5
350	4	1,840	80	95.7
350	7	1,840	8	99.6

The batch reactor was a nominal 1/4 inch (ID) stainless steel coil capable of holding between 5 and 10 milliliters of waste water and equipped with a thermocouple and pressure transducer. The entire assembly was attached to a vibrator and a motor driven rack/pinion which transported the coil between a hot sand bath and a water quenching bath. The reactor was mechanically lowered into the hot sand bath maintained at a pre-determined reaction temperature. Vibration of the reactor continued while in the sand bath and steady state temperature was attained in less than 30 seconds. After allowing a predetermined time (residence time) to elapse, the reactor was removed from the sand and the vibrator turned off. The reactor temperature dropped to approximately 40 C and the pressure dropped to 700 kPa (100 psi) within 3–4 seconds. The reactor was then quenched to 25 C and atmospheric pressure. Elapsed time between removal from the sand and quenching was between 8 and 10 seconds. The volumes of waste water and oxygen charged to the reactor depended on reaction temperature.

Total organic removal efficiencies were calculated for each of the conditions in the experimental program to determine extent of oxidation. These measurements did not take into account destruction of specific compounds nor did they attempt to identify the nature of the organics which contributed to the residual organic carbon.

Organic removal efficiencies were measured in two ways. Where the organics were dissolved in the aqueous medium or present as an oily precipitate, total organic carbon (TOC) was measured before and after the oxidation reaction. This was the technique used for both subcritical and supercritical experiments without added sludge. The results of those experiments are shown in Figure 4.

Due to the difficulties associated with measuring TOC for solids, the relative amount of organics was measured as chemical oxygen demand (COD) for those experiments in which sludge solids were added. The results are shown in Figure 5.

Figures 4 and 5 present the overall organic removal efficiencies (% organic destruction) for all four sets of experiments (subcritical, supercritical, without solids, with solids). Reaction time is shown as a parameter while destruction efficiency is plotted as a function of temperature. Pressure was kept constant at 27,600 kPa (4,000 psi). The temperature axis includes the subcritical ($T < 374$ C) and supercritical ($T > 374$ C) ranges. The destruction efficiency is greatest in the supercritical temperature range for all cases. When no solids were added, the dependency on reaction time is nearly eliminated and the destruction efficiency becomes a very weak function of temperature. However, the linear trends appear to be unaffected when solids are added (Figure 5). Destruction efficiencies in the supercritical region are still strong functions of both temperature and residence time.

Although the trends in Figure 4 are presented as a family of straight lines with a discontinuity at the critical temperature of water, smooth curves through the data points would lead to the same conclusions. Tables 2 through 5 offer the results in numerical form and give a sense of the data precision.

It is apparent from these data that wet oxidation is effective in removing organics from the waste water even at subcritical temperatures if sufficient time is allowed. The highest efficiencies are realized in the supercritical regime but much of the benefit is lost when organic solids are present.

The priority compounds of concern to this investigation were 2-nitrophenol (2-NP); 4-nitrophenol (4-NP); 2,4-dinitrophenol (2,4-DNP); 4,6-dinitro-ortho-cresol (4,6-DNOC); phenol (P) and dinitrotoluene (DNT). All are included in EPA lists of regulated compounds. Initial concentrations in the test waste

Table 3 Supercritical Wet Oxidation Without Added Sludge

Temperature (C)	Time (min)	TOC In (ppm)	TOC Out (ppm)	Removal (%)
400	1	1,840	30	98.5
400	4	1,840	20	99.0
400	7	1,840	20	99.0
450	1	1,840	20	99.2
450	4	1,840	10	99.5
450	4	1,840	10	99.5
450	4	1,840	10	99.5
450	7	1,840	10	99.5
500	1	1,840	5	99.7
500	4	1,840	1	99.9+
500	7	1,840	<1	99.9+

Table 4 Subcritical Wet Oxidation With 3% Added Sludge

Temperature (C)	Time (min)	COD In (ppm)	COD Out (ppm)	Removal (%)
250	1	38,970	18,980	51.3
250	4	38,970	7,440	80.9
250	7	38,970	6,900	82.3
300	1	38,970	7,330	81.2
300	4	38,970	4,560	88.3
300	4	38,970	5,070	87.0
300	4	38,970	5,070	87.0
300	7	38.970	4,330	88.9
350	1	38,970	10,910	72.0
350	4	38,970	10,090	74.1
350	7	38,970	3,550	90.9

Table 5 Supercritical Wet Oxidation With 3% Added Sludge

Temperature (C)	Time (min)	COD In (ppm)	COD Out (ppm)	Removal (%)
400	1	38,970	6,550	83.2
400	4	38,970	4,520	88.4
400	7	38,970	1,910	95.1
450	1	38,970	4,130	89.4
450	4	38,970	900	97.7
450	4	38,970	820	97.9
450	4	38,970	780	98.0
450	7	38,970	740	98.1
500	1	38,970	470	98.8
500	4	38,970	430	98.9
500	7	38,970	270	99.3

Table 6 Supercritical Wet Oxidation Without Added Sludge

		Final Concentration (ppb)					
Temp (C)	Time (min)	DNT	2-NP	4-NP	2,4-DNP	4,6-DNOC	Phenol
250	1	135,000	BD	BD	BD	BD	BD
250	4	151,400	1,400	BD	375	BD	100
250	7	347,200	BD	BD	BD	BD	BD
300	1	157,000	BD	BD	BD	BD	BD
300	4	60,800	BD	BD	BD	BD	BD
300	4	BD	BD	BD	BD	BD	BD
300	4	83,700	BD	BD	BD	BD	BD
300	7	88,500	BD	BD	BD	BD	BD
300	7	208,000	BD	BD	BD	BD	BD
350	1	109,200	BD	BD	BD	BD	BD
350	4	122,600	BD	BD	BD	BD	BD
350	7	102,900	BD	BD	BD	BD	BD

BD = Below Detectable Limits
Detection Limits: 2-NP, 4-NP, 2,4-DNP, 4,6-DNOC, Phenol = 5 ppb, DNT = 1000 ppb

waters have already been shown in Table 1. The analytical results for these specific compounds, after oxidation, are given in Tables 6 through 9. Dinitrotoluene was analyzed using gas chromatographic methods where the lower detection limit was 1 ppm (1,000 ppb). The other compounds were analyzed using a liquid chromatographic/pulsed amperometric detection method and the lower detection limit was 0.005 ppm (5 ppb).

In Table 6, all the priority organics with the exception of DNT were oxidized to less than 5 ppb (detection limit) in the absence of sludge solids at relatively mild temperatures (250 C < T < 350 C). DNT was reduced by an average 60% over the reaction conditions; concentration data below 350 C are, however, imprecise. DNT destruction became significant (below detection) only at temperatures above the critical point of water as shown in Table 7.

Addition of sludge solids to the aqueous waste appears to enhance the destruction efficiency of DNT in the subcritical region (300 C < T < 350 C) but the final concentrations for all other compounds are higher than reported at similar temperatures in the absence of sludge. This is shown in Table 8.

Table 7 Supercritical Wet Oxidation Without Added Sludge

Temp (C)	Time (min)	Final Concentration (ppb) DNT	2-NP	4-NP	2,4-DNP	4,6-DNOC	Phenol
400	1	BD	BD	BD	BD	BD	BD
400	4	BD	BD	BD	BD	BD	BD
400	7	BD	BD	BD	BD	BD	BD
450	1	BD	BD	BD	BD	BD	BD
450	4	BD	BD	BD	BD	BD	BD
450	4	BD	BD	BD	BD	BD	BD
450	4	BD	BD	BD	BD	BD	BD
450	7	BD	BD	BD	BD	BD	BD
500	1	BD	BD	BD	BD	BD	BD
500	4	BD	BD	BD	BD	BD	BD
500	7	BD	BD	BD	BD	BD	BD

BD = Below Detectable Limits
Detection Limits: 2-NP, 4-NP, 2,4-DNP, 4,6-DNOC, Phenol = 5 ppb, DNT = 1000 ppb

Table 8 Subcritical Wet Oxidation With 3% Added Sludge

Temp (C)	Time (min)	Final Concentration (ppb) DNT	2-NP	4-NP	2,4-DNP	4,6-DNOC	Phenol
250	1	15,500	BD	BD	BD	157	43,100
250	4	28,000	976	854	5,888	1,204	1,403
250	7	35,100	516	BD	3,638	BD	514
300	1	8,900	BD	BD	BD	BD	412
300	4	BD	BD	334	1,703	343	383
300	4	6,400	BD	513	3,920	389	647
300	4	21,700	128	BD	BD	45	507
300	7	14,200	BD	1,185	1,756	BD	177
350	1	BD	2,376	BD	721	BD	BD
350	4	BD	BD	BD	350	BD	BD
350	7	BD	BD	BD	236	BD	BD

BD = Below Detectable Limits
Detection Limits: 2-NP, 4-NP, 2,4-DNP, 4,6-DNOC, Phenol = 5, ppb DNT = 1000 ppb

Table 9 Supercritical Wet Oxidation With 3% Added Sludge

Temp (C)	Time (min)	Final Concentration (ppb) DNT	2-NP	4-NP	2,4-DNP	4,6-DNOC	Phenol
400	1	BD	54	120	478	560	792
400	4	BD	BD	BD	BD	BD	825
400	7	BD	33	BD	219	515	223
450	1	BD	BD	BD	BD	BD	3,796
450	4	BD	BD	BD	46	BD	95
450	4	BD	BD	BD	41	BD	57
450	4	BD	BD	BD	BD	BD	112
450	7	BD	BD	BD	BD	BD	BD
500	1	BD	408	826	130	668	BD
500	4	BD	19	BD	BD	556	BD
500	7	BD	BD	BD	BD	BD	BD

BD = Below Detectable Limits
Detection Limits: 2-NP, 4-NP, 2,4-DNP, 4,6-DNOC, Phenol = 5 ppb, DNT = 1000 ppb

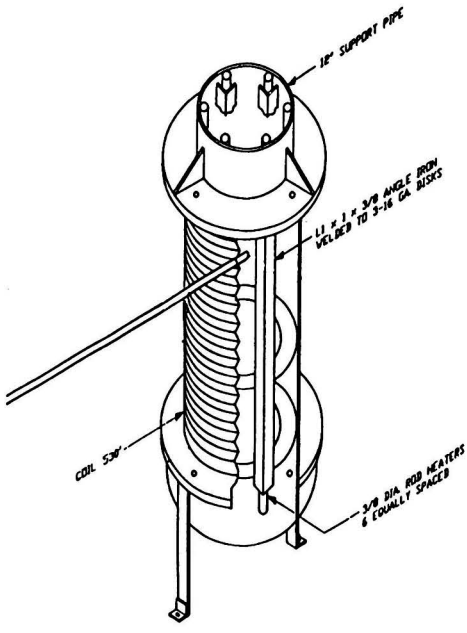

FIGURE 6. Plug flow reactor configuration.

DNT is reduced to detection limits at 350 C in the presence of sludge solids while its level remained high in the absence of solids. All other organics appear in significant, although inconsistent, concentrations throughout the range of experimental conditions. The apparent fluctuations are attributed to difficulties in preparing consistent batch-to-batch feed quality for the reactor due to the nature of sludge solids. Addition of sludge solids adversely affects the oxidation of several of the compounds.

Under supercritical conditions, oxidation appears to be efficient in destroying all organic material. The experiments with sludge solids occasionally show a "high" concentration for some of the compounds (Table 9).

Addition of sludge solids seems to inhibit the oxidation of aromatic organics. One reason is the competition for oxygen by a relatively low concentration of aromatic compounds compared to a high concentration of solid material. Another theory is that DNT is preferentially adsorbed on the sludge solid and then destroyed as the solids are oxidized. Without intensive investigation into this specific area, the reason for this effect is entirely speculative. It must also be recognized that the longest residence time was 7 minutes and longer times would have further reduced all of the organics. The intention was to demonstrate the overall effects of sludge solid addition on the wet oxidation process. That effect is generally negative.

PROCESS DESIGN

The above work was conducted in parallel with small scale continuous reactor investigations using batch results as guidelines for developing process conditions. The continuous reactor was a modified Autoclave Engineering high pressure system. The modifications included the installation of a 1/4 inch (nominal ID) stainless steel tube, approximately six inches long, to serve as a plug flow reactor. The supercritical regime was unsuitable for treating this particular waste stream in a tubular reactor due to severe plugging. In several cases, the pressure drop across the plug was in excess of 1200 psi. The precipitate causing the pluggage was due to high cation concentrations in the stream. Sodium is added in the product washing step and is subsequently found in the waste stream. As mentioned previously, inorganic compounds are virtually insoluble in supercritical fluids.

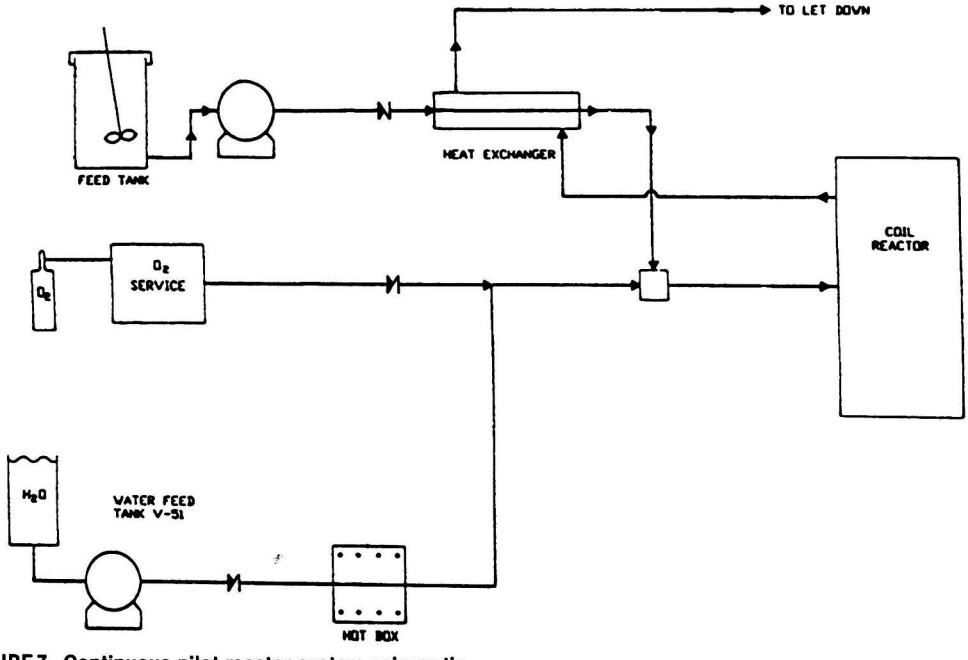

FIGURE 7. Continuous pilot reactor system schematic.

Table 10 Near Critical Wet Oxidation of Nitration Wastewater Continuous Reaction

Wasterwater Flow Rate: 374 cc/min
Supercritical Water Flow Rate: 60 cc/min
Average Reactor Temperature: 343 C
Reactor Pressure: 3450 psi

Residence Time (Min)	TOC (ppm)	DNT Distribution, ppm		Priority Pollutants, ppb					
		2,6-DNT	2,4-DNT	Phenol	4-NP	2,4-DNP	2-NP	4,6-DNOC	NBENZ
0	1,164	114,420	352,420	15,140	BD	1,300	BD	8,520	500
1	525	BD	BD	BD	2,220	7,540	BD	BD	5,220
2	403	BD	BD	BD	BD	1,670	BD	BD	4,640
3	357	BD	BD	BD	BD	BD	BD	BD	13,000
4	331	BD	BD	BD	BD	BD	BD	BD	5,220
5	351	BD	BD	BD	BD	BD	BD	BD	5,200

BD = Below Detectable Limits
Detection Limits: 2-NP, 4-NP, 2,4-DNP, 4,6-DNOC, Phenol = 5 ppb, DNT = 200 ppb

This problem was circumvented by simply lowering the reaction temperature until precipitation no longer occurred. Keeping the pressure above the critical pressure but lowering the temperature to the 350 C range resulted in smooth operation and apparently good organic removal efficiencies.

A series of "verification" tests were planned and carried out in cooperation with Modar, Inc., in their pilot facilities. The overall purpose was to verify the assumptions based on batch tests in small scale continuous tests and to determine the appropriate residence time, a critical parameter which effects capital expenditure. For these tests, a pilot scale continuous tubular reactor was constructed.The inside diameter was nominally 1/4 inch and the length was 162 meters (530 feet). The reactor was wound onto a 30 centimeter (12 inch) diameter cast iron pipe and equipped with internal heating elements to compensate for heat losses. The entire assemble was approximately 1.8 meters (6 feet) high and is shown in Figure 6.

The pilot equipment consisted of a waste water feed system, an oxygen feed system, a supercritical water system, a heat exchanger to preheat the reactor feed and a tubular reactor. The schematic is shown in Figure 7. Waste feed to the reactor was pre-heated by exchanging heat with the reactor effluent. Immediately before entering the reactor, a mixture of supercritical water and oxygen was introduced into the waste to bring it up to reaction temperature. Samples were taken from various points along the reactor's length. These points corresponded to 1, 2, 3 and 4 minutes residence time. The effluent sample had a nominal 5 minute residence in the reactor coil.

The results of those experiments are shown in Table 10. The detection limits are lower than previously stated due to continued improvements in analytical capabilities; toluene and dinitrotoluene have detection limits of 200 ppb while the other priority pollutants have 5 ppb limits. A three minute residence at temperatures between 340 and 360 C is sufficient to reduce priority compounds to acceptable levels. Total organic carbon (TOC) is substantially reduced and the residual is, most likely, the result of low molecular weight organic acids (acetic). A surprising result is the generation of nitro-benzene, a regulated compound. This compound can be easily removed from the stream using conventional technology such as carbon adsorption. All other regulated compounds have been substantially removed from the aqueous waste stream.

Based on this work a system was designed and awaits implementation. Economic analysis shows a higher initial capital cost than most other conventional technologies but this is offset by much lower operating costs. Economically, the cost of a wet oxidation process is in the same range with more conventional systems. Risk is a factor that must be taken into account. Conventional technologies have proven track records whereas this process has yet to be demonstrated on a commercial scale.

CONCLUSIONS

The wet oxidation process has been demonstrated in both small scale batch reactions and in intermediate pilot scale equipment. Destruction of priority pollutants was sufficient to comply with federal regulations. The development of the process was completed in a short time and this was made possible by the cooperative effort and parallel activities of industry, academia and development organizations. This type of interaction will become more prevalent because of the time pressures on industries imposed both externally and internally.

ACKNOWLEDGMENTS

The authors wish to acknowledge the collaboration and assistance of the following people and groups: Dr. Earnest Gloyna and Dr. Lixiong Li of The University of Texas at Austin for their generation of batch reaction data. Mr. William Killilea and Dr. Glenn Hong of Modar, Inc., for constructing and running continuous pilot scale reactions. Mr. C. Y. Haung and Dr. Herb Barner, of Lummus Crest, Inc., for their contributions to the final process design. Mr. Bruce Phillips of Air Products and Chemicals for developing analytical methods and for generating the analytical data.

LITERATURE CITED

1. Rich, Linvil G., "Unit Processes of Sanitary Engineering," John Wiley and Sons, Inc., New York, New York (1963).
2. Zimmerman, F. J., "New Waste Disposal Process," *Chem. Eng.*, pp. 117–120 (Aug. 1958).
3. Teltzke, G. H., "Wet Air Oxidation," *Chem. Eng. Prog.*, 60(1), pp. 33–38 (Jan. 1964).
4. Morrill, G. B., H. C. Delaney, A. Wallum, and W. Schwoyer, "Commercial Scale Demonstration of Below-Ground Aqueous Phase Sludge Oxidation at Longmont," Rocky Mountain AWWA/WPCA Summer Meeting (Sept. 1986).
5. EPA Project Summary, "Aqueous-Phase Oxidation of Sludge Using the Vertical Reaction Vessel System," EPA/600/S2-87/022 (May 1987).
6. Gitchel, W. B., C. A. Hoffman, and E. W. Schoeffel,

"Partial Oxidation of Sewage Sludge," U.S. Patent 3,359,200 (Dec. 1967).
7. Lawless, H. L., "Method of and Apparatus for Carrying Out a Chemical or Physical Process," U.S. Patent 3,606,999 (Sept. 1971).
8. Hover, H. K., D. T. Hulbras, and L. J. Serkamic, "System for Treatment of Secondary Sewage," U.S. Patent 3,607,735 (Sept. 1971).
9. Hoffman, C. A., "Paper Mill Waste Sludge Oxidation and Product Recovery," U.S. Patent 3,876,497 (Apr. 1975).
10. Smith, C. S., E. Garrett, "Treatment of Sewage," U.S. Patent 4,115,258 (Sept. 1978).
11. Crane, T. H., "Pressurized Treatment of Sewage," U.S. Patent 4,217,211 (Aug. 1990).
12. Modell, M., "Processing Method for the Oxidation of Organics in Supercritical Water," U.S. Patent 4,338,199 (July 1982).
13. Freese, R. A., and E. J. Rosinski, "Wet Air Oxidation Studies of Coal Gasification," *J. Haz. Materials*, **8**, pp. 367-375 (Aug. 1984).
14. Bailloid, C. R., B. M. Faith, and O. Masi, "Fate of Specific Pollutants During Wet Oxidation and Ozonation," *Env. Progress*, **1**(3), pp. 217-227 (Aug. 1982).
15. Bailloid, C. R., R. A. Lamperter, and B. A. Barna, "Wet Oxidation for Industrial Waste Treatment," *Chem. Eng. Prog.*, pp. 52-56 (Mar. 1985).
16. Detrich, M. J., T. L. Randall, and P. J. Cannery, "Wet Air Oxidation of Hazardous Organics in Waste Water," *Env. Progress*, **4**(3), pp. 171-177 (Aug. 1985).
17. Wilhelmi, A. R., and R. B. Ely, "A Two-Step Process for Toxic Wastewaters," *Chem. Eng.*, pp. 105 (Feb. 1976).
18. Flynn, B. L., "Wet Air Oxidation of Waste Streams," *Chem. Eng. Prog.*, pp. 66-69 (Apr. 1979).
19. Ito, M. M., K. Akita, and H. Inoue, "Wet Oxidation of Oxygen- and Nitrogen-Containing Organic Compounds Catalyzed by Cobalt (III) Oxide," *Ind. Eng. Chem. Res.*, **28**(7), pp. 894-899 (1989). ◆

Remediation of Metal Contaminated Soil by EDTA Incorporating Electrochemical Recovery of Metal and EDTA

Herbert E. Allen* **and Ping-Hsien Chen+**

Department of Civil Engineering, University of Delaware, Newark, DE 19716

Removal of toxic heavy metals from a soil matrix by the addition of ethylenediamine tetraacetic acid (EDTA) is an effective means of remediation. The liquid stream containing the metal and chelating agent is amenable to further treatment by electrolysis in which the metal can be separated from the chelating agent. This provides a separated metal that can be removed for reuse or treated for final disposal by conventional technologies and a reclaimed EDTA stream that can be used again for treatment of contaminated soil.

Under the diffusion controlled conditions of polarography or voltammetry, we observed reduction of cadmium, copper and lead ions and their protonated EDTA complexes (MHY^-), but not of the non-protonated EDTA complexes (MY^{2-}). Potentials applicable for metal deposition and, consequently, regeneration of the EDTA were established. To prevent electrochemical oxidation of EDTA during electrolysis we used a cell in which the anode and cathode compartments were separated by a cation exchange membrane. Tests with Pb-EDTA demonstrated that over 95 percent recovery of both EDTA and lead could be achieved by electrolysis. The lead that was deposited onto a copper electrode was a mixture of hydrolysis products and salts and the lead could be recovered by dissolution in acid. EDTA was equilibrated with soil before addition of lead. When electrolyzed, this sample released EDTA and deposited Pb to approximately the same extent as did the samples that had not been equilibrated with soil.

The uncontrolled discharge of heavy metals is common and has resulted in contamination of numerous sites [1]. Toxic heavy metals are frequently encountered at elevated levels at Superfund sites [2]. Lead was found at 15 percent of the uncontrolled hazardous waste sites; chromium, cadmium, and copper were reported at 11, 8, and 7 percent of the sites, respectively.

The metal concentrations at uncontrolled sites extend to quite high values compared to those which are normally encountered. In a study of six U.S. Army installations [3], metal concentration ranges in soils were 0.05–453 mg/kg for cadmium; 1.2–3,000 mg/kg for chromium; and 1.2–4,940 mg/kg for lead. At a former battery recycling plant, the soil contained over 50,000 mg lead/kg [4]. Because most metals are highly retained by soils, exposure is likely to persist for a prolonged time. This creates the need to remove the source of potential contamination.

* *To whom correspondence should be addressed.*

+ *Present address: Sinotech Engineering Consultants, Inc., 171, Nanking East Road, Sec. 5, Taipei 10572, Taiwan, Republic of China.*

Several methods have been proposed for the remediation of heavy metal contamination of soil. These are based on two principles (1) immobilization of metal by increasing the retention of metal by soil or by decreasing the mass transfer of rate of the metal or (2) removal of metal from the soil matrix [5].

The chelating agent tetraethylenepentamine (tetren) has been added to soil to form complexes of metals such as cadmium, copper, nickel and zinc that are more strongly retained by clays than are the metal cations [6]. Clays, synthetic resins and zeolites have been added to increase metal retention and to reduce bioavailability [5]. Precipitation of the metals as sulfides, carbonates, phosphates and hydroxides as a means to immobilize metals has also been investigated [5]. The most common means of immobilization is by decreasing the mass transfer coefficient by means of soil vitrification or the addition of pozzolonic agents [7]. One negative aspect of these methods is that they all result in a product that still contains the metal. The soil is not returned to its original state or to a material suitable for most uses.

Two types of metal extraction agents have been used for the removal of heavy metals from soil, acids and chelating agents [7, 8]. Acid washing will change soil properties and result in

large volumes of liquid that must be treated before discharge. Acid washing may be very difficult in carbonate rich soils. Removal of many metals by reaction with chelating agents is quite efficient, but the high cost of chelating agents such as ethylenediamine tetraacetic acid (EDTA) has precluded their uses in remediation of metal-contaminated sites.

This research was undertaken to develop a means by which EDTA used for the extraction of metal from soil could be recovered and reused. Electrolysis of metal chelates was investigated as a means to recover both the EDTA and the associated metal. This technology provides the potential to be applied to contaminated soils and to other solids and slurries, including ash and sludges.

METAL-SOIL INTERACTION

The aqueous concentration of an inorganic contaminant in contact with a soil can be predicted from appropriate thermodynamic measurements. At high concentrations, cationic metals will form insoluble hydroxide, carbonate, or sulfide precipitates [*9-11*]. The solubility is a function of the concentration of metal and precipitant, the solution pH and the concentrations of other interacting metal ions and ligands.

Often trace elements are present in the solid phase as a result of adsorption to components of the soil. The most important factor in controlling the partitioning of a metal to soil is the solution pH. As the pH decreases, the concentration of soluble metal increases [*12-16*]. For anions, such as chromate, a reverse trend is found in which adsorption is maximum at low pH and decreases with increasing pH.

The reaction of metal ions with solid phases has a dependency on pH resulting from the surface chemistry of soil materials. Protons can react with anions capable of forming precipitates to compete with the reaction of the metals, thus increasing solubility. Soils have pH-dependent, or variable, charge associated with the reaction of protons with oxide and hydroxide minerals and with certain functional groups of humic substances [*10, 17*]. Protons and metal ions compete with each other for available surface binding sites, $\equiv S\text{-}OH^0$, on a soil. The following equation represents the reaction for a divalent metal ion, Me^{2+}:

$$\equiv S\text{-}OH^0 + Me^+ \Leftrightarrow \equiv S\text{-}OMe^+ + H^+ \quad (1)$$

Unfortunately, in most situations the concentration of available binding sites and the stability constants for the reaction of metal ions and protons with those sites is not known. Thus, the partitioning of metals to a soil has been difficult to predict.

Table 1 Stability Constants for Metal-EDTA Complexes [*18*]

Element	Cation	log K_{MEDTA}	log K_{MHEDTA}
Cadmium	Cd^{2+}	16.5	2.9
Calcium	Ca^{2+}	10.7	3.1
Chromium	Cr^{3+}	23.0	2.3
Copper	Cu^{2+}	18.8	3.0
Iron	Fe^{2+}	14.3	2.8
	Fe^{3+}	25.1	1.4
Lead	Pb^{2+}	18.0	2.8
Magnesium	Mg^{2+}	8.7	3.9
Manganese	Mn^{2+}	14.0	3.1
Mercury	Hg^{2+}	21.8	3.1
Nickel	Ni^{2+}	18.6	3.2
Zinc	Zn^{2+}	16.5	3.0

CHELATION OF METALS BY EDTA

A complex ion is a species in which the metal ion coordinately bonded to one or more electron-donating groups that are called ligands. Multidentate ligands can contribute two or more electron pairs to the central metal atom when a complex is formed. The complexes, composed of a metal atom and one or more multidentate ligands, are known as chelates and possess high degrees of stability.

A particularly important chelating agent is the aminopolycarboxylic acid, ethylenediaminetetraacetic acid which provides six-fold coordination. EDTA is a tetraprotic acid that can be denoted H_4Y. The four stepwise dissociation constants of the parent acid to yield H_3Y^-, H_2Y^{2-}, HY^{3-} and Y^{4-} are 1.00×10^{-2}, 2.16×10^{-3}, 6.92×10^{-7} and 5.50×10^{-11}, respectively. Unless the pH is very high, the EDTA will not be completely deprotonated. The fraction of EDTA in the deprotonated form can be computed from α coefficients. For EDTA, the fraction present in the completely deprotonated form (Y^{4-}) is

$$\alpha_{Y^{4-}} = \frac{K_{a1}K_{a2}K_{a3}K_{a4}}{[H^+]^4 + K_{a1}[H^+]^3 + K_{a1}K_{a2}[H^+]^2 + K_{a1}K_{a2}K_{a3}[H^+] + K_{a1}K_{a2}K_{a3}K_{a4}} \quad (2)$$

where the four K_a values are those of the stepwise proton dissociation given above. The complexation of metals by EDTA is therefore dependent on pH. The fraction of metal in any other form, e.g., HY^{3-}, can be expressed by a related α coefficient. The reaction of the deprotonated EDTA with a hydrated metal ion, Me^{n+}, can be represented

$$Me^{n+} + Y^{4-} \Leftrightarrow MeY^{(n-4)+} \quad (3)$$

The stability constant, K_{MeY}, for this reaction is represented

$$K_{MeY} = \frac{[MeY^{(n-4)+}]}{[Me^{n+}][Y^{4-}]} \quad (4)$$

Under acidic conditions, the formation of protonated complexes ($MeHY^{(n-3)+}$) will exceed that of the deprotonated complexes ($MeY^{(n-4)+}$). The reaction to form the protonated complex can be represented

$$MeY^{(n-4)+} + H^+ \Leftrightarrow MeHY^{(n-3)+} \quad (5)$$

The stability constant, K_{MeHY}, for this reaction is represented

$$K_{MeHY} = \frac{[MeHY^{(n-3)+}]}{[MeY^{(n-4)+}][H^+]} \quad (6)$$

Table 1 lists the stability constants for the formation of metal-EDTA complexes. The strength of these complexes has led a number of investigators to use EDTA and related aminocarboxylic acids to release metals from soils and sediments.

RELEASE OF METAL FROM SOIL BY EDTA

Ellis *et al.* [*19*] studied the release of cadmium, chromium, copper, lead and nickel from soil collected from a Superfund site near Seattle, WA. They conducted both batch equilibration and column studies using EDTA alone and EDTA followed by hydroxylamine hydrochloride, to reduce iron oxides in the

soil. EDTA used alone removed over 90 percent of the lead and cadmium. EDTA removed approximately one quarter of the chromium. Addition of the reducing agent increased this value to approximately 50 percent. It is not clear if the improvement was due to the solubilization of iron oxides or to the reduction of chromate.

Mobley [20] added cadmium, copper, nickel and zinc to a Lebanon silty soil at contaminant levels of 100 to 300 mg/kg. The soil was packed into a Plexiglas column and extracted by EDTA. Results of his testing indicated that 80 to more than 95 percent of the heavy metals that had bonded to the soil matrix could be recovered. For copper, the total removal was 80 percent for 0.01 M EDTA and 95 percent for 0.1 M EDTA. The effect of column flow rate was not studied, but the flow was stopped for periods of 1 to 3 days, causing only small differences in results.

Connick [21, 22] sorbed cadmium, copper, lead, nickel and zinc onto a Typic Hapludult soil. The soils were placed in columns and rinsed with 8 column volumes of a nonionic surfactant plus 0.144 M EDTA solution. Percentage removals were cadmium (100), copper (82), lead (63), nickel (94) and zinc (93).

A series of four soils were contaminated with organics and with arsenic, cadmium, chromium, copper lead, nickel and zinc to enable efficiencies of various soil treatment technologies to be compared [23]. An EDTA wash (3:1 molar ratio of EDTA to metal) provided a high efficiency for removal of metals even in the <250 μm fraction. For soil contaminated to the 50,000 mg/kg level of total metal, the removal of metal was approximately 80%. There was not an appreciable effect of temperature or pH on the extraction efficiency. Because the extractability of metals decreases as a function of the amount of time the soils have been aged [24], the results of the Esposito study [22] may not reflect conditions present in field contaminated soil.

Secondary recovery of lead from recycling scrap batteries is the source of over 70 percent of the nation's total lead production [25]. However, secondary lead processing has resulted in contamination of soil in the vicinity of battery reclamation operations. For example, the soil at the Lee Farm former battery recycling site in Woodville, Wisconsin had 15,000 cubic yards of soil which was contaminated by lead and contained broken battery casings [4]. The feasibility of soil washing with EDTA to remove lead from the contaminated soil was investigated because EDTA had been shown to be effective at a number of other sites including the Western Processing Site and the Leeds, Alabama site. A 20 percent tetrasodium EDTA solution was adjusted to pH 7.0 to conduct sequential extractions of size separated soil. As would be expected, the lead content is greatest in the smaller-size particles. Total lead reduction of 95 to 97 percent and residual concentrations as low as 696 mg/kg were achieved.

Surficial concentrations of lead in soils in the vicinity of smelters and battery recycling facilities can be in the percent range; the highest concentration reported by Elliot *et al.* [26, 27] was 211,300 mg/kg soil on a dry weight basis. They evaluated the effect of solution pH, EDTA concentration and electrolyte addition on the solubilization of lead from the soil containing 21 percent lead. There was only a modest reduction in the lead removal ability when the solution pH was raised above pH 5. They also found that the concentration of iron extracted from the soil increased as the pH decreased. However, little of the iron was brought into solution during the 5-hour extraction time. At pH 6 only 12 percent of the iron was removed while almost 86 percent of the lead was removed by 0.04 M EDTA.

Peters and Shem [28] have also shown that the removal of lead from contaminated soil is pH insensitive over the range of 4 to 12. They were able to remove over 64 percent of the lead from a soil containing an initial lead concentration of 10,000 mg/kg.

The sequential extraction procedure of Tessier *et al.* [29] was applied to compare the distribution of cadmium, chromium, copper, lead, nickel and zinc in contaminated clay soils before and after extractive cleaning [30]. Both 0.1 M HCl and 0.1 M EDTA were used as the soil extractants. The metals were sorbed to five clay soils; two waste site soils were also investigated. Treatment with 2 portions of 0.1 M EDTA removed metals to roughly the same extent as did a single treatment with the 0.1 N HCl. The sequential extraction procedure indicated significant differences between the samples that had had metals added in the laboratory and those which were from waste sites. Metals in the waste site samples were more difficult to remove. Higher proportions of the metals were in the "organic/sulfidic" and "residual" fractions than was the case for the samples to which metals had been added in the study. The metals in these more resistant phases would be expected to be less mobile than would those in other phases and thus cause less environmental problems. Also, the study points out that using samples to which metals have been added in the laboratory results in an overestimation of the efficiency of extraction by EDTA or other remediation methods.

ELECTROCHEMISTRY OF METAL-EDTA COMPLEXES

Johnson *et al.* [31] reported that during metal deposition at a platinized-Pt anode in acid sulfate solutions, EDTA was anodically oxidized into a variety of compounds, including carbon dioxide, formaldehyde, and ethylenediamine. They found a series of reaction products indicating sequential removal of acetate groups from the EDTA. The decarboxylations were followed by a reverse Schiff-type reaction that produced formaldehyde and the corresponding amine. The overall anodic oxidation of EDTA is given by the following reaction:

$$(HOOCCH_2)_2NCH_2CH_2N(CH_2COOH)_2 + 2H_2O \Rightarrow (HOOCCH_2)_2NCH_2CH_2NH_2 + 2CH_2O + 2CO_2 + 4H^+ + 4e^- \quad (7)$$

Electrolysis has been investigated to recover EDTA from its copper complex [32]. A two-compartment electrolysis cell that was divided by a cation exchange membrane to prevent the oxidation of EDTA at the anode during the electrolysis was used. The anode compartment was filled with sodium carbonate solution and the cathode compartment held the Cu-EDTA solution. A graphite sheet was used as anode and a copper plate as cathode. When a current was applied to the cell, the anolyte, sodium carbonate, provided sodium ions to carry the current through the membrane and to regenerate EDTA to its sodium form. The copper was electrodeposited onto the cathode, so that the Cu-EDTA complex was destroyed and EDTA was regenerated. The results showed the average yield of uncomplexed EDTA was 94%.

Etzel and Tseng [33] used a two-chamber electromembrane reactor to recover copper and zinc from their EDTA complexes. They used a dimensionally stable material designed for evolving oxygen gas as the anode and a copper plate as the cathode. They found that the electrodeposition of Cu and Zn from their chelate complexes was achieved, but no electrodeposition of Ni was possible in the presence of EDTA, NTA, or citrate.

No studies were found in our literature review that suggested the possibility of the electrodeposition of Cd and Pb from their EDTA complexes. By reviewing electrochemistry of these two ions, it was predicted that electrodeposition ions of Cd and Pb as well as Cu and Zn could occur from their EDTA complexes.

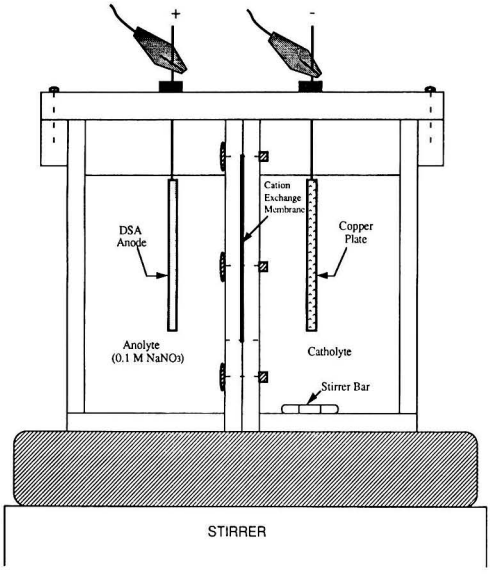

FIGURE 1. Electrolysis cell.

MATERIALS AND METHODS

Soil Extraction

Three different soils were used for this study. A New Jersey soil containing an elevated lead level was used as it was received. Based on extraction with 6 M HCl, it contained 350 mg lead/kg. We added lead to the soil that was collected in Delaware to raise its level to approximately 350 mg lead/kg also. The lead was added in the form of lead nitrate solution which was stirred with the soil in a ratio of 5 g soil per 100 ml $Pb(NO_3)_2$. After 24 hours, the soil was separated from the solution by centrifugation and used in a moist form. The third soil was Downer loamy sandy soil that was from New Jersey. Lead was also added to it to achieve a concentration near 350 mg/kg.

A stock 0.1 M EDTA solution was prepared from reagent grade disodium EDTA. This was diluted as necessary for each test. Lead was extracted from the soils by placing 5 g of soil and 100 ml of 10^{-1}, 10^{-2}, 10^{-3}, 5×10^{-4}, 10^{-4} or 5×10^{-5} M EDTA in flasks. Two tests were conducted at each concentration. After shaking on a reciprocating shaker for 24 hr, 10 ml of solution was removed and filtered through a Gelman FP-450 0.45 μm membrane filter. These solutions were diluted with distilled deionized water, as appropriate, and the concentration of lead in the filtrate was determined by atomic absorption spectroscopy.

Polarography and Voltammetry

For polarographic and voltammetric analysis, 0.1 M solutions of cadmium, copper and lead were prepared from their nitrate salts. The solutions tested were prepared by addition of appropriate volumes of the metal and EDTA solutions. These were diluted to volume with 0.1 M sodium nitrate.

Polarography was conducted using an EG&G Model 364 Polarographic Analyzer and an X-Y recorder. A three-electrode cell was used for d.c. polarographic analysis. The dropping mercury electrode employed a 4-cm length of capillary glass tubing; the reference electrode was a Fisher Scientific Standard Prefilled Calomel Reference Electrode; the platinum counter electrode was B&S Gauge #24 platinum wire. Samples were deoxygenated with nitrogen, and a nitrogen atmosphere was maintained above the solution while the polarogram was run at a 5 millivolt per second scan rate.

On the basis of the results of the polarographic study, we replaced the dropping mercury electrode (DME) with B&S Gauge #22 copper wire as the working electrode. The copper wire was taped by electric tape to maintain a 5-mm length of exposed of copper wire. This ensured a constant surface area to provide reproducibility for the voltammograms.

Electrolysis

Figure 1 depicts the cell developed for electrolysis experiments. The rectangular unit was made of 0.25″ thick Plexiglas. The electrode holding bar was constructed of 0.375″ thick Plexiglas. It was assembled from two independent identical chambers and an electrode holding bar. Both independent chambers had an inner mounting wall with a 2″ by 2.5″ cut-out and 0.75″ flanges. Then the two chambers were attached by means of inserting six screws on their flanges with a cation exchange membrane between. The screw holes on the flange of chamber 1 were drilled and those of chamber 2 were threaded so that the two chambers could be tightly attached. The membrane was cut 3.5″ by 3.5″ square and glued into the inner mounting wall of the two chambers with Dow Corning 100% Silicone Rubber Sealant (Dow Corning Corp., Midland, MI) to prevent any leakage between the chambers. The outer wall of each chamber had a boss with a tapped hole for affixing the electrode holding bar that was placed on the top of the cell. The electrodes, which were totally immersed in the solution, were suspended from the electrode holding bar and were approximately 1″ from the membrane surface.

The anode was a dimensionally stable anode of iridium oxide coated on titanium with dimensions of 2 in × 2 in × 0.0565 in. designed for evolving oxygen (Electrosynthesis Company, ES2 ICI Metcote flag anode, East Amberst, NY). Copper plate cathodes having dimensions of 2 in × 2 in × 0.022 in. were made from copper scrap by the roofing shop of the University of Delaware.

The cation exchange membrane used in this study was Ionics Modacrylic fiber-backed cation-transfer membrane (Ionics Incorporated, 61CZL386, Watertown, MA). It is a homogeneous film comprised of cross-linked sulfonated copolymers of vinyl compounds on synthetic reinforcing fabric.

The power supply used in these experiments was capable of supplying a potential of up to 200 volts and a direct current of up to 1 amp. A built-in current integrator recorded the quantity of electricity passed through the cell. Figure 2 shows the circuit diagram of the power supply.

For electrolysis experiments, 250 ml of 0.1 M sodium nitrate solution was added to the anode chamber. The cathode chamber contained 250 ml of metal or metal-EDTA solution. The catholyte was magnetically stirred to enhance mass transfer and obtain representative samples.

During electrolysis, samples were taken at regular time intervals from the cathode chamber. An appropriate portion of the solution was rapidly transferred into a graduated polystyrene tube, using a micropipette. This sample was acidified and then diluted with deionized distilled water prior to determination of the metal concentration by atomic absorption spectrophotometry. The pH of the catholyte was measured and the cumulative time and cumulative electricity consumed were recorded each time samples were taken.

Chemical Analysis

Samples for metal analysis were preserved and stored according to Standard Methods [*34*]. Cadmium, copper, and lead were determined using a Perkin-Elmer 5000 atomic absorption spectrophotometer. The standards were prepared and

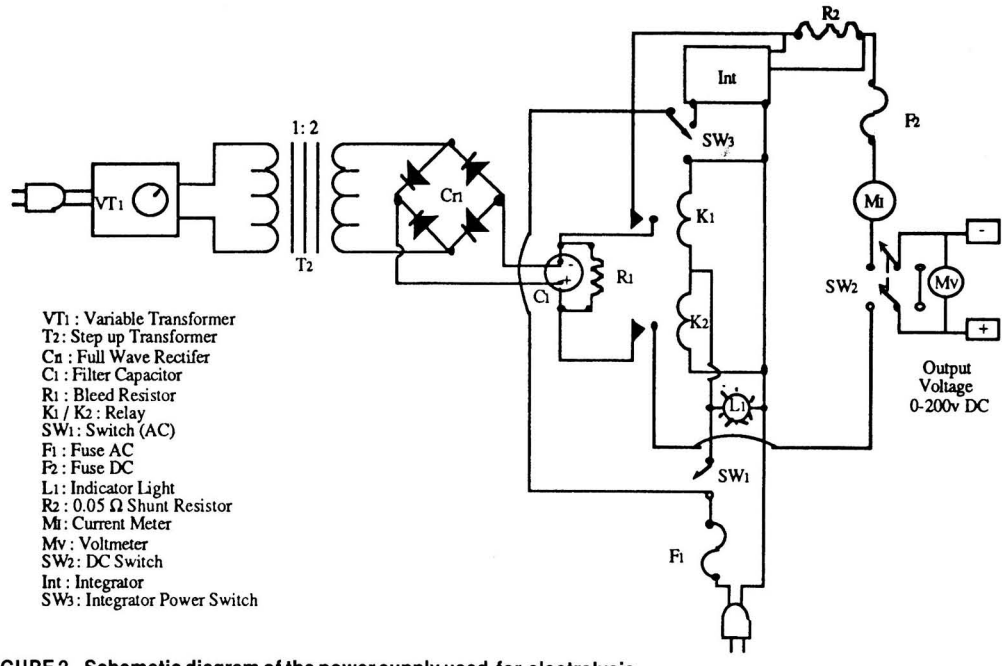

FIGURE 2. Schematic diagram of the power supply used for electrolysis.

the samples were diluted according to the procedures in Standard Methods.

A Cole Parmer DigipHase pH meter was used to determine pH. The meter was calibrated with standard pH 4 and pH 7 buffer solutions.

The concentration of EDTA was determined by EDTA titration [*35*]. The catholyte samples were adjusted to about pH 4.7 for titration. For a copper-EDTA catholyte, the yield of free EDTA was determined by titration with copper. For a lead-EDTA catholyte, the yield of free EDTA was determined by titration with lead.

Materials deposited onto the electrode during electrolysis were analyzed using x-ray diffraction (Philips Electronic Instruments, XRG-3000, Mount Vernon, NY) to identify the chemical composition of the material.

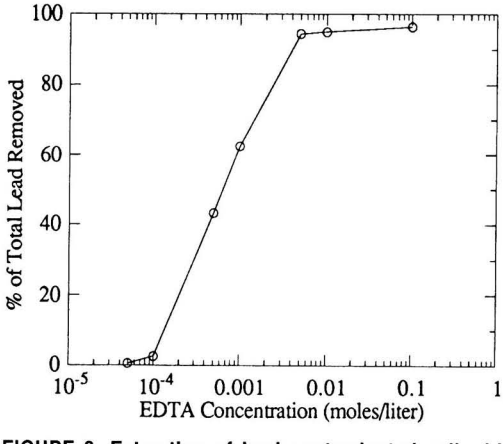

FIGURE 3. Extraction of lead contaminated soil with EDTA.

RESULTS AND DISCUSSION

Removal of Lead from Soil by EDTA

Extraction of the contaminated New Jersey soil with 0.1 M HCl indicated that the soil contained 350 mg Pb/kg dry weight. The soil was extracted with various concentrations of EDTA at pH 4.3 ± 0.1, and the concentration of lead in the extract was determined. The extraction efficiency, plotted in Figure 3, reached nearly 100 percent at a 10^{-3} M concentration of EDTA.

In a separate test, the pH was found to not affect the extraction efficiency over the range of 4–8 that was employed. This is consistent with previous results that have also shown that solution pH does not greatly influence extraction efficiency [*26, 28*].

At 10^{-3} M or lower concentrations of EDTA, the recovery of lead that had been added to the Delaware soil was greater than that for the New Jersey soil that had been previously contaminated. The greater strength of metal partitioning to soil after aging is supported by other work in this laboratory on the effect of wetting and drying on metal partitioning [*24*]. Conclusions regarding treatment efficiency based on the removal of metal salts added in laboratory experiments must be evaluated with caution. Removal is also highly dependent on the form of metal present in the soil.

Polarography and Voltammetry of Metal and Metal-EDTA Complexes

Polarography was carried out at various pH values and at various metal-to-EDTA ratios. The metals are reduced at more negative potentials in the presence of EDTA than when no EDTA is present. For the metal plus EDTA solutions, two waves are found in the polarogram; one is for metal reduction and the other is for reduction of the metal-EDTA complex. The metal-EDTA wave only can be observed at pH less than 4 and the diffusion current decreased as the pH increased.

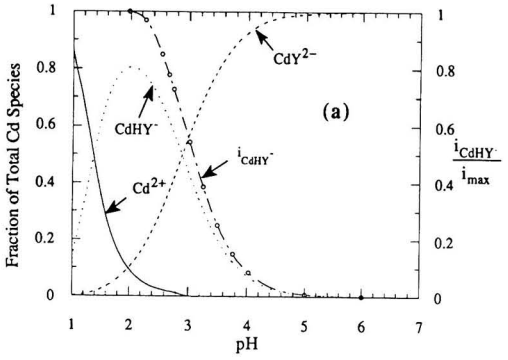

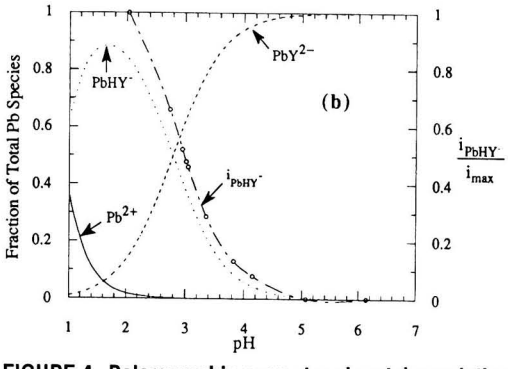

FIGURE 4. Polarographic current and metal speciation diagram for (a) cadmium-EDTA and (b) lead-EDTA.

These observations imply that the protonated MHY^-, rather than MY^{2-} species, are responsible for the polarographic signal.

The current has been plotted for the reduction of the complexes at various pH values superimposed on speciation diagrams for Cd and Pb (Figure 4). These show that the current follows the relative proportion of the $CdHY^-$ or $PbHY^-$ complexes.

The concentration of M^{2+} and MHY^- in solutions of various pH values and of various ratios of metal-to-EDTA have been calculated. The MHY^- concentration versus the measured reduction current is linear [*36*]. Thus, the Ilkovic equation is followed.

Table 2 Polarographic (Dropping Mercury Electrode) and Voltammetric (Copper Electrode) Half Wave Potentials of Metal and Metal-EDTA Complexes (Volt vs. SCE)

	Polarography—Hg electrode		Voltammetry—Cu electrode	
Species	Metal Solution	Metal-EDTA solution	Metal Solution	Metal-EDTA solution
Cd	−0.578	−0.623	−0.426	−0.573
Cu	N.D.	N.D.	−0.150	−0.200
Pb	−0.378	−0.415	−0.350	−0.388
Cd-EDTA	—	−0.833	—	−0.806
Cu-EDTA	—	N.D.	—	−0.598
Pb-EDTA	—	−0.701	—	−0.657

N.D.—not determined

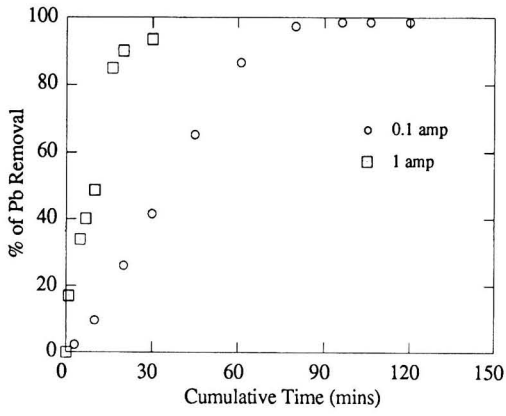

FIGURE 5. The percentage of lead removed from 0.01 M $Pb(NO_3)_2$ as a function of electrolysis time at 0.1 and 1 amp applied current using a copper plate electrode.

Because mercury electrodes can not be used for the recovery of metal and EDTA due to the toxicity of mercury, we investigated other electrodes that would provide the suitable conditions of low cost and a sufficient hydrogen overpotential to permit the reduction of a metal from its EDTA complex. The hydrogen overpotential at a copper electrode was expected to be sufficient to allow the electrolysis of lead-EDTA solutions [*37*]. We evaluated the reduction of cadmium, copper and lead and of their EDTA complexes on a copper wire electrode to evaluate the utility of this electrode for the deposition of metal from its EDTA complex. Half-wave potentials for the reduction of cadmium, copper and lead and for their EDTA complexes on a dropping mercury electrode and on a copper electrode are given in Table 2.

Electrolysis of Metal-EDTA Solutions

The recoveries of Pb, Cd, Cu and their EDTA complex solutions were studied in the electromembrane cell. The maximum one amp current developed a current density at the membrane surface of approximately 25.8 milliamps/cm^2. That is well below the 30 milliamps/cm^2 found to be limiting in industrial electrodialysis systems [*38*]. The cell voltage was allowed to vary to maintain constant current. As the metal ion concentration decreased in the cathode chamber, the voltage required to maintain a given current decreased to a minimum value. The pH value at the cathode increased during the electrolysis due to the production of hydroxide ion at the cathode. Hydrogen ion was produced at the anode.

Based on the voltammetric study using a copper electrode, a copper plate was used as the cathode in the electromembrane cell. Electrodeposition of Pb from 0.01 M $Pb(NO_3)_2$ was carried out at 0.1 and 1 amp controlled current. The Pb removal rate was greater at the higher the current density (Figure 5). The percentage of Pb removal was 98.6% and the current efficiency, computed for metal deposition, was 52.4% at 0.1 amp controlled current. For 1 amp controlled current, the percentage of Pb removal and the current efficiency decreased to 93.4% and 17.2%, respectively.

A one amp controlled current was applied to the cell for the electrodeposition of the Cd-EDTA complex. No cadmium precipitation was observed during the electrolysis nor was Cd plated on the copper electrode. It is possible that use of an electrode having a larger overpotential would permit the electrolysis of Cd.

Copper was successfully electrodeposited on the copper electrode from Cu-EDTA at a controlled current of 0.75 amp or

Table 3 Recovery Cu and EDTA from Cu-EDTA Solutions by Electromembrane Process on Different Cathodes

Cathode	Initial Cu (mg/l)	Initial EDTA (M)	Initial pH	Current Applied (amp)	Reaction Time (min)	Final pH	Final Cu (mg/l)	Cu Removal %	Free EDTA %	Current Efficiency %
nickel	572.4	0.01	2.28	1.00	75	12.36	15.6	97.3	95.0	9.0
copper	437.1	0.01	3.27	0.75	221	12.78	10.2	97.7	99.3	3.1

higher. For the 0.01 M Cu-EDTA solution tested, the percentage of Cu removal and EDTA recovered are 97.7% and 99.3% respectively, but the current efficiency was only 3.2%. Table 3 shows the results of Cu deposition from Cu-EDTA solution.

The most important application of this electrolysis is the treatment of Pb-EDTA solutions to regenerate EDTA. The percentage of Pb deposited is greater in the absence of EDTA than in its presence (Figure 6), however, the difference is less at a 0.1 amp applied current (Figure 6a) than at a 1 amp applied current (Figure 6b). We electrolyzed Pb-EDTA solutions at 0.1, 0.25, 0.5 and 1 amp controlled current, which correspond to current densities at the copper electrode of 1.90, 4.74, 9.48, and 18.96 milliamps per square centimeter, respectively. Figure 7 describes the Pb removal as a function of electrolysis time at various current densities for a 0.01 M Pb-EDTA solution. Figure 8 plots the relationship of current efficiency versus current density. The current efficiency decreases linearly with increasing current density. There was significant hydrogen evolution at high current density. The reduction in current efficiency at higher current density is probably also due to hydroxide ion production that consumes energy. Therefore, it is best to operate at lower current densities.

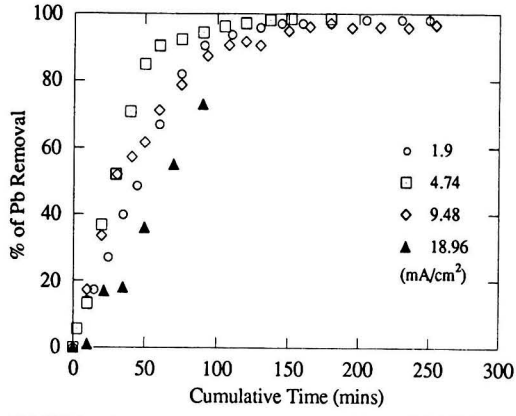

FIGURE 7. Percentage of lead removed from 0.01 M lead-EDTA as a function of electrolysis time at various current densities.

The regeneration of Pb and EDTA from Pb-EDTA is indicated in Table 4. The recovery of lead and EDTA should be the same, but the yield of EDTA at 0.1 amp is less than the percentage of Pb recovered. After 250 minutes of electrolysis time, the pH of catholyte for this sample was adjusted from 11.48 to 3.01. Then the electrolysis went on 250 minutes more and EDTA was recovered from final solution. Due to maintaining a long time with the pH of the anolyte less than 2, we suspect that some of the recovered EDTA was precipitated

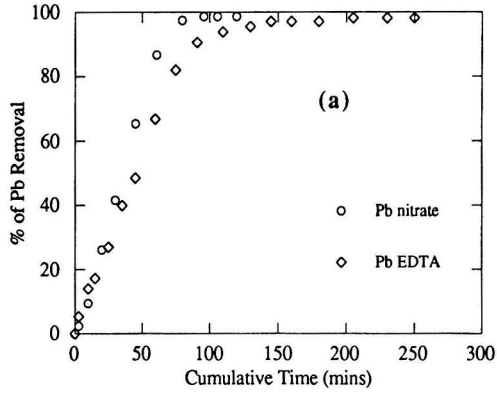

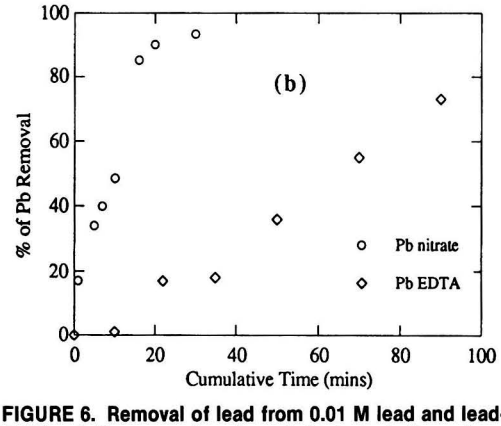

FIGURE 6. Removal of lead from 0.01 M lead and lead-EDTA solutions as a function of electrolysis time at applied currents of (a) 0.1 and (b) 1 amp.

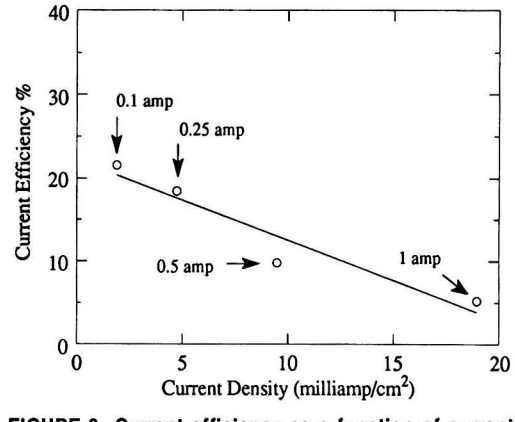

FIGURE 8. Current efficiency as a function of current density for deposition of Pb from 0.01 M Pb-EDTA onto a copper plate electrode.

Table 4 Recovery of Pb and EDTA from Pb-EDTA Solutions by Electromembrane Process Using a Copper Cathode

Initial Pb (mg/l)	Initial EDTA (M)	Initial pH	Current Applied (amp)	Reaction Time (min)	Final pH	Final Pb (mg/l)	Pb Removal %	Free EDTA %	Current Efficiency %
1786.2	0.01	2.12	0.10	500	11.48	34.2	98.1	74.2	21.5
1946.6	0.01	2.17	0.25	180	12.16	27.8	98.6	92.0	18.4
1707.7	0.01	2.20	0.50	255	12.50	141.1	91.7	90.8	9.8
1746.0	0.01	2.14	1.00	90	12.20	470.2	73.1	74.2	5.2

and attached onto the surface of the cation exchange membrane. EDTA is almost insoluble in water up to a pH of approximately 3.5 which suggests that, to prevent EDTA precipitation, the pH of the anolyte must not be too low. On the other hand, membrane degradation can occur at pH > 10. Therefore, pH control is very important.

Gordievskii and Gurinov [*32*] studied the effect of anolyte composition in the electromembrane process. Hydrochloric and sulfuric acid and sodium carbonate solutions were used. They found that when hydrochloric or sulfuric acid was used, EDTA was partially deposited during the regeneration in the cathode chamber, primarily on the membrane surface, thus reducing the conductivity of the membrane. This problem could be conquered if sodium carbonate was used instead of acid in the anode chamber. If we had used sodium carbonate as the anolyte, we believe that the yield of free EDTA would have increased. However, as noted above, the high pH can result in membrane degradation.

We were able to recover the deposited lead by either reversal of potential or by immersing the copper electrode in a dilute solution of acid. We further investigated the composition of the deposited lead by x-ray diffraction analysis. Figure 9 shows the x-ray diffraction pattern of the lead coating formed on the copper electrode from the Pb-EDTA solution. The sharp peaks at 2θ equals 29.16 and 30.42 are due to PbO and $Pb_4O_3Cl_2 \cdot H_2O$, respectively. As no chloride was added, it is likely degradation of plastic was the source of the chloride.

All studies of electrolysis reported above have been based on pure Pb-EDTA solutions. To test whether other soil components would affect the process, 75 grams of the Downer loamy sandy soil was extracted with 1500 ml of 0.01 M EDTA. The concentrations of Fe and Mn of the filtrate were 2.82 and 0.17 mg/l, respectively. The EDTA concentration remaining in the filtrate was analyzed by EDTA titrations with calcium and lead. The results show that the EDTA concentration was 9.56×10^{-3} M (by calcium) or 9.68×10^{-3} M (by lead). Then, 0.5935 grams of $Pb(NO_3)_2$ (fw = 331.20) was dissolved in the filtrate and the volume was brought to 250 ml with filtrate to give a solution that was 7.17×10^{-3} M in lead. Thus, a solution having a 0.75:1 ratio of Pb:EDTA was obtained.

Figure 10 shows the percentage of total lead remaining in the catholyte as a function of electrolysis time for an applied current of 0.1 mA (current density = 1.9 mA/m^2). The percentage of Pb removal and EDTA recovered are 99.0% and 91.7%, respectively, and the current efficiency was 14.1%. The percentage of Pb removal in this study was compared with

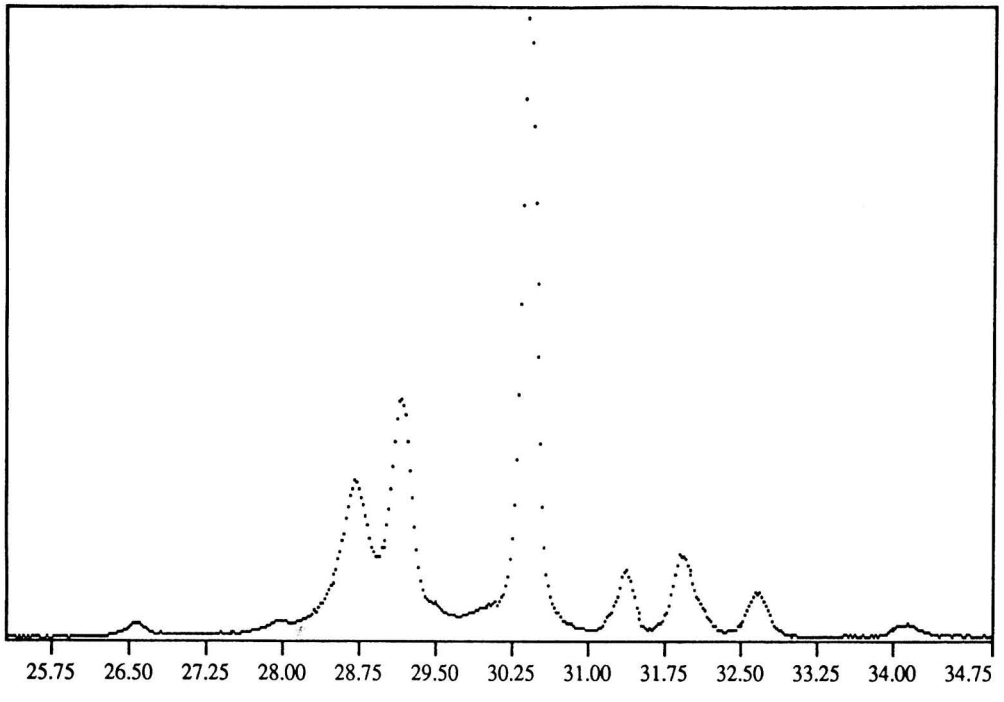

FIGURE 9. X-ray diffraction pattern of the material that was deposited onto a copper plate electrode from a 0.01 M Pb-EDTA solution.

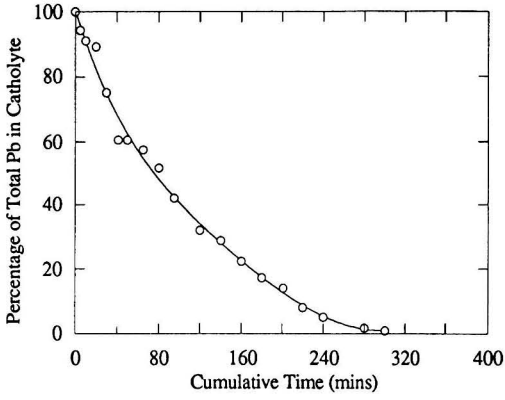

FIGURE 10. Deposition of Pb onto a copper plate electrode from a solution of EDTA that had been contacted with soil and that was 7.17×10^{-3} M Pb and 9.56×10^{-3} M EDTA.

that of the previous study (see Figure 7). Only slightly less Pb was deposited after the soil extraction than when pure Pb-EDTA was electrolyzed. However, it took longer to recover 90+% of the lead in the soil test than it did in the $Pb(NO_3)_2$ test.

In this study we made no attempt to achieve the high current efficiency necessary for full-scale operation. As shown in Figure 7, lowering the current density increased the current efficiency as a result of decreasing side reactions. High current efficiency also requires properly designed electrochemical cells.

High efficiency electrochemical processes have been the focus of a significant amount of research in mining and chemical engineering. There has been a large amount of work directed to the electrowinning of metals [*39*, *40*]. Much of this has been to optimize cell design by minimizing the electrical current requirement. Current efficiency is reduced as metal concentration decreases and under mass transfer limited conditions [*41*]. Fluidized bed electrolysis with fluidized electrodes [*42–46*] or fluidized beds of inert beads [*47*, *48*] have shown that (a) metals can be extracted from solutions with low metal concentrations, (b) electrochemical separations can be achieved, and (c) economic advantages can be achieved when the process is compared to alternatives. The anode and cathode compartments can be separated by inert plates of polyethylene or other inert permeable materials, or by ion exchange resins.

SUMMARY AND CONCLUSIONS

This study demonstrates the feasibility of development of a system for the remediation of soil contaminated by lead, and potentially, other heavy metals, by extraction of the soil with EDTA and subsequent recovery and reuse of the EDTA. The lead is deposited on the electrode in a form that is easily reclaimed for subsequent recycling and reuse.

We have demonstrated that under diffusion limited conditions of polarography and voltammetry, the free metal ion protonated metal complexes, M^{2+} and MHY^{-}, are reduced at the electrode surface. We constructed a two-chamber electrolysis cell in which the anode compartment was separated from the cathode compartment by a cation exchange membrane. This prevented the EDTA from being oxidized at the anode during the electrolysis. High recoveries of copper, lead, and EDTA could be achieved by electrolysis of Cu-EDTA or Pb-EDTA complexes. In most cases the recoveries greatly exceeded 90 percent. As the current density increased, the current efficiency decreased. The current efficiency was greater for free metal ion than for the metal-EDTA complexes. No attempt was made to develop a high current efficiency in the present study. To achieve high current efficiency, it is necessary to have a low current density to minimize side reactions and to use an electrolysis cell having a high efficiency.

Most of the cells described in the literature have been developed to optimize current utilization in electrodeposition processes. In the present case it is also necessary to recover a purified chelator product in the resultant solution. Thus, optimization may be somewhat different in this case. It is clear that a high concentration of chelator should be used for the extraction of soil and that this should be cycled through the soil until its capacity to remove metal is exhausted or is nearly exhausted. This highly concentrated solution will provide an optimum current utilization. This must be balanced against chelator loss in the soil washing process. To minimize loss of chelator, a minimum concentration is best. Obvious the overall optimal chelator concentration is one that minimizes the cost of non-recovered chelator and the use of electricity. The recovered chelator can also be concentrated by several membrane processes. A method to monitor the process of metal extraction from soil must be devised. A countercurrent flow, in which the most contaminated soil is treated with nearly spent chelator should provide the best process. New chelator solution can be used to polish the clean-up.

Additional work is underway to develop a cell meeting the above-described requirements. This is the first step required in the development of a full-scale functioning process that can be routinely utilized for the recovery of metals from soil, ash, and sludge materials.

ACKNOWLEDGMENTS

We wish to thank Michael Davidson and Douglas Baker, of the Department of Civil Engineering of the University of Delaware who respectively designed and constructed the power supply and the cell used in the electrolysis experiments. We are appreciative of the assistance of other faculty at the University of Delaware. We want to thank Dr. C. P. Huang for his advice and Drs. George W. Luther III and Dennis H. Evans for the use of equipment. We also wish to thank Dr. Paul F. Sanders of the New Jersey Department of Environmental Protection and Energy for supplying soil samples and Miss Xiaoping Shao of the Department of Materials Science of the University of Delaware for assistance with the x-ray diffraction analysis.

LITERATURE CITED

1. U.S. Environmental Protection Agency, Hazardous Waste Sites: Descriptions of Sites on Current National Priority List, October, 1984.
2. Ellis, W. D., J. R. Payne, and G. D. McNabb, Treatment of Contaminated Soils with Aqueous Surfactants, U.S. Environmental Protection Agency EPA/600/S2-85/129, 1985.
3. Kesari, J., P. S. Puglionesi, S. Popp, and M. H. Corbin, Heavy Metal Contaminated Soil Treatment: Conceptual Development, U.S. Army Toxic & Hazardous Materials Agency AMXTH-TE-CR-86101, 1987.
4. Evangelista, R. A., and A. P. Zownir, "Lead Extraction from Excavated Soil," paper presented at Fifth National RCRA/Superfund Conference, Las Vegas, NV, April 19–21, 1988.
5. Sims, R. C., J. L. Sims, D. L. Sorensen, J. McLean, R. Mahmood, and R. R. Dupont, Review of In-Place Treatment Techniques for Contaminated Surface Soil, Vol. 1, Technical Evaluation, National Technical Information Service PB 85-124 881, 1985.

6. Smeulders, F. A., A. Maes, J. Sinnaeve, and A. Cremers, "In Situ Immobilization of Heavy Metals with Tetraethylenepentamine (tetren) in Natural Soils and Its Effect on Toxicity and Plant Growth," *Plant and Soils*, **70**: 37–47, 1983.
7. Ehrenfeld, J., and J. Bass, Evaluation of Remedial Action Unit Operations at Hazardous Waste Disposal Sites, Noyes Publications, Park Ridge, NJ, 1984.
8. Rulkens, W. H., and J. W. Assink, "Extraction as a Method for Cleaning Contaminated Soil: Possibilities, Problems and Research," Proceedings of the 5th National Conference on Management of Uncontrolled Hazardous Waste Sites, Washington, D.C., 1984, pp. 576–583.
9. Stumm, W., and J. J. Morgan, Aquatic Chemistry, 2nd ed., New York, Wiley, 1981.
10. Evans, L. J., "Chemistry of Metal Retention by Soils," *Environ. Sci. Technol.*, **23**: 1046–1056 (1989).
11. Sposito, G., The Chemistry of Soils, New York, Oxford University Press, 1989.
12. Shuman, L. M., "The Effect of Soil Properties on Zinc Adsorption by Soils," *Soil Sci. Soc. Am. Proc.*, **39**: 454–458 (1975).
13. Kuo, S., and A. S. Baker, "Sorption of Copper, Zinc and Cadmium by Some Acid Soils," *Soil Sci. Soc. Am. Proc.*, **44**: 969–974 (1980).
14. Harter, R. D., "Effect of Soil pH on Adsorption of Lead, Copper, Zinc, and Nickel," *Soil Sci. Soc. Am. Proc.*, **47**: 47–51 (1983).
15. Elliott, H. A., M. R. Liberti and C. P. Huang, "Competitive Adsorption of Heavy Metals by Soils," *J. Environ. Qual.*, **15**: 214–219 (1986).
16. Fu, G., and H. E. Allen, "Cadmium Adsorption by Oxic Sediment," *Water Res.*, **26**: 225–233 (1992).
17. Sposito, G., The Surface Chemistry of Soils, New York, Oxford University Press, 1984.
18. Ringbom, A., Complexation in Analytical Chemistry, New York, Interscience, 1963.
19. Ellis, W. D., T. R. Fogg, and A. N. Tafuri, "Treatment of Soils Contaminated with Metals," Proceedings of the 12th Annual Research Symposium: Land Disposal, Remedial Action, Incineration and Treatment of Hazardous Waste, 1986, pp. 201–207.
20. Mobley, K., "Potential Use of Chelating Agents for Decontamination of Soils," M.S. Thesis, Dartmouth, 1988.
21. Connick, C. C., "Mitigation of Heavy Metal Migration in Soil," *New Eng. Water Pollut. Control Assoc. J.*, **19**: 4–21, 1985.
22. Connick, C. C., F. Blanc and J. O'Shaughnessy, "Adsorption and Release of Heavy Metals in Contaminated Soil," Proceedings of the 1985 Specialty Conference ASCE Environmental Engineering Division, 1045–1052, 1985.
23. Esposito, P., J. Hessling, B. B. Locke, M. Taylor, M. Szabo, R. Thurnau, C. Rogers, R. Traver and E. Barth, "Results of Treatment Evaluations of a Contaminated Synthetic Soil," *J. Air Pollut. Control Assoc.*, **39**: 292–304, 1989.
24. Yang, H-H., "Cadmium Adsorption-Desorption on Soils," M.S. Thesis, Dept. Civil Engineering, University of Delaware, 1993.
25. U.S. Bureau of Mines, Mineral Comodity Summaries 1993, Washington, 1993.
26. Elliott, H. A., J. H. Linn, and G. A. Shields, "Role of Fe in Extractive Decontamination of Pb-Polluted Soils," *Haz. Waste and Haz. Mater.*, **6**: 223–229, 1989.
27. Elliott, H. A., G. A. Brown, G. A. Shields, and J. H. Linn, "Restoration of Pb-Polluted Soils by EDTA Extraction," Proceedings of the Seventh International Conference on Heavy Metals in the Environment, Vernet, J.-P., ed., Geneva, Vol. II, pp. 64–67, 1989.
28. Peters, R. W., and L. Shem, "Use of Chelating Agents for Remediation of Heavy Metal Contaminated Soil," *in* Environmental Remediation, G. F. Vandegrift, D. T. Reed and I. R. Tasker, eds., ACS Symposium Series 509, American Chemical Society, Washington, 1992, pp. 70–84.
29. Tessier, A., P. G. C. Campbell and M. Bisson, "Sequential Extraction Procedure for the Speciation of Particulate Metals," *Anal. Chem.*, **51**: 844–851, 1979.
30. Tuin, B. J. W., and M. Tels, "Distribution of Six Heavy Metals in Contaminated Clay Soils Before and After Extractive Cleaning," *Environ. Technol.*, **11**: 935–948, 1990.
31. Johnson, J. W., H. W. Jiang, S. B. Hanna and W. J. James, "Anodic Oxidation of Ethylenediaminetetraacetic Acid on Pt in Acid Sulfate Solutions," *J. Electrochem. Soc.*, **119**: 574–580, 1972.
32. Gordievskii, A. V., and Y. S. Gurinov, "Regeneration of Trilon B from Copper EDTA Solutions by Electrolysis with Ion Exchange," *Zhurnal Prikladnoi Khimii*, **34**: 936–938, 1961.
33. Etzel, J. E., and D. Tseng, Cation Exchange Removal of Heavy Metals with a Recoverable Chelant Regenerant, *in* Metal Speciation, Separation, and Recovery, J. W. Patterson and R. Passino, eds., Lewis Publishers, Chelsea, MI, 1987.
34. Standard Methods for the Examination of Water and Wastewater, 17th edition, Washington, DC, American Public Health Association, 1989.
35. Flaschka, H. A., EDTA Titration, New York, Pergamon Press, 1959.
36. Chen, P-H., Recovery of Metal and EDTA from Metal-EDTA Solutions by Electromembrane Deposition, M.S. Thesis, Dept. Civil Engineering, University of Delaware, 1992.
37. Weinberg, N. L., and B. V. Tilak, eds., Technique of Electroorganic Synthesis Scale-up and Engineering Aspects, Technique of Chemistry, Vol. V, Part III, p. 226, New York, John Wiley & Sons, 1982.
38. Lacey, R. E., and S. Loeb, Industrial Processing with Membranes, New York, Wiley-Interscience, 1992.
39. Gilroy, D., The Electrowinning of Metals, *in* Industrial Electrochemical Processes, A. T. Kuhn, ed., Amsterdam, Elsevier, 1971.
40. Bautista, R. G., ed., Hydrometallurgical Process Fundamentals, New York, Plenum, 1984.
41. Avci, E., "Electrolytic Recovery of Nickel from Dilute Solutions," *Sep. Sci. Technol.*, **24**: 317–324, 1989.
42. Hiddleston, J. N., and A. F. Douglas, "Fluidized Bed Electrodes. Fundamental Measurements and Implications," *Nature*, **218**: 601–602 (1968).
43. Coeuret, F., "The Fluidized Bed Electrode for the Continuous Recovery of Metals," *J. Appl. Electrochem.*, **1**: 103 (1971).
44. Flet, D. S., "The Fluidized-Bed Electrode in Extractive Metallurgy," *Chem. Ind.*, **24**: 983–988, 1972.
45. Leroy, R. L., "Fluidized-Bed Electrowinning. I. General Modes of Operation," *Electrochim. Acta*, **23**: 815–826, 1978.
46. Wei, T., I. Shaw, and Y. Hoh, "Electrolytic Recovery of Low Concentration Cupric Ions by a Fluidized-Bed Electrode Reactor," *J. Chinese Inst. Chem. Eng.*, **18**: 83–91, 1987.
47. Lopez-Cacicedo, C. L., "The Electrolytic Recovery of Metals from Dilute Effluent Streams," *J. Separ. Proc. Technol.*, **2**: 34–39, 1981.
48. Boyanov, B. S., J. D. Donaldson, and S. M. Grimes, "Removal of Copper and Cadmium from Hydrometallurgical Leach Solutions by Fluidized Bed Electrolysis," *J. Chem. Tech. Biotechnol.*, **41**: 317–328, 1988.

Effects of Salts on Limestone Dissolution Rate in Wet Limestone Flue Gas Desulfurization

Naohiko Ukawa and Toru Takashina

Hiroshima Research & Development Center, Mitsubishi Heavy Industries, Ltd., 4-6-22, Kanonshin-machi, Nishi-ku, Hiroshima 733 JAPAN

and

Michio Oshima and Tsuyoshi Oishi

Engineering and Construction Center, Mitsubishi Heavy Industries, Ltd., 15-1, Tomihisa-cho, Shinjuku-ku, Tokyo 162 JAPAN

To understand how the dissolution rate of limestone used for absorbent in a wet flue gas desulfurization plant is affected by the soluble salts formed from hydrogen chloride gas in flue gas as well as from the impurities contained in the used raw material limestone itself, various limestone slurries each added with a single salt of $CaCl_2$, $MgCl_2$, NaCl, Na_2SO_4 and $MgSO_4$ were titrated with sulfuric acid. From the titration results the dissolution rate was found to vary greatly with the kind and the concentration of the salts with a general tendency to decrease in chloride solution but to increase in sulfate solutions.

Based on this finding, the authors proposed a semi-empirical simplified model. The evaluated results using this model closely agreed with the measured values of the limestone dissolution rate both in single-salt solutions and mixed salt solutions.

INTRODUCTION

In wet limestone flue gas desulfurization (FGD) process, powdered limestone dissolves and neutralizes acidity produced by SO_2 absorption in liquid phase.

It is known that the soluble salts have effects [*6, 9*] on the dissolution rate of the limestone used as the absorbent but sufficient quantitative examinations had not yet been conducted to clarify the phenomena.

It is thus very important to obtain quantitatively the effects of the salts because the most dominant factor which determines the performance of the FGD is the limestone dissolution rate.

Under normal operating conditions in the FGD process, the kinds and concentrations of salts accumulating in the absorbent slurry vary widely and are governed by the concentrations of impurities in the flue gas, the chemical composition of the limestone, and the water balance of the FGD process.

In this study, various limestone slurries, each added with a single salt, were titrated with sulfuric acid to measure the dissolution rate. Salts used were calcium chloride ($CaCl_2$), magnesium chloride ($MgCl_2$), sodium chloride (NaCl), sodium sulfate (Na_2SO_4) and magnesium sulfate ($MgSO_4$).

As it became clear that the dissolution rate of limestone was affected significantly by the kind and concentration of salts, the authors proposed the semi-empirical dissolution rate model in which ionic strength and bisulfate ion were introduced as the affecting factors.

Consequently, the dissolution rates evaluated by the proposed dissolution model closely agreed with the experimental results. The dissolution rates of limestone in mixed salts were also examined in detail since various salts exist in mixed states in commercial FGD processes.

EXPERIMENTAL APPARATUS AND PROCEDURE

The dissolution rate of the limestone was measured in a batch reactor shown in Figure 1.

Two methods such as "pH-stat" and "free-drift" have been used to determine the dissolution rate of limestone. In the present study, the pH-stat method used by many other investigators [*1, 2, 8*] was selected due to its high reproducibility.

The reactor was agitated at 600 r.p.m., by a turbine (6 blades, 50 mm diameter, 10 mm width) to fully fluidize the sample.

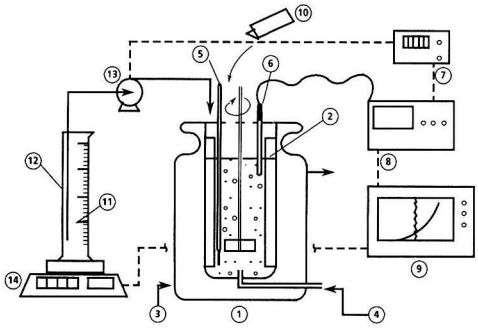

FIGURE 1. Limestone dissolution rate measurement apparatus

A sulfuric acid solution (1.0 mol/ℓ) was titrated into a limestone slurry of 2 ℓ in the reactor to maintain the pH at 5.2 ± 0.1. The experiment was initiated by the addition of 20 g of limestone and 200 g of seed gypsum.

Sulfuric acid was selected as the acid to simulate the totally oxidizing condition in absorber tank by so called "in-situ oxidation" [4] which is usually being applied to the current FGDs. The use of the sulfuric acid eliminated the strong inhibition of limestone dissolution by sulfite which had been previously investigated by Chan and Rochelle [1, 8]. The operating pH was determined from the pH range in the commercial FGD and the operability of the experiments.

The titration rate of sulfuric acid was automatically controlled by a feed pump monitoring the pH of the slurry. The slurry temperature was thermostated at 50 ± 1°C by a water jacket outside the reactor. Air was sparged at 13 ℓ/min into the slurry to release carbon dioxide gas into the atmosphere to eliminate the effect of dissolved CO_2.

The weight of sulfuric acid was continuously measured by a balance and recorded. The titration speed was calculated from the periodic decrease in the sulfuric acid weight.

The titrated sulfuric acid dissolves limestone by following reaction:

$$H_2SO_4 + CaCO_3 + H_2O \rightarrow CaSO_4 \cdot 2H_2O + CO_2 \qquad (1)$$

The mass balance equation of SO_4^{2-} for the titration is given by:

$$F \cdot Cs \cdot dt = r \cdot V \cdot dt + V \cdot dC + C \cdot dV \qquad (2)$$

Where F is the titration rate of H_2SO_4 [ℓ/h], Cs is the concentration of H_2SO_4 [mol/ℓ], t is time [h], r is the dissolution rate of limestone with H_2SO_4 [mol/ℓ·h] which is thought to express removal rate of SO_4^{2-} by gypsum crystallization, V is the volume of limestone slurry in the reactor [ℓ] and C is the concentration of H_2SO_4 in the slurry [mol/ℓ].

In this experiment, the volume change of the slurry was small and the steady state for SO_4^{2-} in the slurry was attained due to the prevention of supersaturation by addition of the seed gypsum. Thus, the limestone dissolution rate was expressed by:

Table 1 Properties of limestone used for the tests

CaO		[wt %]	54.6
MgO		[wt %]	0.23
Fe_2O_3		[wt %]	0.013
SiO_2 + Acid insoluble		[wt %]	0.12
Al_2O_3		[wt %]	0.011
Purity		[wt %]	97.5
Particle size	45 [μm]	97.2 [wt %]	passing

$$r \simeq \frac{F \cdot Cs}{V} \qquad (3)$$

Here, because the limestone dissolution rate (r) varies with its particle size distribution and chemical composition, limestone from specified mine with a consistent particle size distribution was used throughout the experiments to eliminate this source of variability.

Properties of the used limestone are shown in Table 1.

As the comparison standard, the limestone dissolution rate (r) was employed when 70% of initially charged limestone dissolved because the r varies with the change in the limestone particle size and the limestone concentration during the titration.

To investigate the effects of salts, Na_2SO_4, $MgSO_4$, $MgCl_2$, NaCl and $CaCl_2$ were added individually or as mixtures. The reagents used were of pure grade made by Hayashi Pure Chemical Industries, Ltd.

RESULTS AND DISCUSSION

Limestone Dissolution Rate in Single Salt Solutions

Figure 2 shows the relationship between concentrations of various coexisting salts and the relative dissolution rates (R)

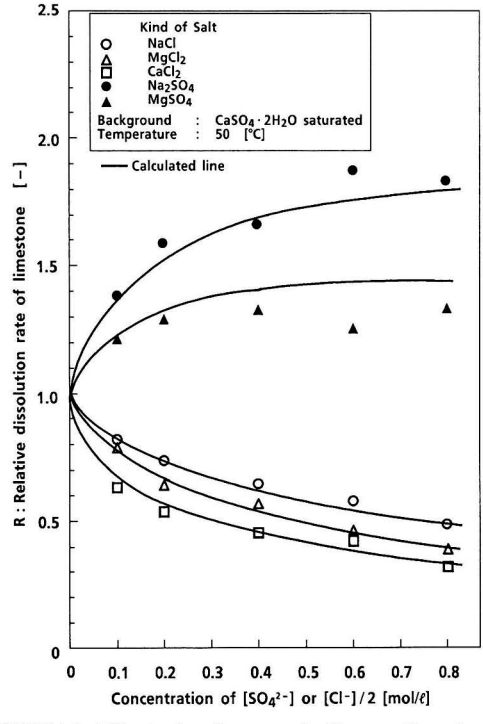

FIGURE 2. Effect of salt concentration on limestone dissolution rate

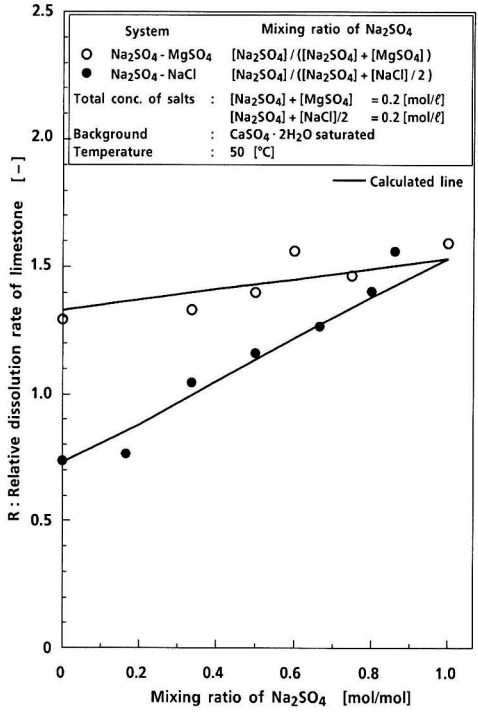

FIGURE 3. Limestone dissolution rate in mixed salts solution

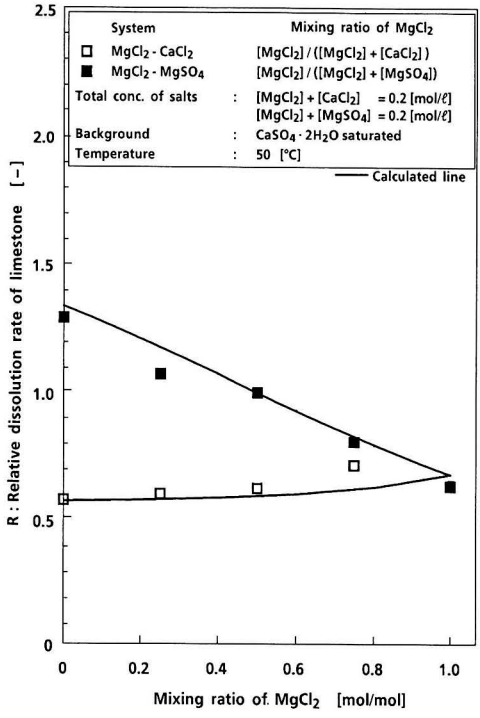

FIGURE 4. Limestone dissolution rate in mixed salts solution

of limestone. The relative dissolution rate (R) is a ratio of the dissolution rate (r_o) in a standard solution containing no salt and the dissolution rate (r) in a solution containing a salt, and is defined by:

$$R = \frac{r}{r_o} \tag{4}$$

In chloride solutions such as $CaCl_2$, $MgCl_2$ and NaCl, the dissolution rate decreases with the concentration of salt. At the same Cl^- concentration, the decrease in dissolution rate is greater in the $CaCl_2$ and $MgCl_2$ solutions than that in the NaCl solution.

When sulfates such as Na_2SO_4 and $MgSO_4$ were added, the dissolution rate increased. The effects of the sulfates were entirely different from those of the chlorides.

Limestone Dissolution Rate in Mixed-Salt Solutions

Figure 3 shows how the dissolution rate of limestone changed in the solution containing Na_2SO_4 and $MgSO_4$ at different mixing ratios. With a greater mixing ratio of Na_2SO_4, the dissolution rate increased mildly. This agrees with previously described results where the dissolution in solution containing Na_2SO_4 exhibits a slightly greater rate than that containing $MgSO_4$.

Figure 3 also depicts the dissolution rate change in the solution containing Na_2SO_4 and NaCl.

As also mentioned previously, the individual salts had an entirely different effect on the dissolution rate.

The effects of the mixed salts on the dissolution rate are located midway between the effects of these salts when they were added alone. That is, the dissolution rate decreased in a solution containing a greater amount of NaCl, and increased in a solution containing a greater amount of Na_2SO_4.

Figure 4 expresses the dissolution rate as a function of the $MgCl_2$–$CaCl_2$ mixing ratio.

With a greater mixing ratio of $MgCl_2$, the dissolution rate increased mildly. This also agrees with the result that a reduction in dissolution rate is less affected by $MgCl_2$ than that by $CaCl_2$.

Figure 4 also shows the dissolution rates in solutions containing $MgCl_2$ and $MgSO_4$. Similar to the case of the sodium salts in Figure 3, the dissolution rate decreased in a solution containing a greater amount of $MgCl_2$ and increased in a solution containing a greater amount of $MgSO_4$.

SIMPLIFIED MODEL FOR THE EVALUATION OF SALT EFFECTS

Influencing Factors

The test results concerning the limestone dissolution rate were summarized as follows:

—The dissolution rate decreases as the concentration of a chloride increases.
—The dissolution rate increases as the concentration of a sulfate increases.

To explain these results qualitatively, the authors assumed the following influencing factors:

a) The dissolution rate decreases when the ionic strength (I) increases as observed in a chloride solution.
b) The increase of the dissolution rate in a sulfate solution is brought about by the effect of bisulfate ions coexisting in the solution in equilibrium.

The factor a) is based on the previous report [5] that the dissolution of limestone is controlled primarily by the diffusion of H^+ from the bulk of solution to the limestone surface, and

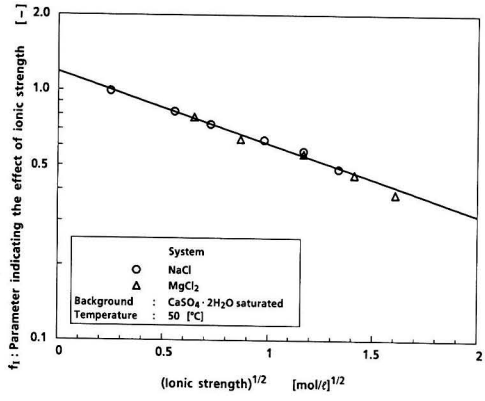

FIGURE 5. Effect of ionic strength on limestone dissolution rate

high ionic strength inhibits the dissolution by decreasing the diffusivity of the H^+.

The factor b) is due to the idea that sulfates enhance the dissolution rate by providing an additional species of diffusing acidity i.e. the bisulfate ion (HSO_4^-) to the limestone surface.

In the case of chlorides, only the effect of a) occurs and the dissolution rate decreases. While in the case of sulfates, the effects of a) and b) offset each other and depending on its degree, the dissolution rate increases.

Previous studies [*1*, *8*] had demonstrated precious theoretical approach to the effect of solution composition on the dissolution rate of limestone. However, the strong effect of sulfate or bisulfate ion as shown in the present study had not been discussed sufficiently. Therefore, the authors tried to propose a semi-empirical simplified model for the evaluation of limestone dissolution rate, considering the effect of bisulfate ion as a dominant factor.

Modeling of the Dissolution Rate

First, it is assumed that the relative dissolution rate (R) defined in equation 4 is expressed by the product of the effects of the above two mutually independent factors as follows:

$$R = f_I \cdot f_S \tag{5}$$

f_I and f_S are parameters indicating the degrees of effects of the ionic strength and bisulfate ions respectively. The f_I means relative diffusion rate of acid and the f_S corresponds to the relative acid concentration. In the system containing no salt, both f_I and f_S are defined to be 1.0.

Determination of f_I

Using data of NaCl and $MgCl_2$ system in Figure 2, f_I is obtained. As this system contains no sulfates, f_S should be 1.0 and f_I is obtained directly from the observed R.

After trying to find out the most fittable curve to the measured value, an empirical formula shown in equation 6 was obtained.

$$\log f_I = 0.0730 - 0.286\sqrt{I} \tag{6}$$

As shown in Figure 5, the solid line calculated by equation 6 shows close agreement to measured values. Strictly speaking, the ionic strength I should be calculated using the molality, but considering the relatively low salt concentration, it was calculated in terms of molarity for easiness in practical use.

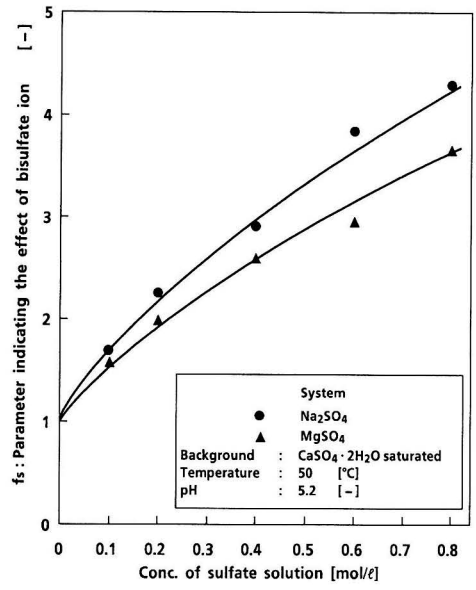

FIGURE 6. Relation between sulfate solution concentration and parameter f_S

The pattern of the relation expressed in equation 6 was similar to that of the previous study [*8*] and closely agreed with the reported dependence of the H^+ diffusivity on the ionic strength. But in the present research, the weaker dependence of dissolution rate of limestone on the ionic strength than in the previous study [*8*] was found. The cause of the difference probably is due to the differences of experimental conditions such as pH and the flow rate of sparging gas.

Determination of f_S

The effects of sulfates are separated using the data of the Na_2SO_4 and $MgSO_4$ system and considering the above-mentioned effect of the ionic strength.

From the measured R and calculated f_I by equation 6, f_S could be obtained by equation 5.

Figure 6 shows the relation between f_S and the sulfate concentration. It is found that f_S increases as the concentration of sulfate increases. The probable reasons for this are thought to be as follows:

When a sulfate exists, bisulfate ions are formed in the following equilibrium.

$$SO_4^{2-} + H^+ \rightleftharpoons HSO_4^- \tag{7}$$

In addition to H^+, the bisulfate ions also react with the limestone and enhance the dissolution rate.

$$HSO_4^- + CaCO_3 + 2H_2O \rightarrow CaSO_4 \cdot 2H_2O + HCO_3^- \tag{8}$$

From previous report [*7*], it was thought that the dissolution rate of limestone was nearly proportional to the H^+ ion concentration within the pH range conducted in this study. If this was true, the dissolution rate would become equal regardless of the kinds of salts when pH is the same, and differences in the dissolution rate with kinds of the salts would not be explainable. If it is presumed that HSO_4^- also reacts directly as shown in equation 8 with $CaCO_3$ as well as H^+ and its reaction rate is α times greater than the reaction of H^+, the following expression can be applied.

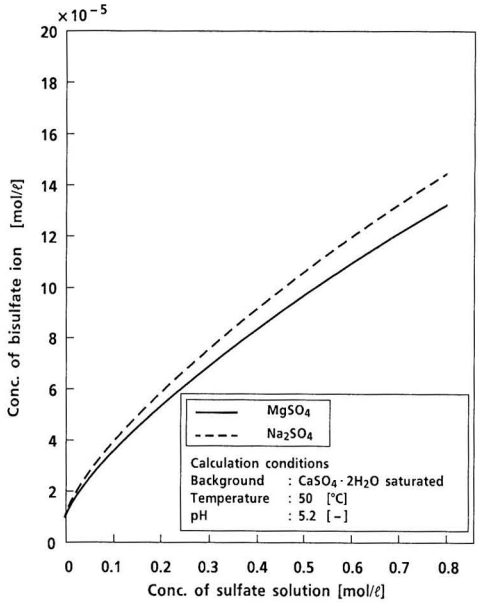

FIGURE 7. Concentration of bisulfate ion in sulfate solutions

$$r = k([H^+] + \alpha[HSO_4^-]) \cdot f_I \tag{9}$$

Where, k is a reaction rate constant. A similar relation holds under the standard condition without salt.

$$r_o = k([H^+]_o + \alpha[HSO_4^-]_o) \tag{10}$$

Where, the suffix stands for the standard condition with no salts addition. From the definitions in equations 4 and 5 and from equations 9 and 10, the following relation is obtained.

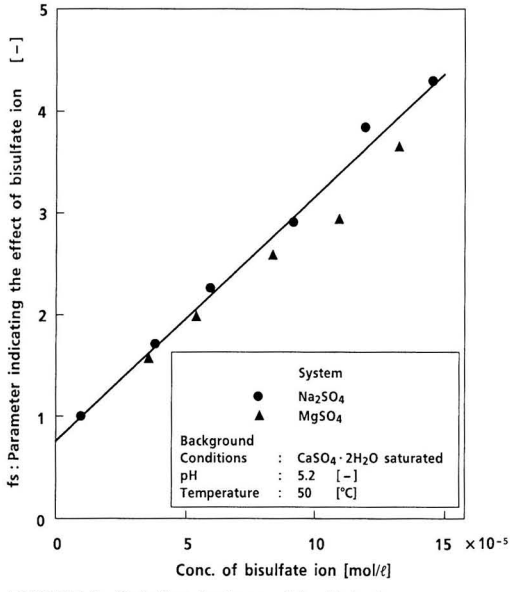

FIGURE 8. Relation between bisulfate ion concentration and parameter f_S

$$f_S = \frac{r}{r_o \cdot f_I} = \frac{[H^+] + \alpha[HSO_4^-]}{[H^+]_o + \alpha[HSO_4^-]_o} \tag{11}$$

The value of $[H^+]$ is obtained by:

$$[H^+] = 10^{-pH}/\gamma_{H^+} \tag{12}$$

The pH value at the standard conditions is 5.2. Therefore, equation 11 can be rewritten as follows:

$$f_S = \frac{10^{-5.2} + \beta[HSO_4^-]}{10^{-5.2} + \beta[HSO_4^-]_o}$$

$$\beta = \alpha \cdot \gamma_{H^+} \tag{13}$$

Strictly speaking, the activity coefficient γ_{H^+} of hydrogen ion varies with the ionic strength and liquid composition, but is assumed to be constant within the test range of this study for simplification.

That is, when f_S is plotted as a function of $[HSO_4^-]$, a linear relation is obtained and β is obtained from its y intercept or gradient.

The concentration of bisulfate ion can be calculated by:

$$[HSO_4^-] = Kc[H^+][SO_4^{2-}]$$

$$= Ka \cdot 10^{-pH}[SO_4^{2-}](\gamma_{SO_4^{2-}}/\gamma_{HSO_4^-}) \tag{14}$$

Ka is the equilibrium constant of formation reaction of bisulfate shown in equation 7 and has the following value at 50°C according to the literature [5].

$$Ka = 194.6 \tag{15}$$

Using the method reported by Helgesen [3] which is regarded relevant in the range of high salt concentration, the activity coefficient is evaluated as follows:

$$\log \gamma_{SO_4^{2-}} = -4AI^{1/2}(1 + 4 \cdot B \cdot I^{1/2}) + C \cdot I \tag{16}$$

$$\log \gamma_{HSO_4^-} = -AI^{1/2}(1 + 4.5 \cdot B \cdot I^{1/2}) + C \cdot I \tag{17}$$

Where, A, B and C are evaluated to be 0.535, 0.333 and 0.043, respectively.

Figure 7 shows a relation between the concentration of salt and the concentration of calculated $[HSO_4^-]$ taking into consideration the gypsum saturated background.

In Figure 8, f_S values obtained are plotted against the concentration of HSO_4^-, and the linear relation between $[HSO_4^-]$ and fs therein gives following β in equation 13

$$\beta = 0.20 \tag{18}$$

Comparison of Measured and Calculated Dissolution Rates of Limestone

The effects of the ionic strength and sulfate on the limestone dissolution rate are calculated by equations 6 and 13, and R is evaluated by equation 5.

The solid lines in Figure 2 show the calculated R in the systems of the various salts. The results of calculation nearly agree to those of the measured.

Solid lines in Figure 3 show the calculated relations between the R and the mixing ratios of salts in the Na_2SO_4-$MgSO_4$ and Na_2SO_4-NaCl systems. In both systems, the calculated results also fit in with the observed. In the $CaCl_2$-$MgCl_2$ and $MgSO_4$-

$MgCl_2$ systems, the calculated results of R approximately agree to the measured values as shown in Figure 4. As mentioned above, it has become clear that the simplified model proposed in this section provides a quantitative explanation of the effects of various salts and their mixtures on the limestone dissolution rate.

CONCLUSION

In the wet limestone FGD process, various kinds of soluble salts formed from impurities contained in the flue gas and limestone accumulate in the absorbent slurry.

These soluble salts influence the dissolution rate of limestone used as the absorbent. Experimental investigation was made to clarify the effects of the various kinds of salts and their concentrations on the dissolution rate of limestone. As a result, it was made clear that the dissolution rate decreased in the chloride solutions but increased in the sulfate solutions.

To explain these phenomena, a semi-empirical simplified model based on the following fundamental mechanisms was proposed:

a) The dissolution rate decreases as the ionic strength increases.
b) The dissolution rate in a sulfate solution increases due to the effect of coexisting bisulfate in equilibrium.

The model provides a quantitative explanation of the experimental results.

It is possible to evaluate the effects of salts on the limestone dissolution rate not only in single salt systems but also in their mixtures.

In the actual FGD process, the characteristics of flue gas, impurities in limestone and operating conditions such as water balance vary greatly from plant to plant resulting in the accumulation of various kinds of salts in the absorbent slurry.

The effects of these salts on the limestone dissolution rate are complicated and were difficult to evaluate so far. The results of this study would give a practical means of evaluating these complicated effects. Paying attention to the effects of the salts is important for improving the design accuracy, since the dissolution rate of limestone is a key factor which governs the desulfurization efficiency.

NOTATION

C = concentration of H_2SO_4 in slurry [mol/ℓ]
Cs = concentration of H_2SO_4 used for titration [mol/ℓ]
F = titration rate of H_2SO_4 [ℓ/h]
f_I = parameter indicating the effect of ionic strength on the limestone dissolution rate [−]
f_S = parameter indicating the effect of bisulfate ion on the limestone dissolution rate [−]
I = ionic strength [mol/ℓ]
Ka, Kc = equilibrium constant based on activity, and concentration respectively [ℓ/mol]
k = reaction rate constant [h^{-1}]
R = relative dissolution rate of limestone [−]
r = dissolution rate of limestone [mol/ℓ·h]
t = time [h]
V = volume of limestone slurry in the reactor [ℓ]
γ_i = activity coefficient of ion i [−]
α, β = empirical constant [−]

SUBSCRIPT

o = standard condition with no salts addition

LITERATURE CITED

1. Chan, P. K., and G. T. Rochelle, "Limestone Dissolution: Effects of pH, CO_2 and Buffers Modeled by Mass Transfer," ACS Symposium Series, No. 188, 75 (1982).
2. Ellis, A. R., "An Investigation of UK Limestone Reactivity for the Limestone-Gypsum FGD Process," I ChemE Symposium Series, No. 106, 251 (1989).
3. Helgesen, H. C., *Am. J. Sci.*, 267, 729 (1969).
4. Heydorn, E. C., C. L. Yeh, K. Muramatsu and N. Ukawa, Proc. of Seventh Annual International Pittsburgh Coal Conference, Pittsburgh (1990).
5. Kharaka, Y. K., and I. Barnes, "Solution-Mineral Equilibrium Computations," U.S. Geological Survey Menlo Park, California (1973).
6. Owen, D. G., W. D. Halstead and J. R. P. Cooper, I. Chem. E. Symposium Series, No. 116, 349 (1990).
7. Plummer, L. N., T. M. L. Wigley and D. L. Parkhurst, *Am. J. Sci.*, 278, 179 (1978).
8. Rochelle, G. T., P. K. R. Chan and A. T. Toprac, "Limestone Dissolution in Flue Gas Desulfurization Process," EPA Report No. EPA-600/7-83-043 (1983).
9. Schöngrundner, W., R. J. Marr and H. Maier, VGB Kraftwerkstechnik, 8, 70 (1990).

Simultaneous NO_x-SO_x Removal by Ammonia using Methanol Injection and Partial Flue Gas Condensation

Klaus Hjuler and Kim Dam-Johansen

Department of Chemical Engineering, Technical University of Denmark, DK-2800 Lyngby, Denmark

The feasibility of combining selective reduction of nitric oxide by ammonia, or nitric oxide oxidation by methanol, with partial flue gas condensation has been studied in the laboratory. It was demonstrated that both combinations may result in high removal efficiencies for nitric oxide and sulfur dioxide. High-temperature reactors (600–900°C) and low-temperature (20–40°C) tubular condensers were applied in series, and each one was tested individually. The flow of simulated flue gas ranged from 1 to 5 Nl/min. In the condenser simultaneous absorption of ammonia, sulfur dioxide, oxygen, and nitrogen dioxide took place. At certain conditions large quantities of aerosols were formed, particularly when NO_2 was present.

INTRODUCTION

Recent laboratory experiments have shown that the addition of methanol (and other organic compounds) to simulated flue gas at 500–800°C provides a rapid and nearly quantitative conversion of NO to NO_2. At the same time, reduction of SO_3 to SO_2 can be obtained. Thus, methanol injection in combination with ammonia or urea-based selective non-catalytic NO_x-reduction processes (SNR) may be advantageous: it reduces the necessary amount of methanol, byproduct CO is lowered (approximately one mole of CO is produced per mole NO or SO_3 converted), and NH_4HSO_4 formation may be eliminated due to the reduction of SO_3 [*1*]. However, a combination requires that the flue gas is scrubbed before discharge to remove NO_2 (and SO_2).

If traditional limestone scrubbing is applied, problems with oxidation of calcium sulfite and subsequent crystallization of calcium sulfate on scrubber surfaces may be intensified due to the presence of NO_2. Rosenberg and Grotta [*2*] studied the influence of NO_2 on the oxidation of $CaSO_3$ to $CaSO_4$ and found that NO_2 acts as a promoter either catalytically or as a direct oxidant. They suggested the use of an NO_2 prescrubber in order to avoid sulfate scaling. Thus, other types of flue gas desulfurization processes, such as spray drying using $Ca(OH)_2$ or ammonia solution wet scrubbing, may be even more suitable for combination with SNR and methanol injection. In these processes the sulfite content of the byproduct may be converted into the more usable sulfate.

The reaction between sulfur dioxide and ammonia in flue gas has been extensively studied in a previous work (Hjuler and Dam-Johansen, [*3*]) at temperatures above the water dew point. It was observed that ammonium salts containing sulfur in the (IV) and the (VI) oxidation states were formed on surfaces. The presence of NO_2 accelerated sulfite oxidation significantly. The rate of reaction increased when the temperature decreased. In the present work a high sulfur dioxide removal efficiency was obtained by lowering the temperature below the water dew point.

EXPERIMENTAL SET-UP

High-temperature (600–900°C) and low-temperature (20–40°C) serial reactors were applied in this study, and each one was tested individually. In both reactors the flow pattern was

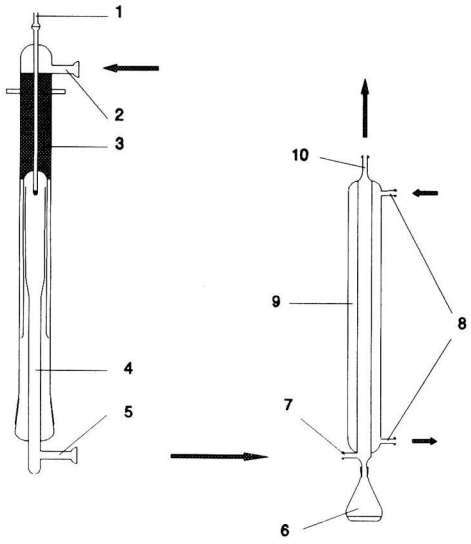

FIGURE 1. Experimental set-up with 100 cm³ high-temperature reactor (left) and condenser (right). The arrows indicate the normal flow directions using air as a coolant. 1: NH_3 or CH_3OH inlet, 2: main gas inlet, 3: pre-heat section, 4: reaction tube outlet, 5: reactor outlet, 6: Erlenmeyer flask for condensate, 7: gas inlet/outlet, 8: coolant inlets/outlets, 9: thermostating jacket, 10: gas inlet/outlet.

close to plug flow in the flow range used (1-5 Nl/min). Simulated flue gas was mixed from cylinders of the individual components by means of reduction valves and mass flow controllers. In all experiments the oxygen and water concentrations were constant at about 4.5 and 6.0 vol-% respectively. Except for nitrogen and oxygen, the gases used were pre-mixed with nitrogen. Water was added by evaporating known quantities from a micro pump.

In the two high-temperature reactors either selective non-catalytic reduction of NO or NO oxidation by methanol was carried out. Both reactors were constructed in quartz glass; one with a reaction volume of about 100 cm³ with a gas pre-heating section filled with quartz glass spheres, Figure 1, and the other with a reaction volume of 11.5 cm³ (presented in Kristensen *et al.*, [4]). The reactors were mounted in a three zone oven. Methanol was added by evaporating a water/methanol mixture.

In the low-temperature reactors (condensers), the reactor wall temperature was maintained below the water dew point of the inlet gas. Typically about 20% of the water content was condensed. The reactors were jacket thermostated vertical pyrex glass tubes (dimensions 4.0 or 8.8 mm i.d., 43 cm in length) with Erlenmeyer flask glass connections in the bottom for collection of the condensate, Figure 1. Water or air was used as coolant.

Inlet and outlet concentrations of SO_2, NH_3 and NO were measured in the UV range using differential absorption spectrometry. NO_2 was measured by converting it to NO in a molybdenum oxide converter. The spectrometer was operated by means of a built-in personal computer, which was also used for data acquisition and analysis.

EXPERIMENTAL RESULTS

The experimental results presented in the following fall in three parts. First, the optimal reaction temperatures were found for selective non-catalytic reduction of NO and NO oxidation by methanol. Next, the performance of the condenser was investigated at various reaction conditions to determine SO_2 removal efficiencies by NH_3 and the accompanying NH_3 emissions. Finally, these reactors were combined.

High-temperature Reactors

For NO reduction using NH_3 the optimal operating temperature of the 100 cm³ high-temperature reactor was found to be about 860°C at a residence time of 340 K·s (i.e. 0.34 s at 1000 K). The NO reduction was about 64% for an NO inlet concentration of about 500 ppm and an inlet NH_3/NO molar ratio of 1. This result compares quite well with the results obtained by Duo *et al.* [5]. Moreover, it was observed that the NO reduction decreased about 30% in the presence of 800 ppm SO_2, probably due to radical quenching.

When methanol was introduced upstream of the 11.5 cm³ reactor at an inlet CH_3OH/NO molar ratio of 1, NO was oxidized almost completely to NO_2, Figure 2. At the isothermal

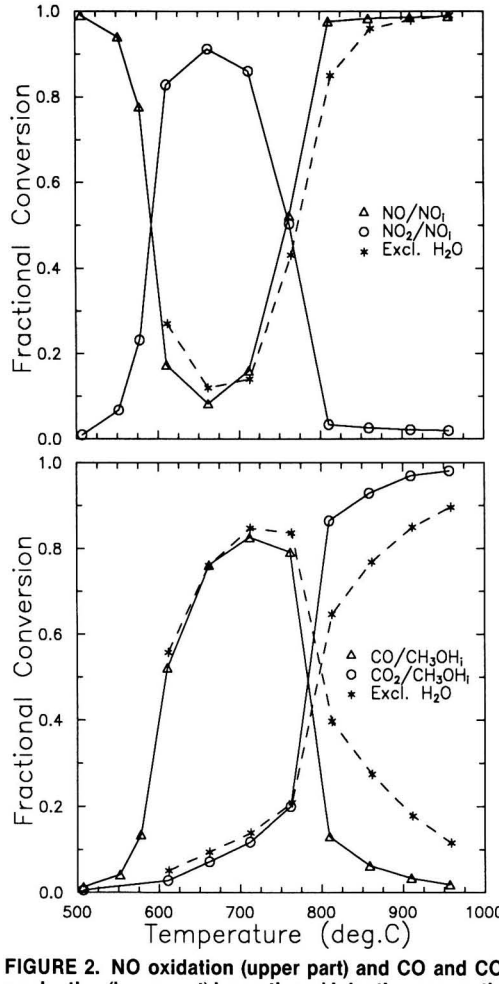

FIGURE 2. NO oxidation (upper part) and CO and CO_2 production (lower part) by methanol injection versus the temperature. The 11.5 cm³ reactor was used. Inlet: 580 ppm NO, 510 ppm CH_3OH, 4.6 vol-% O_2, no H_2O/0.7 vol% H_2O, residence time 218 k·s.

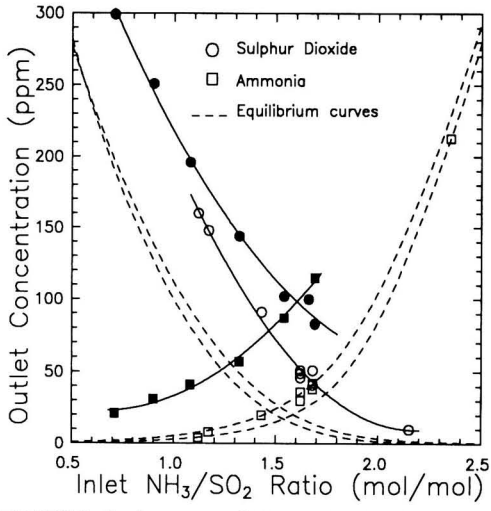

FIGURE 3. Performance of 4.0 mm i.d. (gas flow 1.0 Nl/min, open symbols) and 8.8 mm i.d. (gas flow 3.3 Nl/min, closed symbols) condensers with water cooling (35°C) and gas flow downward (cocurrent). Outlet concentrations of SO_2 and NH_3 are shown versus inlet N-to-S molar ratio. The equilibrium curves were calculated using a water condensation rate of 9.0 (upper) and 12.0 mg/(Nl/min) (lower). Inlet: 500 ppm SO_2, 6.5 vol-% H_2O, and 4.3 vol-% O_2.

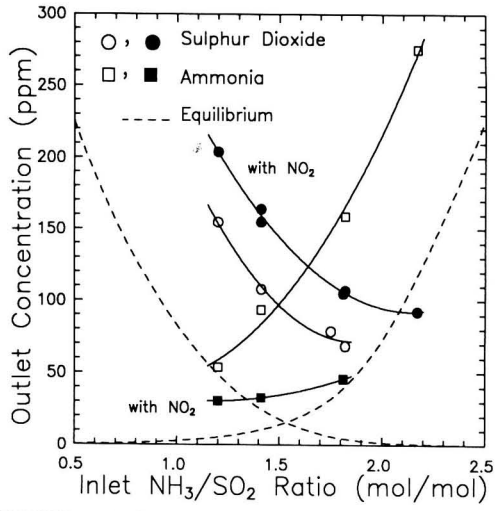

FIGURE 4. Performance of air cooled (20 Nl/min, 0°C) 8.8 mm i.d. condenser with 5.0 Nl/min gas flow upward (countercurrent). Outlet concentrations of SO_2 and NH_3 are shown versus inlet N-to-S molar ratio without NO_2 present (open symbols) and with 20 ppm NO_2 (closed symbols) present. The equilibrium curves were calculated using a water condensation rate of 11.0 mg/(Nl/min). Inlet: 400 ppm SO_2, 5.5 vol-% H_2O, and 4.6 vol-% O_2.

temperature optimum, which was found to be 680°C at a residence time of 214 K·s, the fractional conversion of NO was about 0.9. A comparison between data obtained with about 0.7 vol-% water and without water present shows that water increases the NO conversion slightly. In Figure 2 the corresponding CO and CO_2 production profiles are also shown. Nearly one mole of CO is produced per mole of NO oxidized. Above about 750°C the NO oxidation rate drops rapidly and at the same time the CO oxidation rate increases. The presence of water accelerates CO oxidation in agreement with Yetter and Dryer [6]. The optimum temperatures for NO_2 production were found to be 650°C at a residence time of about 300 K·s and 760°C at 14 K·s.

Low-temperature Condensers

Condensation was tested as a means to remove NH_3 and SO_2 by simultaneous absorption. The temperature of the inlet gas was typically 120°C. Figure 3 shows the outlet concentrations of SO_2 and NH_3 versus the inlet NH_3/SO_2 molar ratio using 4.0 mm and 8.8 mm i.d. condenser tubes thermostated at 35°C with water. The inlet SO_2 concentration was about 500 ppm. The gas residence time was 1.5 s for the 8.8 mm i.d. tube (Re ≅160) and 0.09 s for the 4.0 mm i.d. tube (Re≅1170). The gas flow was directed downwards, i.e. cocurrent flow of gas and condensed droplets. At steady state the weighed quantity of condensing water was 9–12 mg/(Nl gas/min). In Figure 3 it is seen that the removal of SO_2 increases when more NH_3 is added, but that the NH_3 emission increases accordingly. Apparently, the condenser performance improves with the specific surface area, which for the results shown is 11.9 $m^2/(Nm^3/min)$ and 1.6 $m^2/(Nm^3/min)$ for the 8.0 mm i.d. and the 4.0 mm i.d. tube respectively.

For comparison, calculated equilibrium curves (dashed lines) are shown in Figure 3 for water condensation rates of 9.0 mg/(Nl gas/min) and 12.0 mg/(Nl gas/min). The equilibrium model is discussed below. It is found that the experimental data for NH_3 at a high specific surface area lies close to the equilibrium curves, while this is apparently not the case for SO_2.

The condenser performance was not significantly improved when the temperature was lowered to 32°C. Assuming that the limiting factor is the gas-liquid interfacial area, this may be due to the fact that the tube surface was already wetted at 35°C from drops moving downwards. When the gas flow was directed upwards (countercurrent), the removal of both SO_2 and NH_3 decreased. In this case the condensate drops formed primarily in the lower end of the tube and the upper part was almost not wetted, i.e. the gas-liquid contact area decreased.

In order to obtain a better performance in countercurrent operation, experiments were performed with air as a coolant to obtain a lower gas cooling rate and formation of droplets at the top of the condenser tube. 25 Nl/min air was cooled to 0°C and fed at the top of the cooling jacket. 4.7–5.0 Nl/min gas at about 130°C was introduced from the bottom end of the 8.8 mm i.d. condenser (specific surface area 2.4 $m^2/(Nm^3/min)$). In this way an outlet gas temperature of about 40°C and a water condensation rate of about 10 mg/(Nl gas/min) were measured, which is quite similar to what was obtained previously. Figure 4 shows the outlet concentration of SO_2 and NH_3 versus the inlet NH_3/SO_2 ratio, and the corresponding calculated equilibrium curves. It is seen that the performance at countercurrent operation with air cooling (Figure 4, open symbols) is about the same as that for cocurrent operation with water cooling (Figure 3, closed symbols) (in these experiments the specific surface areas are comparable).

Also seen in Figure 4 is the result of introducing 20 ppm NO_2. When NO_2 is added, the outlet SO_2 concentration increases, while the outlet NH_3 concentration decreases markedly, *i.e.* the observed NH_3-to-SO_2 reaction stoichiometry increases. The effect of the inlet NO_2 concentration on the removal of SO_2 and NH_3 at an inlet molar N-to-S ratio of 1.8 is shown in Figure 5. Calculated equilibrium curves are shown for comparison, assuming complete absorption of NO_2 (as NO_2^- or NO_3^-) and no further reactions of absorbed NO_2 with sulfite. Although the calculated results must be taken with

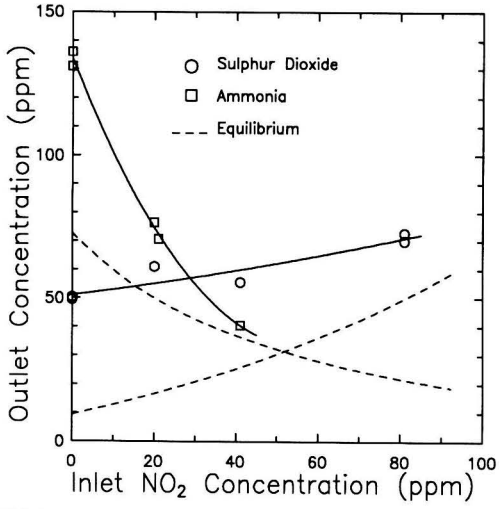

FIGURE 5. Performance of air cooled (20 Nl/min, 0°C) 8.8 mm i.d. condenser with 5.0 Nl/min gas flow upward (countercurrent). Outlet concentrations of SO_2 and NH_3 are shown versus the inlet NO_2 concentration. The equilibrium curves were calculated assuming an outlet NO_2 concentration of zero, and that NO_2 is absorbed as a monovalent completely ionized acid without further reaction. The water condensation rate was 11.0 mg/(Nl/min). Inlet: 780 ppm SO_2, 1400 ppm NH_3, 5.6 vol-% H_2O, and 4.5 vol-% O_2.

care, it is indicated that the outlet gas composition approaches equilibrium as more NO_2 is added, i.e. the absorption rates increases. During the experiments a white fog (aerosols) was visible downstream of the condenser, particularly at high NO_2 concentrations.

Combining the Reactors

When selective reduction of NO by NH_3 is combined with partial flue gas condensation, the inlet NH_3/NO molar ratio may be increased by a factor of 3 or more as the outlet NH_3 concentration is reduced in the condenser. In this way the NO removal efficiency may be increased significantly. The actual inlet NH_3/NO molar ratio which can be used depends on the SO_2 content of the gas and the acceptable NH_3 emission.

The 100 cm^3 high-temperature reactor was installed upstream of the condenser and about 5 Nl/min gas was fed to the reactor, containing about 500 ppm NO, 850 ppm SO_2, 5 vol-% water and 4 vol-% O_2. Using it for selective nitrogen oxide reduction, the temperature selected was 860°C as discussed previously. When about 1700 ppm NH_3 was added (inlet NH_3/NO molar ratio of 3.4), the overall NO and SO_2 conversion obtained was 95% and 77% respectively. The outlet NH_3 concentration was 60–75 ppm.

When the 100 cm^3 high-temperature reactor was used for nitrogen oxide oxidation by methanol, the temperature was maintained at 650°C. 1500 ppm of NH_3 was added at the condenser inlet (NH_3/SO_2 molar ratio of 1.8). The conversion of NO obtained by the injection of 480 ppm methanol was about 0.80 (inlet CH_3OH/NO molar ratio of 0.96), while SO_2 was removed almost completely (about 98% conversion). The outlet NH_3 concentration varied between 20 and 50 ppm, probably due to variations in the gas-liquid interfacial area (drops moving downwards).

When samples of condensate were analyzed by ion chromatography, no sulfite or nitrite was found, but only sulfate and nitrate. Sulfite is partly oxidized in the condenser in the presence of absorbed NO_2, while nitrite and the rest of the sulfite probably oxidize slowly by reaction with oxygen in the sample containers. The NH_4^+ and SO_4^{2-} contents of the condensate were 0.06–0.12 and 0.025–0.035 mol/mol H_2O respectively. The measured pH value was about 5.

According to the equilibrium calculations (discussed below), $[NH_4^{2+}]$ (C) is 0.03–0.06 mol/mol and the sum of $[SO_3^{2-}]+[HSO_3^-]$ (S) is about 0.021–0.032 mole/mole depending on the inlet NH_3/SO_2 molar ratio. These values vary with a factor of about 2 for water condensation rates ranging from 8–14 mg/(Nl gas/min). The calculated pH values are typically in the range 5.0–6.0.

Unfortunately, NO_2 was not measured at the condenser outlet due to problems with salt formation in the gas lines. However, in the experiment with combined reactors and methanol addition mentioned above, the condensate contained 0.01–0.02 mol/mol NO_3^- and about 400 ppm NO_2 was produced. If all of the NO_2 was completely absorbed, the dissolved concentration would be about 0.028 mol/mol H_2O. Thus, based on the measured condensate concentrations, the NO_2 removal was between 40 and 70%. Any reactions of absorbed NO_2 with sulfite etc. are neglected when making this assumption.

Formation of Aerosols

Several experiments carried out with inlet SO_2, NH_3 and NO_2 concentrations of about 750 ppm, 1000–1400 ppm and 20–100 ppm respectively were interrupted due to the formation of aerosols. Gas lines and monitoring equipment were blocked up by a white, solid material. Significant quantities of aerosols were produced which were visible at the gas outlet as a white fog, especially when methanol was added. When a 0.5 μm sintered steel filter was installed just downstream of the high-temperature reactor, at least the visible part of the aerosols was removed. By using a 7 μm filter the removal efficiency as well as the pressure drop were initially low, but increased slowly probably due to the formation of a filter cake. No aerosols were observed without SO_2 or without NH_3 present. The visibility of the aerosols was increased by direct cooling of the outlet gas in ice water.

CALCULATED EQUILIBRIUM

In the following the outlet gas is considered to be in equilibrium with the condensing liquid. The condensing liquid is considered to be well mixed due to condensate drops moving downwards when they are large enough. At steady state, the liquid "feed" rate is equal to the flow of condensing water, which has been measured experimentally to 9–12 mg/(Nl gas/min). The liquid temperature is approximated by the cooling water outlet temperature, or, using air cooling, calculated from the inlet water vapor pressure and the measured quantity of condensed water assuming equilibrium at the condenser outlet.

The mole balances with respect to SO_2 and NH_3 can be formulated as:

$$G \cdot y^o_{SO_2} = G \cdot y_{SO_2} + N_{SO_2} \quad (1)$$

$$G \cdot y^o_{NH_3} = G \cdot y_{NH_3} + N_{NH_3} \quad (2)$$

where G is the total flow rate of gas (mol/s), y_i^o and y_i are the inlet and outlet (equilibrium) mole fractions of components i (SO_2 or NH_3) respectively, and N_i is the rate of absorption (mol/s).

According to Johnstone [7], the equilibrium partial pressures of SO_2 and NH_3 can be related to the liquid phase concentrations of dissolved SO_2 (S) and dissolved NH_3 (C) as:

$$p_{SO_2} = M \cdot \frac{(2S - C + nA)^2}{C - S - nA} \quad (3)$$

and:

$$p_{NH_3} = N \cdot \frac{C(C - S - nA)}{2S - C + nA}, \quad (4)$$

where $\log M = 5.865 - 2369/T$ and $\log N = 13.680 - 4987/T$. Johnstone uses T in Kelvin, p in mmHg, and C and S in mol/100 mol H_2O. A is the concentration (mol/100 mol H_2O) of any completely ionized acid species present, such as SO_4^{2-}, NO_2^-, or NO_3^-, and n is the valence of the acid ion. Notice that SO_4^{2-} may be formed by oxidation of HSO_3^- and SO_3^{2-}, thus increasing the equilibrium pressure of SO_2 and decreasing that of NH_3 according to equations (3) and (4) respectively. Specifically, in the pH range 4.5-6, S and C are approximately:

$$C = [NH_4^+], \text{ and } S = [HSO_3^-] + [SO_3^-] \quad (5)$$

Equations (1) and (2) may now be written:

$$y^o_{SO_2} = y_{SO_2} + S \cdot L/G \quad (6)$$

$$y^o_{NH_3} = y_{NH_3} + C \cdot L/G, \quad (7)$$

where L is the condensing water flow (mol/s), and C and S the liquid concentrations in mol/mol H_2O (notice the conversion from mol/100 mol to mol/mol). Inserting equations (3) and (4) with given L, G, and inlet partial pressures, equations (6) and (7) can be solved to give C and S. Then the equilibrium partial pressures are calculated.

Moreover, knowing C and S, the pH of the condensate can be found from an empirical equation given by Johnstone [7]:

$$pH = 9.20 - 4.62 \cdot (S/C) \quad (8)$$

The resulting water vapor pressure can also be found: according to Raoult's law the vapor pressure is reduced by a factor of $1/(1 + C + S)$.

DISCUSSIONS AND CONCLUSIONS

The overall reactions taking place in the SNR process may be described as two competitive (for NH_3) or successive (for NO) reactions:

$$NH_3 + NO + 1/4\ O_2 \leftrightharpoons N_2 + 3/2\ H_2O$$

$$NH_3 + 5/4\ O_2 \leftrightharpoons NO + 3/2\ H_2O$$

A simple empirical model was successfully developed by Duo *et al.* [5] to describe the kinetics. At present, the homogeneous reactions taking place are relatively well known from detailed kinetic modeling.

Experiments performed in our laboratory have shown that the efficiency in converting NO to NO_2 follows the sequence $CH_3OH > CH_2O > CO$ in the temperature range 850-1050 K. The suitability for NO oxidation of a specific fuel depends on its ability to create HO_2 radicals during the oxidation process. In the presence of NO, $\cdot HO_2$ reacts selectively with NO through $NO + HO_2 \rightleftharpoons NO_2 + OH$. Apart from oxidizing NO, the process exchanges a comparatively unreactive radical, HO_2, with a reactive one, OH, thus enhancing the oxidation of the parent fuel. Further experimental and theoretical results on NO oxidation by combustible additives will be presented in a following paper.

The reactions taking place in the condenser are quite complicated. Ammonia, sulphur dioxide, nitrogen dioxide, and oxygen are simultaneously absorbed in the condensing water:

$$NH_3 + H_2O \leftrightharpoons NH_4^- + OH^-$$

$$SO_2 + SO_3^{2-} + H_2O \leftrightharpoons 2\ HSO_3^-$$

$$2\ NO_2 + H_2O \leftrightharpoons 2H^+ + NO_2^- + NO_3^-$$

$$O_2(g) \leftrightharpoons O_2(sol)$$

In the presence of NO_2, sulfite is effectively oxidized to sulfate, and, on the other hand, in the presence of sulfite, NO_2 is effectively absorbed with 20-30 times higher rates than for pure water [8]. The reaction is first order in both the gas concentration and the sulfite or bisulfite concentrations. The reaction rate coefficient is more than 10 times higher for reaction with SO_3^{2-} than with HSO_3^-. NO is not effectively absorbed due to its low solubility. In the presence of both NO and NO_2, N_2O_3 is formed in the gas phase which has a relatively high solubility, thereby indirectly enhancing NO absorption.

Takeuchi *et al.* [9] investigated the absorption rate of NO_2 in various 0.1 M sulfite solutions and found the order $NH_4^+ > K^+ > Na^+$, corresponding to the order of viscosity of the solutions. This indicates that the diffusivity of NO_2 in the liquid film has significant importance for the NO_2 absorption.

Little is known about the kinetics and products of the reaction between absorbed NO_2 and HSO_3^-/SO_3^{2-} in the presence of dissolved oxygen. A sequence of reactions probably leads to the formation of nitrosyl sulfuric acid. A wet process for SO_x-NO_x removal has been developed [10], where the absorption fluid contains nitrosyl sulfuric acid formed by the reaction:

$$NO + NO_2 + 2\ H_2SO_4 \leftrightharpoons 2\ HNOSO_4 + H_2O,$$

and the nitrosyl sulfuric acid is subsequently decomposed by SO_2 absorption due to the heat of oxidation of S(IV):

$$SO_2 + 2\ HNOSO_4 + 2\ H_2O \leftrightharpoons 3\ H_2SO_4 + 2\ NO.$$

The formation of nitrosyl species has also been reported for the absorption of NO and NO_2 in aqueous sulfite solutions containing Fe(II)-EDTA [11].

In Denmark, a widely developed district heating system has allowed optimal use of thermal energy from heating plants; the water return temperature typically being 45-50°C. Especially when burning biomass with a higher water content, such as wood chips, the heat recovered by using the return water for flue gas condensation is quite significant. An additional advantage is that particulate material may be captured in the condenser [12]. Injection of ammonia and methanol as discussed in this paper may turn such condensing units into effective gas cleaning plants. Moreover, the condensate may be used as e.g. fertilizers.

ACKNOWLEDGEMENTS

This work is part of the research program CHEC (Combustion and Harmful Emission Control) funded by the Danish Technical Research Council, Elsam (the Jutland-Funen Electricity Consortium), Elkraft (the Zealand Electricity Consortium) and the Danish Ministry of Energy. The fruitfull collaboration with Aalborg Ciserv International A/S is gratefully acknowledged.

LITERATURE CITED

1. Lyon, R. K., J. A. Cole, J. C. Kramlich, and S. L. Chen, "The Selective Reduction of SO_3 to SO_2 and the Oxidation of NO to NO_2 by Methanol," *Combustion and Flame*, Vol. 81, pp. 30-39 (1990).
2. Rosenberg, H. S., and H. M. Grotta, "NO_x Influence on

Sulfite Oxidation and Scaling in Lime/Limestone Flue Gas Desulfurization (FGD) Systems," *Env. Sci. & Tech.*, Vol. 14, No. 4, pp. 470–472 (1980).
3. Hjuler, K., and K. Dam-Johansen, "The Reaction between Sulphur Dioxide and Ammonia in Flue Gas," *Ind. Eng. Chem. Res.*, Vol. 31, No. 9, pp. 2110–2118 (1992).
4. Kristensen, P. G., P. Glarborg, and K. Dam-Johansen, "CO Oxidation in Quartz Flow Reactors. Effect of H_2O Concentration and Carrier Gas," To be submitted (1993).
5. Duo, W., K. Dam-Johansen, and K. Østergaard, "Kinetics of the Gas Phase Reaction Between Nitric Oxide, Ammonia and Oxygen," *The Canadian Journal of Chemical Engineering*, Vol. 70, pp. 1014–1020 (1992).
6. Yetter, R. A., and F. L. Dryer, "A Comprehensive Reaction Mechanism for Carbon Monoxide/Hydrogen/Oxygen Kinetics," *Combust. Sci. and Tech.*, Vol. 79, pp. 97–128 (1991).
7. Johnstone, H. F., "Recovery of Sulphur Dioxide from Waste Gases—Equilibrium Partial Vapor Pressures over Solutions of the Ammonia-Sulphur Dioxide-Water System," *Industrial and Engineering Chemistry*, Vol. 27, No. 5, pp. 587–593 (1935).
8. Weisweiler, W., and R. Blumhofer, "Untersuchungen zur Absorption von Stickoxiden in wäßrigen Lösungen von Natriumsulfit und -hydrogensulfit sowie zur Simultan-Absorption von Stickoxiden und Schwefeldioxid in Natronlauge mittels einer Doppel-rührzelle," *Chem.-Ing. Tech.*, Vol. 55, No. 10, pp. 810–811 (1983).
9. Takeuchi, H., M. Ando, and N. Kizawa, "Absorption of Nitrogen Oxides in Aqueous Sodium Sulfite and Bisulfite Solutions," *Ind. Eng. Chem., Proc. Des. Dev.*, Vol. 16, No. 3, pp. 303–308 (1977).
10. Fauth, P., P. Cedraschi, and G. Hess, "Das Ciba-Geigy-Stickoxid-Schwefelsäure-Verfahren zur Reinigung von SO_2- und NO_x-haltigen Abgasen," *Chem.-Ing.-Tech.*, Vol. 59, No. 2, pp. 145–148 (1987).
11. Weisweiler, W., R. Blumhofer, and T. Westermann, "Absorption of Nitrogen Monoxide in Aqueous Solutions Containing Sulfite and Transition-Metal Chelates such as Fe (II)-EDTA, Fe (II)-NTA, Co (II)-Trien and Co (II)-Treten," *Chem. Eng. Process.*, Vol. 20, pp. 155–166 (1986).
12. Evald, A., and H. H. Jakobsen, "Flue Gas Condensing Systems—Practical Experiences in Denmark," Danish Boiler Owners' Association, Gladsaxe Møllevej 15, DK-2860 Søborg, Denmark.

Biodegradation of Xenobiotics in a Fixed Bed Reactor

Chantal Seignez, Vincent Mottier, Cesar Pulgarin, Nevenka Adler and Paul Péringer

Bioengineering Laboratory, Swiss Federal Institute of Technology, CH-1015 Lausanne, Switzerland

The specific example of an at-source biological wastewater treatment has been elaborated and developed. A two-phase fixed-bed bioreactor system was tested for its efficiency using phenol as a test substance and then, the degradation of sodium anthraquinone-2-sulfonate (SAS) was studied and performed.

The continuous aerobic degradation of phenol or SAS as the sole source of carbon was investigated. For SAS degradation with an immobilized mixed bacterial culture, industrial activated sludge was used as inoculum, while for phenol a domestic activated sludge from a municipal wastewater treatment plant and activated Actizym-sludge prepared with Actizym® powder were applied. In our laboratory fixed bed reactor system the adapted mixed culture was able to degrade up to 0.17 g L^{-1} h^{-1} of SAS and 0.28 g L^{-1} h^{-1} of phenol at dilution rates of 0.149 h^{-1} and 0.059 h^{-1}, respectively. The removal efficiency of our two-phase continuous bioreactor system was about 99% of primary and 90% of ultimate SAS degradation.

In the adapted bacterial culture degrading SAS, pure bacterial strains were isolated and identified; three were gram negative and six were gram positive.

INTRODUCTION

Industrial wastewaters must be subject of individual treatment before being passed to a municipal sewage treatment plant. The legislation concerning wastewater is becoming more strict in terms of particular pollutant concentration and load. The industry will therefore be obliged in the near future to reduce not only total pollution levels, but also the concentration of specific pollutants.

The use of biological processes is of particular interest for the treatment of effluents from individual sources, especially if a well defined chemical compound had to be degraded instead of a complex or even unknown mixture of pollutants. In this case, optimal adaptation of biomass is possible, which ensures a degradation without added chemicals or waste production. Such a system must be designed to operate at the pollution source, at each production line, whereas classical techniques are usually centralized and treat wastewaters from several production lines containing many different pollutants. The industrial process can improve production and separation processes in general, as well as recycling secondary products, reagents, catalysts, solvents, and process water. The interaction of production and treatment processes represents a promising means of obtaining biocompatible effluents in the future.

For effluents highly contaminated with recalcitrant compounds and their breakdown intermediates, biological pretreatment by fixed-bed reactors is particularly convenient. An adapted biomass in a fixed-bed reactor can be designed to operate at the pollution source. The main advantage of a fixed-bed reactor containing immobilized biomass over conventional biological processes is in significantly lower sludge production,

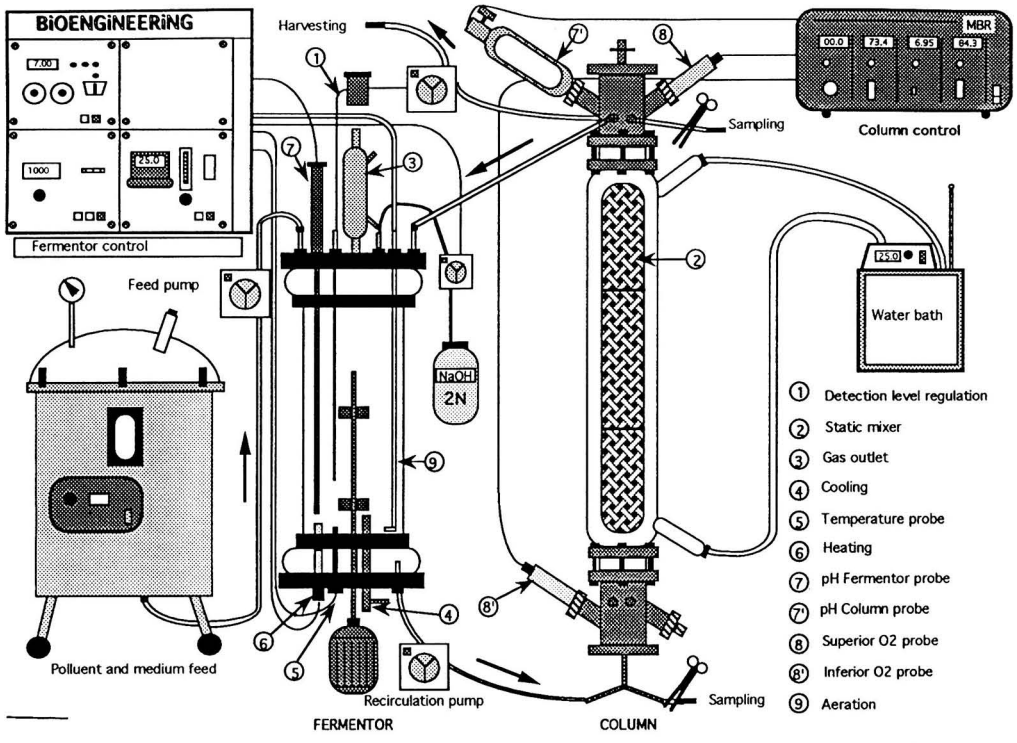

FIGURE1. Schematic drawing of fixed bed bioreactor system: fermentor with column and additional apparatus.

greater loading for a given purification performance and consequently lower reactor volume, using optimally adapted and specialized mixture or individual bacteria for degrading resistant chemicals. The immobilized microbial culture has advantages in treatment of municipal as well as industrial sewage because of its high degradation efficiency and operational stability. The system can readily be adapted to changes in operating conditions when xenobiotic concentration shock and other upsets occur.

Although phenol biodegradation has been the subject of many publications over the years, phenol still remains one of the most widespread wastewater pollutants, alone or in combination with other xenobiotics. It was shown recently that phenol biodegradation is possible in the presence of other toxic substances, even inorganic ones such postassium cyanide. Different strains of *Pseudomonas* are even able to simultaneously degrade phenol and cyanide to a limited degree, depending on the adaptation of bacteria to these substrates [*1*]. Phenol degradation, either by pure or mixed immobilized continuous cultures, has been studied by many authors, especially by Rehm and coworkers [*2, 3, 4, 5*] and Anselmo and Novais [*6, 7*].

Furthermore, SAS and other substituted sulfonated aromatics are important water pollutants that accumulate because they are very recalcitrant compounds and are ubiquitous in the environment [*8*]. Their source is in the chemical industry, where they serve as precursors in production of many pharmaceuticals, pesticides, dyestuffs and tensides; SAS is also used in the production of paper pulp. There are only a few reports about its degradation, for example published by Knackmuss [*9*], Locher *et al.* [*10, 11*], Thurnheer *et al.* [*12*] and Zürrer *et al.* [*13*]. To our knowledge there has been no report on the process biodegradation of SAS.

The purposes of the present work are therefore the:
a) adaptation of a microbial immobilized mixed culture from a sludge for the degradation of phenol as a test substance to prove the efficiency of our bioreactor system and
b) degradation of SAS as a representative of one of the most important groups of water pollutants using industrial activated sludge as inoculum.

MATERIALS AND METHODS

Two-phase Reactor

The fixed-bed laboratory bioreactor system shown in Figure 1 consisted of a 1.5-L fermentor (Bioengineering, Switzerland) and a column. The temperature was maintained at 24°C, the agitation speed at 1200 rpm, the aeration at 150 L h^{-1} and the pH at 7. A peristaltic pump (Watson-Marlow type 501, England) fed the fermentor with the pollutant at a constant flow rate. Medium recirculation was maintained at 35 L h^{-1}. The second part of the system was a 1.2-L fixed-bed column that contained three Kerapak® structured supports (Sulzer, Switzerland) with 420 m^2 m^{-3} of specific effective area. Figure 2 shows the structures of ceramic particles. Each Kerapak support had an area of 0.19 m^2, on which bacteria became attached. The pH and the dissolved oxygen were measured at the bottom and the top of the column, with the oxygen probes being polarographic sensors of 0.004 mg L^{-1} sensitivity (Ingold, Switzerland). The medium circulated between these two reactors at a rate of 88 L h^{-1}. The sampling and harvesting were at the top of the column.

FIGURE 2. Ceramic particles of Kerapak® support. The white line represents 1 mm.

Mineral Medium

The composition of the mineral salts medium making up synthetic wastewater is shown in Table 1. Sodium anthraquinone-2-sulfonate, SAS, from Fluka, Switzerland, (1.2 g L^{-1}) or phenol (4.8 g L^{-1}) were added to the medium as the only carbon and energy source. Ammonium chloride was added to the medium as the nitrogen source, 450 mg L^{-1} for SAS and 700 mg L^{-1} for phenol, respectively, so that the ratio C/N was always about 5.

Inoculum

A sludge from a Ciba-Geigy wastewater treatment plant (Monthey, Switzerland) was used as inoculum for SAS degradation, while for phenol degradation the inocula were adapted sludges from a municipal wastewater treatment plant (Vidy, Switzerland) or activated Actizym [*14*]. The inocula were adapted at pH 7 and 25°C in the same medium with SAS or phenol at a concentration of 0.2 or 0.75 g L^{-1}, respectively. After five repetitive inoculations in shaker flasks, the heterogeneous microbial population that was obtained was used as inoculum for the reactor. After purification of isolates, usual microbiological techniques were applied to identify pure strains of present microorganisms [*15*, *16*].

Table 1 Composition of mineral salt medium

Component	Concentration
	mgL^{-1}
SAS	1200
Phenol	4800
Solution A	
$FeCl_3 \cdot 6\ H_2O$	5
HCl 1N	0.01
Nitrogen Solution	
$MgSO_4 \cdot 7\ H_2O$	40
$CaCl_2$	50
NH_4Cl for phenol	700
NH_4Cl for SAS	450
Phosphates	
Na_2HPO_4	340
KH_2PO_4	140
	μgL^{-1}
Trace Elements	
$FeSO_4 \cdot 7\ H_2O$	400
$ZnSO_4 \cdot 7\ H_2O$	20
$MnCl_2 \cdot 4\ H_2O$	6
H_3BO_3	60
$CoCl_2 \cdot 6\ H_2O$	40
$CuCl_2 \cdot 2\ H_2O$	2
$NiCl_2 \cdot 6\ H_2O$	4
$Na_2MoO_4 \cdot 2\ H_2O$	6

FIGURE 3. Detailed electromicrograph of the Actizym® biofilm degrading phenol. Up on the edge of the photo on the right, bacteria around a yeast cell.

Analytical Methods

After acidification and filtration of samples to remove microbial cells, SAS and phenol concentrations were determined quantitatively in a UV spectrophotometer U-3200 (Hitachi, Japan) at 256 and 235 nm, respectively. The concentration of organic matter was measured as dissolved organic carbon (DOC) using a TOC-500 analyser (Shimadzu, Japan).

RESULTS AND DISCUSSION

The continuous fixed-bed two-step reactor system shown in Figure 1 has been in operation for more than one year with phenol as a test substance. Stirring, aeration, pH adjustment and media addition were performed in a fermentor containing free cells. The whole culture media passed through the column containing immobilized cells on Kerapak® support. Figure 3 shows the electron micrograph of the Actizym biofilm on the support. At the beginning of the experiment yeast cells were surrounded by bacteria, while later the yeast cells lysed and only bacteria were observed. The column was equipped with oxygen pressure and pH controls at the entrance on the bottom and at the exit on the top of the column, where sampling and harvesting occurred. Phenol was used as a test substance. Its initial concentration was 5.0 g L^{-1}, but it was rapidly and totally degraded. Apparently, there were no difference in cells between domestic activated sludge and activated Actizym immobilized on the support.

In 25 days of continuous operation, maximal flow rate (F) with the heterogenous microbial population obtained from the municipal treatment plant was about 80 mL h^{-1}, while with Actizym as inoculum, during the same time under the same

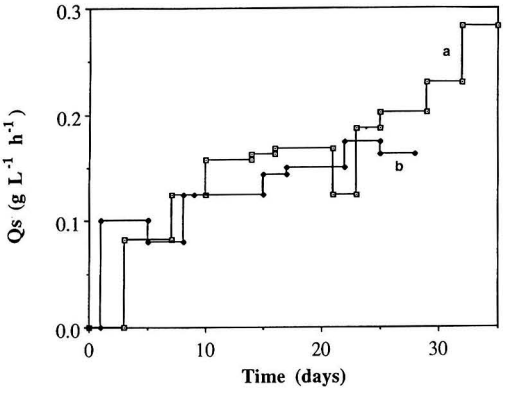

FIGURE 4. Continuous degradation of phenol by · curve a) adapted sludge from municipal wastewater treatment plant (Vidy, Switzerland) · and · curve b) activated Actizym®. Consumption rate (Q_s) vs. time; initial concentration of phenol: 5.0 g L^{-1}.

culture conditions a maximal flow rate of about 65 mL h^{-1} could be achieved. Through stepwise increases of the dilution rate up to D = 0.06 h^{-1} and 0.03 h^{-1}, maximal phenol degradation could be reached with domestic sludge and Actizym, respectively. Better consumption rates (Q_s = 0.202 g L^{-1} h^{-1}) were obtained with domestic activated sludge than with Actizym (Q_s = 0.163 g L^{-1} h^{-1}) as inoculum after 25 days (Figure 4). Similar results were obtained by Beltrame *et al.* [*17*] with activated sludge in a combined continuous-batch system, but with an initial concentration of phenol about one order of magnitude less. In a packed-bed bioreactor, the degradation rate of phenol obtained by Holladay *et al.* [*18*] was 0.200 g L^{-1} h^{-1} from phenolic waste liquors, depending on the flow rate and concentration (0.5 g L^{-1}). Much better results can be obtained by defined mixed culture with species which use phenol as a sole source of carbon and energy. Mörsen and Rehm [*5*] studied immobilized mixture of the yeast *Cryptococcus elinovii* H – 1 and the bacterium *Pseudomonas putida* P – 8 and obtained a maximal degradation rate of 0.383 g L^{-1} h^{-1}.

In our bioreactor system continuous degradation with domestic sludge over 32 days allowed the dilution rate to reach 0.059 h^{-1} (Figure 5), flow rate 112 mL h^{-1} and resulted in a maximal consumption rate of 0.283 g L^{-1} h^{-1} (Figure 4, curve

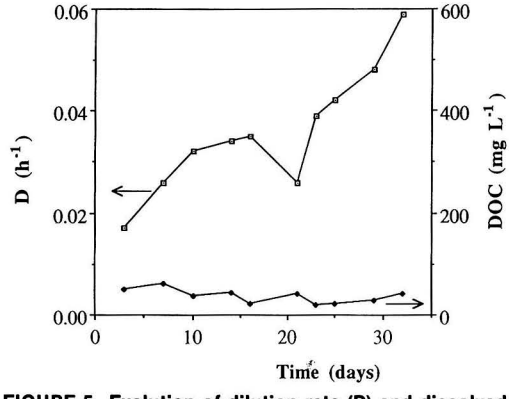

FIGURE 5. Evolution of dilution rate (D) and dissolved organic carbon (DOC) in the course of phenol degradation by domestic sludge. (The lines of curves are just guide for eyes).

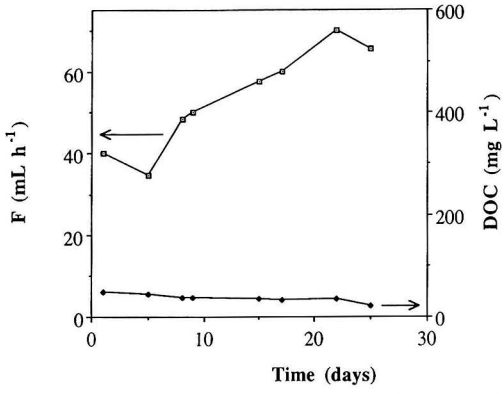

FIGURE 6. Flow (F) and DOC evolution in the course of phenol degradation by activated Actizym®.

a), concentration of phenol being always zero. When the dilution rate attained 0.06 h^{-1} or more, the degradation drastically decreased so that phenol concentration increased from zero to 4.2 g L^{-1}. Figure 6 shows the results of the experiment when activated Actizym was used as inoculum. In that case maximal flow rate of 70.0 mL h^{-1} was achieved.

Continuous microscopic observation of the domestic sludge culture shows that at the beginning of the experiment, bacterial bacilli and cocci, as well as some filamentous fungi, yeasts and protozoae were present while later bacteria predominated. Using phenol as a sole source of carbon, seven bacterial strains were isolated and two of them identified as *Acinetobacter calcoaceticus* and *Alcaligenes denitrificans* subsp. *xylosoxydans*; these were also the main population of the film immobilized on the Kerapak supports. We concluded that in activated sludge these strains were most adapted for phenol degradation.

The same media (Table 1) with SAS as the sole source of carbon and energy at a concentration of 1.2 g L^{-1} was used for biodegradation assays in our continuous reactor system using sludge from Ciba-Geigy as inoculum. Figure 7 shows evolution of Q_s in the course of continuous degradation of SAS during 36 days, while Figure 8 depicts D and DOC during the same period and Figure 9 the evolution of consumption rate Q_s and DOC with different dilution rate. From Figure 10 it can be seen that SAS input increased from 28 mg L h^{-1} up to 179 mg L h^{-1}. In the same time the output was zero during 8 days and only about 1–2 mg L^{-1} h^{-1} at the end of the

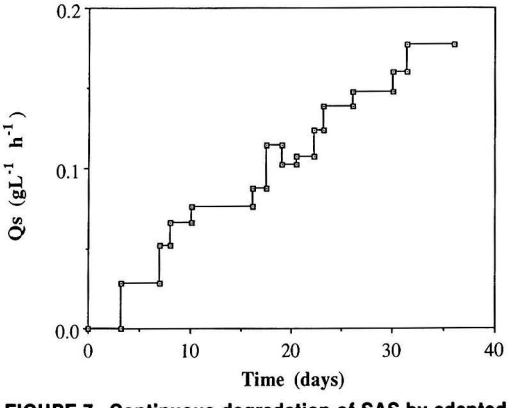

FIGURE 7. Continuous degradation of SAS by adapted industrial sludge (Ciba-Geigy, Monthey, Switzerland). Initial concentration of SAS: 1.2 g L^{-1}.

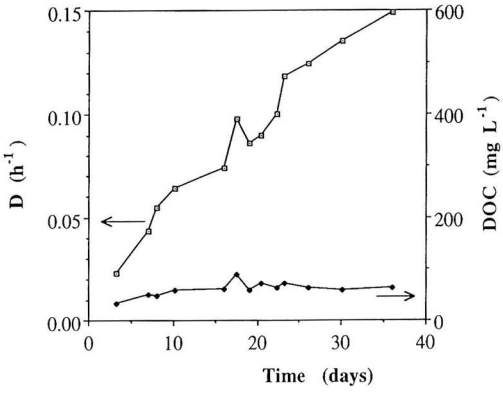

FIGURE 8. Evolution of dilution rate (D) and DOC during SAS degradation.

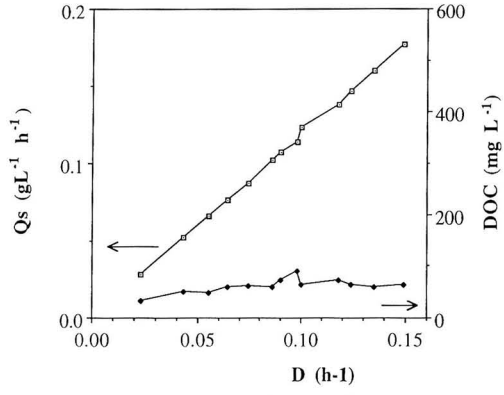

FIGURE 9. Evolution of dilution rate (D) with consumption rate (Q_s) and DOC during SAS degradation.

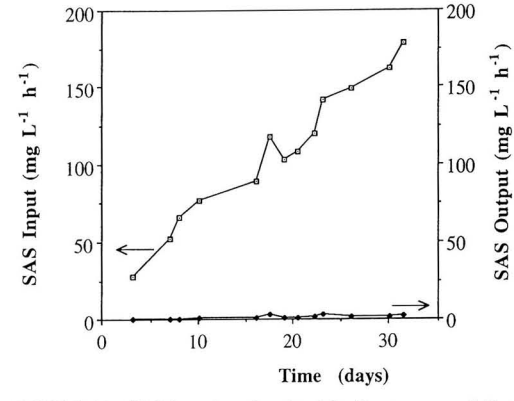

FIGURE 10. SAS input and output in the course of the experiment (culture conditions the same as in Figures 8 and 9).

experiment (about 99% of ultimate degradation), at a dilution rate of D = 0.15 h^{-1} in 32 days. Results presented in Figures 7-10 show that the capacity of the system for SAS degradation was not achieved in that period. The time of the experiment was limited to about one month.

CONCLUSIONS

A two-step laboratory continuous bioreactor system, consisting of two main parts airlift fermentor and packed column with immobilized mixed bacterial culture on Kerapak® support, was effective for the degradation of refractory chemicals. Using phenol as a test substance and activated sludge from municipal wastewater treatment plant, a maximal phenol degradation of 0.28 g L^{-1} h^{-1} was achieved after 32 days. The mixed immobilized biomass on the Kerapak support consists mainly of bacteria. For SAS degradation, industrial activated sludge was adapted so that consumption rates Q_s up to 0.17 g L^{-1} h^{-1} were reached at D = 0.15 h^{-1}.

In the adapted bacterial culture degrading SAS, the following bacteria were isolated; gram-negative strains: *Pasteurella aerogenes*, *Aeromonas salmonicida*, and *Vibrio* ssp. and gram-positive strains: *Enterococcus durans*, one *Staphylococcus*, three strains belonging to the genus *Micrococcus*, and one bacillus, belonging probably to the genus *Corynebacterium*.

ACKNOWLEDGEMENT

The authors express their thanks to Prof. Peter J. Reilly from Iowa State University for his useful suggestions and help during his stay at Ecole Polytechnique Fédérale de Lausanne (EPFL) as Invited Professor.

LITERATURE CITED

1. Labuzek, S., J. Pajak, and I. Pajak, "Degradation of Phenol and Potassium Cyanide by Pseudomonas sp. Strains," *Biotechnologia*, **1**(16), pp. 28-38 (1992).
2. Bettman, H., and H. J. Rehm, "Degradation of Phenol by Polymer Entrapped Microorganisms," *Appl. Microbiol. Biotechnol.*, **20**, 285-290 (1984).
3. Bettman, H., and H. J. Rehm, "Continuous Degradation of Phenol(s) by *Pseudomonas putida* P8 Entrapped in Polyacrylamide-hydrazide," *Appl. Microbiol. Biotechnol.*, **22**, 389-393 (1985).
4. Mörsen, A., and H. J. Rehm, "Degradation of Phenol by Mixed Culture of *Pseudomonas putida* and *Cryptococcus elinovii* Adsorbed on Activated Carbon," *Appl. Microbiol. Biotechnol.*, **26**, 283-288 (1987).
5. Mörsen, A., and H. J. Rehm, "Degradation of Phenol by a Defined Mixed Culture Immobilized by Adsorption on Activated Carbon and Sintered Glass," *Appl. Microbiol. Biotechnol.*, **33**, 206-212 (1990).
6. Anselmo, A. M., and J. M. Novais, "Isolation and Selection of Phenol Degrading Microorganisms from an Industrial Effluent," *Biotechnol. Lett.*, **6**, 601-606 (1984).
7. Anselmo, A. M., and J. M. Novais, "Biological Treatment of Phenolic Wastes: Comparison Between Free and Immobilized Cell System," *Biotechnol. Lett.*, **14**, 239-244 (1992).
8. Pitter, P., and J. Chudoba, "Biodegradability of Organic Substances in the Aquatic Environment," CRC Press, Boca Raton, Florida, p. 220 (1990).
9. Knackmuss, H. J., "Halogenierte und sulfonierte Aromaten—Eine Herausforderung für Aromaten abbauende Bakterien," *Forum Mikrobiol.*, **6**, 311-317 (1979).
10. Locher, H. H., T. Thurnheer, T. Leisinger, and A. M.

Cook, "3Nitrobenzenesulfonate, 3-Aminobenzenesulfonate and 4-Aminobenzenesulfonate as Sole Carbon Sources for Bacteria," *Appl. Environ. Microbiol.*, **55**, 492–494 (1989a).
11. Locher, H. H., T. Leisinger, and A. M. Cook, "Degradation of *p*-Toluenesulphonic Acid via Sidechain Oxidation, Desulphonation and *meta* Ring Cleavage in *Pseudomonas* (*Comamonas*) *testosteroni* T-2," *J. Gen. Microbiol.*, **135**, 1969–1978 (1989b).
12. Thurnheer, T., A. M. Cook, and T. Leisinger, "Co-culture of Defined Bacteria to Degrade Seven Sulfonated Aromatic Compounds: Efficiency, Rates and Phenotypic Variations," *Appl. Microbiol. Biotechnol.*, **29**, 605–609 (1988).
13. Zürrer, D., A. M. Cook, and T. Leisinger, "Microbial Desulfonation of Substituted Naphthalenesulfonic Acids and Benzene Sulfonic Acids," *Appl. Environ. Microbiol.*, **53**, 1459–1463 (1987).
14. Tabka, H., C. Seignez, N. Adler, C. Pulgarin, and P. Péringer, "Inoculum Standardization for Biodegradability Tests," *Biotechnol. Techn.*, **7**, 217–222 (1993).
15. Holt, J. G. (ed.), "Bergey's Manual of Systematic Bacteriology," Vol. 1 to 4, 10th edition, Williams & Wilkins, Baltimore, (1984).
16. Bokhamy, M., N. Adler, C. Pulgarin, M. Deront, C. Seignez, and P. Péringer, "Degradation of Sodium Anthraquinone Sulfonate by Free and Immobilized Bacterial Culture," in press.
17. Beltrame, P., P. L. Beltrame, P. Carniti, and D. Pitea, "Kinetics of Phenol Degradation by Activated Sludge: Value of Measurements in a Batch Reactor," *Water Res.*, **13**, 1305–1309 (1979).
18. Holladay, D. W., C. W. Hancher, C. D. Scott, and D. D. Chilcote, "Biodegradation of Phenolic Waste Liquors in Stirred Tank, Packed-bed and Fluidized-bed Bioreactors," *Jour. Water Poll. Control Fed.*, **50**, 2573–2589 (1978).

Index to Volume 12

Authors

Titles

Subjects

Statement of Ownership, Management, and Circulation (required by 39 U.S.C. 3685) of September 22, 1993, for *Environmental Progress* Publication No. 689-390, issued quarterly for an annual subscription price of $125 from 345 E. 47th St., New York, NY 10017, which is the location of its publication and business offices. The name and address of the Publisher, Editor, and Managing Editor are: Publisher, Gary M. Rekstad, 345 E. 47th St., New York, NY 10017; Editor, Gary F. Bennett, 345 E. 47th St., New York, NY 10017; Managing Editor, Maura Mullen, 345 E. 47th St., New York, NY 10017. The owner is: American Institute of Chemical Engineers, 345 E. 47th St., New York, NY 10017. The known bondholders, mortgagees, and other security holders owning or holding one percent or more of the total amounts of bonds, mortgages, or other securities are: None. The purpose, function, and nonprofit status of this organization, and the exempt status for federal income tax purposes have not changed during the preceding 12 months. The following figures describe the nature and extent of *Environmental Progress*' circulation. In each category the first number (*in italics*) is the average number of copies of each issue during the preceding 12 months. The number next to it, within parentheses ( ), is the actual number of copies of the single issue published nearest to the filing date. Total number of copies printed (net press run), *4,975* (4,800). Paid circulation: 1. Sales through dealers and carriers, street vendors, and counter sales: None; 2. Mail subscriptions, *4,362* (4,321). Total paid circulation *4,362* (4,321). Free distribution by mail carrier, or other means; samples, complimentary, and other free copies, *59* (55). Total distribution *4,422* (4,376). Copies not distributed: 1. Office use, left over, unaccounted, spoiled after printing *554* (424). 2. Returns from news agents: None. Total *4,975* (4,800).
I certify that the statements made by me are correct and complete. Gary M. Rekstad, Publisher.

PROCESS CONTROL THEORY AND THE CPI...

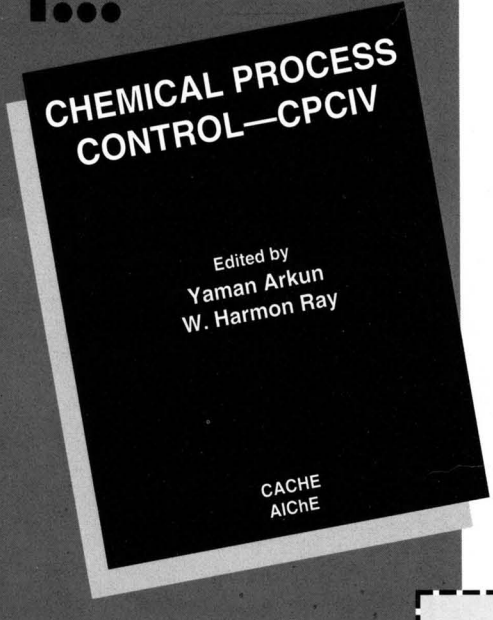

IS THERE A BRIGHTER FUTURE SHINING THROUGH ALL THAT JARGON?

Despite its advances, process control theory has been slow to realize its full potential in the chemical processing industry.Control experts have "theorized" themselves out of the industrial loop. Control remains mostly an afterthought to process design.Yet safety and economics clearly demand more high-performance, non-linear control techniques in the CPI. Those are among the important issues addressed in the new volume of Chemical Process Control—CPCIV. This 700-page compendium contains 37 of the most significant papers from the Fourth International Conference on Chemical Process Control. It covers virtually every topic in the field that chemical engineers should know about. From inventory control in Japanese plants to modeling in neurobiology, these papers sum up five years of the very latest control applications from industry, academia, and government. This fully indexed volume covers:

- Industrial overviews from Japan, Europe, and North America
- On-line sensors and data analysis
- Dynamic process simulation, modeling, and identification
- Model-based process modeling and control
- Recent approaches to the control of nonlinear processes
- Learning systems, adaptive, and AI control
- Control technology in the year 2000

CHEMICAL PROCESS CONTROL—CPCIV, 1991, edited by Yaman Arkun,Georgia Institute of Technology, and W. Harmon Ray, University of Wisconsin. BE SURE TO ORDER YOUR COPY OF THIS IMPORTANT NEW REFERENCE! Mail this form to: AIChE Publications Dept. 345 E. 47th St., New York, NY 10017. or call (212) 705-7657, Fax (212) 752-3294.

Please send me a copy of CHEMICAL PROCESS CONTROL—CPC IV ISBN 0-8169-0549-5

___ Enclosed is my check or money order for $95.00. AIChE members take 20% off list price. International Price $133.00

Please bill my ____Visa ____Mastercard # _____

Expiration date _____ Signature_____

SHIP TO:

Name _____

Organization _____

Address _____

City_____State_____Zip _____

Country _____

Pollution Prevention:

Homework and Design Problems for Engineering Curricula

"One of the greatest needs in industry, as we approach waste elimination, is to change the mindsets of people who have been trained to maximize yield or minimize immediate process costs. This manual goes a long way toward teaching tomorrow's engineers that the real 'process' does not end with just the intended product."

Earl R. Beaver
Monsanto Company

"Through the use of this manual, we hope to instill increased recognition and acceptance of the professional and ethical responsibilities which engineers must have as they develop the next generation of environmentally-compatible, cost-effective process technologies."

Lawrence L. Ross
AIChE's Center for Waste Reduction Technologies

The American Institute of Chemical Engineers' Center for Waste Reduction Technologies is offering a workbook introducing a new resource of pollution prevention technologies and methodologies. This workbook is of value to the novice as well as expert environmental engineers working in the pollution prevention field. Ordered by 600+ faculty members, it is ideal for those seeking:

- Review of pollution prevention techniques
- Introduction to pollution prevention
- Environmental research
- Pollution prevention tutorials
- Use as an educational supplement
- Integration of environmental issues into existing company training courses

Filled with quantitative engineering problems and solutions, this 155 page workbook provides background material, case studies, references, and coverage of six significant pollution prevention concepts.

A driving force behind the creation of this workbook was the American Institute of Pollution Prevention with their members, comprising experts drawn from a wide range of professional and trade organizations, contributing key case studies. The workbook was developed by faculty and professionals active in pollution prevention research, teaching, and practice. Each problem has been reviewed for accuracy, completeness and applicability by engineers in industry, and critiqued by members of CWRT.

Order your Workbook Now!

Call (212)705-7657, Fax (212)752-3294, Or send your order to:

Center for Waste Reduction Technologies
The American Institute of Chemical Engineers

Publication Sales Department, 345 E. 47th Street, New York, NY 10017
All orders must be prepaid (US $35.00). International prices slightly higher.